REVIEWS OF MODERN PHYSICS, VOLUME 82, APRIL–JUNE 2010

Baryon spectroscopy

Eberhard Klempt*

Helmholtz-Institut für Strahlen- und Kernphysik der Rheinischen Friedrich-Wilhelms Universität, Nußallee 14-16, D-53115 Bonn, Germany

Jean-Marc Richard†

Laboratoire de Physique Subatomique et Cosmologie, Université Joseph Fourier-CNRS-IN2P3-INPG, Grenoble, France,
and Institut de Physique Nucléaire de Lyon, Université de Lyon, CNRS-IN2P3-Université Claude Bernard, 4, rue Enrico Fermi, F-69622 Villeurbanne, France

(Published 8 April 2010)

About 120 baryons and baryon resonances are known, from the abundant nucleon with u and d light-quark constituents up to the $\Xi_b^-=(bsd)$, which contains one quark of each generation and to the recently discovered $\Omega_b^-=(bss)$. In spite of this impressively large number of states, the underlying mechanisms leading to the excitation spectrum are not yet understood. Heavy-quark baryons suffer from a lack of known spin parities. In the light-quark sector, quark-model calculations have met with considerable success in explaining the low-mass excitations spectrum but some important aspects such as the mass degeneracy of positive-parity and negative-parity baryon excitations remain unclear. At high masses, above 1.8 GeV, quark models predict a very high density of resonances per mass interval which is not yet observed. In this review, issues are identified discriminating between different views of the resonance spectrum; prospects are discussed on how open questions in baryon spectroscopy may find answers from photoproduction and electroproduction experiments which are presently carried out in various laboratories.

DOI: 10.1103/RevModPhys.82.1095   PACS number(s): 12.39.−x, 13.60.−r, 13.75.−n, 14.20.−c

CONTENTS

*klempt@hiskp.uni-bonn.de
†j-m.richard@ipnl.in2p3.fr

I. INTRODUCTION

A. Why baryons?

Understanding meson resonances and the search for glueballs, hybrids, and multiquark states have remained an active field of research since the time when the high-energy frontier brought into light the existence of the zoo of elementary particles. At that time, baryon spectroscopy flourished as well; but it came to a standstill when the complexity of the three-quark system was realized.

In recent years, interest in baryon spectroscopy has grown again. In his memorable closing speech at the workshop on Excited Nucleons and Hadronic Structure in Newport News, 2000, Nathan Isgur asked "Why N^*'s ?" (Isgur, 2001), and gave three answers: "The first is that nucleons are the stuff of which our world is made. My second reason is that they are the simplest system in which the quintessentially non-Abelian character of quantum chromodynamics (QCD) is manifest. The third reason is that history has taught us that, while relatively simple, baryons are sufficiently complex to reveal physics hidden from us in the mesons." Indeed, baryons were at the roots of the development of the quark model. For references to some early papers, see Gell-Mann and Ne'eman (1964) and Kokkedee (1969). For an introduction to QCD, see Ynduráin (1999) and Narison (2004).

Today, we have a series of precise questions for which we would like to see answers from experiments which are presently on the floor or are being planned. While the spectroscopy of baryons with b quarks is still in its infancy, the number of known charmed baryon ground states and resonances has increased substantially in recent years. But we do not know the following:

(1) Will baryons with triple charm reveal the genuine spectroscopy of three color charges bound by gluons, which is somewhat hidden by the chiral dynamics in light baryons?

(2) Will baryons with two heavy quarks combine a charmoniumlike heavy-quark dynamics and a charmed-meson-like relativistic motion of a light quark bound around a static color source?

(3) Will single-charm baryons and their beauty analogs help understanding the hierarchy of light-quark excitations and provide keys to disentangle the pattern of highly excited nucleon and Δ resonances?

The following questions should be answered by studying light baryons:

(4) Can we relate the occurrence of Regge trajectories and the confinement property of QCD?

(5) Can high-mass excitations be described by the dynamics of three quarks (in symmetric quark models) or do diquark effects play an important role? Quark models describe baryons as dynamics of three flavored quarks. Chiral symmetry breaking is supposed to provide constituent masses; the color degrees of freedom are integrated out. In spite of the indisputable success of the quark model, the question needs to be raised if this type of mean-field theories can be applied to the full resonance spectrum.

(6) Can we identify leading interactions between constituent quarks? Can we find signatures for the property of flavor independence which is expected in QCD?

(7) Are hyperfine splittings and other spin-dependent effects generated by an effective one-gluon exchange, even for light quarks? Or by the exchange of Goldstone bosons? Or are instanton-induced interactions at work?

(8) What are missing resonances and why are they missing? Mostly, missing resonances are defined as resonances which are predicted by symmetric quark models but which have not yet been found. More restricted is a definition where baryons expected in symmetric but not in diquark models are considered to be missing resonances. The lowest-mass example of this type of resonances is the not-well-established quartet of nucleon resonances consisting of $N_{1/2^+}(1880)$, $N_{3/2^+}(1900)$, $N_{5/2^+}(1890)$, and $N_{7/2^+}(1990)$.

(9) The observed spectrum of baryon resonances seems to exhibit a rather simple pattern. Is this pattern accidental or does it reflect a phase transition which may occur when baryons are highly excited?

(10) Are high-mass baryons organized in the form of spin-parity doublets or chiral multiplets of mass-degenerate states having identical spin and parity?

(11) Do we understand baryon decays, or what can be learned studying decays?

B. The structure of baryons

From deep inelastic scattering we know that the nucleon has a complicated structure. The structure functions reveal the longitudinal momentum distributions of valence and sea quarks; generalized parton distributions give access to their transverse momenta and their correlation with the longitudinal momenta. By integration, a few interesting global features follow. The number N_v of valence quarks (integrated over Feynman x) is $N_v=N_q-2N_s=3$. The nucleon has a strange quark sea with $N_s\approx 0.1N_{u,d}$. In the infinite momentum frame, gluons carry a large (≈ 0.5) fraction of the total momentum. From the hadronization of e^+e^- pairs it is known that there are three colors, $N_c=3$. The width of the neutral weak interaction boson Z^0 reveals the number of generations N_G (with at least one neutrino with mass below 45 GeV), $N_G=3$. Timelike and spatial form factors of protons differ by factor of 2 at $Q^2\approx 10$ GeV^2. Perturbatively, this factor should be 1. The discrepancy tells us that even at this large momentum transfer quark correlations play an important role.

C. Naming scheme

The Particle Data Group (PDG) (Amsler *et al.*, 2008) identifies a baryon by its name and its mass. The particle name is N or Δ for baryons having isospin $1/2$ or $3/2$, respectively, with three u, d quarks; the name is Λ or Σ for baryons having two u, d quarks and one s quark; the two light quarks couple to isospin 0 or 1, respectively. Particles with one u or d quark are called Ξ, they have isospin $1/2$. The Ω with no u or d quark has isospin 0. If no suffix is added, the remaining quarks are strange. Thus, the Ω has three s quarks. Any s quark can be replaced by a c (or b) quark which is then added as a suffix. Depending on isospin, Λ_c or Σ_c (or Λ_b or Σ_b) are formed by replacing one s quark by a heavy quark. Resonances with one charmed and one strange quark are called Ξ_c, those with two or three charmed quarks Ξ_{cc} or Ω_{ccc}. The Ξ_b with one b, one s, and one u or d quark has already been mentioned.

Resonances are characterized by adding $L_{2I,2J}$ behind the particle name, where L defines the lowest orbital angular momentum required when they disintegrate into the ground state and a pseudoscalar meson; I and J are isospin and total angular momentum, respectively.

We deviate from this definition, for example, the two particles $N(1535)S_{11}$ and $N(1520)D_{13}$ derive their name from the fact that they form an S wave (D wave) in πN scattering. The first 1 indicates that they have isospin 1/2 (which is already clear for a nucleon excitation), the second 1 defines its total spin to be $J=1/2$. The parity of the states is deduced from the positive parity of the orbital angular momentum state and the intrinsic parities of the ground-state baryon (which is +1) and of the pseudoscalar meson (which is −1).

We call these two states $N_{1/2^-}(1535)$ and $N_{3/2^-}(1520)$. These are the observed states. They can be mixtures of quark-model states. The $N_{1/2^-}(1535)$ and $N_{1/2^-}(1650)$ can be written in the form

$$N_{1/2^-}(1535) = \cos\Theta_{1/2^-}|^2N_{1/2^-}\rangle - \sin\Theta_{1/2^-}|^4N_{1/2^-}\rangle,$$
$$N_{1/2^-}(1650) = \sin\Theta_{1/2^-}|^2N_{1/2^-}\rangle + \cos\Theta_{1/2^-}|^4N_{1/2^-}\rangle, \tag{1}$$

where ${}^2N_{1/2^-}$ has intrinsic quark spin $s=1/2$ while ${}^4N_{1/2^-}$ belongs to the $s=3/2$ quartet. It is often useful to classify baryons according to a baryon model in which the interaction between the constituent quarks are approximated by harmonic oscillators (HOs). In the HO approximation, baryons develop a band structure. Mixing between states belonging to different bands but having identical external quantum numbers is possible. Further components to the states in Eq. (1) could come from the third-excitation band with N=3. A state

$$|^2N_{1/2^-}, D_{56}(L=1)^{P=-1}_{\mathrm{N}=3}\rangle \tag{2}$$

is a spin-doublet quark-model state belonging to the third-excitation band with one unit of orbital angular momentum, having a 56-plet SU(3) flavor structure. Explicit quark-model calculations give a small mixing between different bands and the band structure is preserved.

D. Guide to the literature

Prime sources of original information is found in the proceedings of three conference series on the Structure of Baryons and on N^*. The latest conferences were held as tri-annual International Conference on the Structure of Baryons, Baryons'07, in Seoul, Korea (2007), and as bi-annual International Conference on Meson-Nucleon Physics and the Structure of the Nucleon (MENU 2007) in Jülich, Germany (2007). Irregularly, mostly bi-annual, took place the NSTAR Workshop (Physics of Excited Nucleons) which, in 2009, was hosted in Beijing.

Experimentally indispensable is the Review of Particle Properties published by the Particle Data Group (Amsler *et al.*, 2008) which will be used throughout this review. It includes a few minireviews on baryons (Höhler and Workman, 2008; Trilling, 2008; Wohl, 2008a, 2008b). Still useful is the review by Hey and Kelly (1983). The advances of the quark model to describe the baryon excitation spectrum and baryon decays are reviewed by Capstick and Roberts (2000). Low-energy photoproduction and implications for low-lying resonances are critically discussed by Krusche and Schadmand (2003). Not included here is the physics of cascade resonances of Ξ's and Ω's where little information has been added since the review of Hey and Kelly (1983). There is a proposal to study Ξ resonances at Jefferson Laboratory, and first results demonstrated the feasibility (Guo *et al.*, 2007). The latest review on Ξ baryons can be found in Meadows (1980).

E. Outline

Exciting new results have been obtained for heavy baryons containing a charmed or a bottom quark. The results are reviewed in Sec. II. Most information on light-quark baryons stems from πN or KN elastic or charge exchange (CEX) scattering but new information is now added from photoproduction and electroproduction experiments. The progress is discussed in Sec. III. Section IV provides a framework within which baryon excitations can be discussed and gives an outline of current theoretical ideas. The rich spectrum of light-baryon resonances reveals symmetries and a mass pattern. Based on these observation, a tentative interpretation of the baryon spectrum is offered. In the summary (Sec. V), conclusions are given to what extent the new experiments have contributed to baryon spectroscopy and suggestions for further work are made.

II. HEAVY-QUARK BARYONS

With the discovery of the J particle (Aubert *et al.*, 1974) at Brookhaven National Laboratory (BNL) and of the ψ (Augustin *et al.*, 1974) and ψ' (Abrams *et al.*, 1974) at Stanford and their interpretation as $(c\bar{c})$ bound states, and with the discovery of charmed mesons (Goldhaber *et al.*, 1976), charmed baryons had of course to exist as well, and their properties were predicted early (De Rújula *et al.*, 1975; Gaillard *et al.*, 1975). Experimental evidence for the first charmed baryon was reported at BNL in the reaction $\nu_\mu p \to \mu^- \Lambda \pi^+\pi^+\pi^+\pi^-$ with Λ decaying into $p\pi^-$ (Cazzoli *et al.*, 1975). None of the π^+ could be interpreted as K^+ and no $\pi^+\pi^-$ pair formed a K^0; hence the event could signal either violation of the $\Delta S=\Delta Q$ rule or production of a baryon with charm. Now we know that a Σ_c^{++} was produced.

At present, 34 charmed baryons and 7 beauty baryons are known. For most of them, spin and parity have not been measured; for some states the quantum numbers can be deduced from their decay modes or by comparison of measured masses with the expectation from quark models (Copley *et al.*, 1979).

The study of charmed baryons is mostly pursued by searching for resonances which decay into Λ_c^+ plus one (or more) pion(s). The momenta of the comparatively slow pions can be measured with high precision. Hence the best precision is obtained for the mass difference to the Λ_c^+. The Λ_c^+ is sometimes reconstructed from up to 15 different decay modes. In other cases, the most promi-

TABLE I. Lifetime of flavored mesons and baryons (in s) (Amsler *et al.*, 2008). Lifetimes of Ξ_b^- and Ω_b^-; see also Aaltonen *et al.* (2009).

$K^\pm$	$(123.85\pm0.24)\times10^{-10}$	K_S^0	$(0.8953\pm0.0005)\times10^{-10}$
K_L^0	$(511.4\pm2.1)\times10^{-10}$	$D^\pm$	$(1040\pm7)\times10^{-15}$
D^0	$(410.1\pm1.5)\times10^{-15}$	D_s	$(500\pm7)\times10^{-15}$
$B^\pm$	$(1638\pm11)\times10^{-15}$	B^0	$(1530\pm9)\times10^{-15}$
B_s	$(1466\pm59)\times10^{-15}$		
Λ	$(2.631\pm0.020)\times10^{-10}$	$\Sigma^\pm$	$(0.8018\pm0.0026)\times10^{-10}$
Ξ^0	$(2.90\pm0.09)\times10^{-10}$	Ξ^-	$(1.639\pm0.015)\times10^{-10}$
Ω^-	$(0.821\pm0.011)\times10^{-10}$	Λ_c	$(200\pm6)\times10^{-15}$
Ξ_c^+	$(442\pm26)\times10^{-15}$	Ξ_c^0	$(112^{+13}_{-10})\times10^{-15}$
Ω_c^0	$(69\pm12)\times10^{-15}$	Λ_b	$(1230\pm74)\times10^{-15}$
Ξ_b^-	$(1490^{+200}_{-180})\times10^{-15}$	Ω_b^-	$(1130^{+530}_{-400})\times10^{-15}$

nent and well measurable modes $\Lambda_c^+\to p\bar{K}^0$ and $\Lambda_c^+\to pK^-\pi^+$ are sufficient to obtain a significant signal. The study of charmed baryons was often a by-product: the main aim of the experiments at Cornell, SLAC, or KEK was the study of *CP* violation in B decays from $\Upsilon(4S)$ and, perhaps, the study of the Υ family. Charmed baryons are then produced in the $e^+e^-\to q\bar{q}$ continuum and in B decays.

A. The lifetime of charmed particles

Weak interaction physics is not covered in this review. However, the finite lifetime of hadrons with heavy flavors plays an important role in their experimental identification. In Table I the measured lifetimes of flavored mesons and baryons are summarized. The precision is truncated to 100 keV.

The following comments are in order:

- While the lifetimes of particles carrying a b quark are very similar, this is not the case with strangeness where more than a factor of 3 is observed from the most stable hyperon to the shortest lived.
- The differences are even more pronounced for charmed baryons. When the difference between the charged and the neutral D-meson lifetime was discovered, this was a striking surprise, and it took some time to realize that besides the simplest mechanism, where the c quark emits a virtual W boson which dissociates into a lepton pair or a quark-antiquark pair, there are diagrams in which the W is exchanged. This is, however, permitted for D^0 and D_s but forbidden for $D^\pm$. The lifetime is also influenced by interferences. If $c\to s+W^+\to s+u+\bar{d}$, which initiates some hadronic decay, this $\bar{d}$ should antisymmetrize with the $\bar{d}$ of D^0, an effect that does not exist for D^+. In principle, a fusion mechanism such as $c+\bar{s}\to u+\bar{d}$ should also contribute to the D_s decay.
- The analysis was then extended to charmed baryons, with predictions by Guberina *et al.* (1986); see also Fleck and Richard (1990) and Guberina *et al.* (2000). Some effects are enhanced with respect to the case of mesons, for instance, the role of antisymmetrization. The fusion mechanism, on the other hand, is suppressed as requiring an antiquark from the sea. The trend of the predicted hierarchy is well reproduced by the experimental data, but the observed differences are even more pronounced.
- It would be particularly interesting to measure the lifetime of double-charm baryons, or heavier baryons with triple charm, or with charm and beauty. Another effect should be taken into account is that of the deep binding of the heavy quarks. This is already discussed for the B_c meson with quark content $(b\bar{c})$.
- At the Common Muon Proton Apparatus for Structure and Spectroscopy (COMPASS), the Large Hadron Collider (LHC), and the Antiproton Annihilations at Darmstadt (PANDA), or at a second generation of B factories, there is the possibility to search for weak decays of $\Xi_{cc}(3520)^+$ and Ξ_{cc}^{++} double-charmed baryons into charmless final states (Liu *et al.*, 2008). Such decays could signal new physics.
- The lifetimes of charmed particles are just sufficiently long to identify them by a decay vertex separated from the interaction vertex. For $\beta\gamma\approx1$, the lifetime of B mesons leads to a separation of 500 μm. Precise vertexing is therefore a major experimental requirement.

B. Summary of heavy baryons

The masses of heavy baryons known so far are summarized in Table II; an account of their discoveries and the most recent experimental results is given below. For most resonances, the quantum numbers have not been measured, except for $\Lambda_c(2593)^+$ with $J^P=1/2^-$ and $\Lambda_c^+(2880)$ for which $J^P=5/2^+$ is suggested. The quantum numbers of the lowest-mass states are deduced from the quark model.

Figure 1 shows the flavor dependence of the mass difference between $J^P=5/2^+$ and ground states. The mass gap between $\Lambda_c^+(2880)$ and Λ_c^+ is smaller than that of light-quark baryons. To test this conjecture we compare the spectrum of all observed Λ_c^+ baryons with their light-quark analog states.

In Fig. 2, the excitation spectra of Λ, Λ_c^+, and Ξ_c are compared. In the three lowest states, the light-quark pair has spin 0. In the Ξ_c spectrum, there are two additional states, the Ξ_c' with spin 1/2 and $\Xi_c(2645)$ with spin 3/2, in which the light-quark pair has spin 1. These are forbidden for the isoscalar Λ and Λ_c^+. Above these states, a doublet of negative-parity states are the lowest excitations with fully antisymmetric wave functions. In the Λ spectrum, the Roper-like $\Lambda_{1/2^+}(1600)$ follows, and then a doublet—$\Lambda_{1/2^-}(1670)$ and $\Lambda_{3/2^-}(1690)$—and a

TABLE II. Masses (in MeV) of heavy baryons quoted from (Amsler *et al.*, 2008) except for Σ_b and Ω_b (see text). The isospin of $\Lambda_c^+/\Sigma_c^+(2765)$ (two bold entries) is not known.

Λ_c^+	2286.5 ± 0.2	2595.4 ± 0.6	2628.1 ± 0.6	$\mathbf{2766.6\pm2.4}$	2881.5 ± 0.4
Σ_c^+	2454.0 ± 0.2	2518.4 ± 0.6	2801^{+4}_{-6}	$\lvert\Lambda_c^+$:	2939.3 ± 1.4
Σ_c^+	2452.9 ± 0.4	2517.5 ± 2.3	2792^{+14}_{-5}	$\mathbf{2766.6\pm2.4}$	
Σ_c^+	2453.8 ± 0.2	2518.0 ± 0.5	2802^{+4}_{-7}		
Ξ_c^+	2467.9 ± 0.4	2575.7 ± 3.1	2646.6 ± 1.4	2789.2 ± 3.2	2816.5 ± 1.2
		2969.3 ± 2.8	3054.2 ± 1.3	3077.0 ± 0.5	3122.9 ± 1.3
Ξ_c^0	2471.0 ± 0.4	2578.0 ± 2.9	2646.1 ± 1.2	2791.9 ± 3.3	2818.2 ± 2.1
		2972.9 ± 4.7		3079.3 ± 1.1	
Ω_c^0	2697.5 ± 2.6	2768.3 ± 3.0		$\lvert\Xi_{cc}^+$:	3518.9 ± 0.9
Λ_b^0	5620.2 ± 1.6				
Σ_b^+	5807.8 ± 2.7	5829.0 ± 3.4	$\lvert\Sigma_b^-$:	5815.2 ± 2.0	5836.4 ± 2.8
Ξ_b^-	5792.4 ± 2.2		$\lvert\Omega_b^-$:	6165 ± 17 or	6054.4 ± 6.8

triplet—$\Lambda_{1/2^-}(1800)$, $\Lambda_{3/2^-}(xxx)$, and $\Lambda_{5/2^-}(1830)$—of negative-parity states. The $\Lambda_{1/2^+}(1810)$, not shown in Fig. 2, might be the analog of $N_{1/2^+}(1710)$ and $\Delta_{1/2^+}(1750)$.

Far above, a spin doublet $\Lambda_{3/2^+}(1890)$ and $\Lambda_{5/2^+}(1820)$ is known. It is tempting to assign $1/2^+$ quantum numbers to the isolated states in all three spectra, followed by a doublet of negative-parity states. This scenario is, however, ruled out by the $5/2^+$ assignment to $\Lambda_c^+(2880)$. We urge that the quantum number measurement should be repeated; below we present arguments why the $5/2^+$ assignment is unlikely. In general, the determination of the quantum numbers of heavy baryons remains an important task for the future.

C. Major experiments in heavy-baryon spectroscopy

A large fraction of our knowledge of charmed baryons presented in Table II comes from the CLEO detector at the intersecting storage ring Cornell Electron Storage Ring (CESR). The CLEO detector was upgraded continuously. It consisted of a four-layer silicon-strip vertex detector, a wire drift chamber and a particle identification system based on Cherenkov ring imaging, time-of-flight counters, a 7800-element CsI electromagnetic calorimeter, a 1.5 T superconducting solenoid, iron for flux return and muon identification, and muon chambers (Kopp, 1996; Viehhauser, 2000). The integrated luminosity on the $\Upsilon(4S)$ resonance accumulated in the years 1999–2003 was 16 fb^{-1}.

Of course, the B factories have reached a much higher luminosity; BABAR and BELLE 700 fb^{-1} both collected about 1300 fb^{-1}. The data shown are mostly based on a fraction of the data. Both B factories operated mostly at the peak cross section for formation of the $\Upsilon(4S)$, at 10.58 GeV, with energies of the colliding electron and positron beam of 9 (8) GeV and 3.1 (3.5) GeV, for BABAR (BELLE), respectively, resulting in a Lorentz boost of the center of mass of $\beta=0.55$ (0.425).

The inner part of the BABAR detector (Aubert *et al.*, 2002) includes tracking, particle identification, and electromagnetic calorimetry. It is surrounded by a supercon-

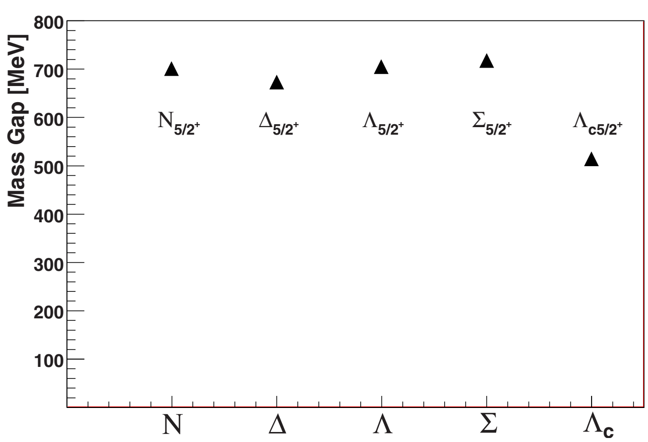

FIG. 1. (Color online) Mass gap from the respective ground states to the lowest excitation with $J^P=5/2^+$.

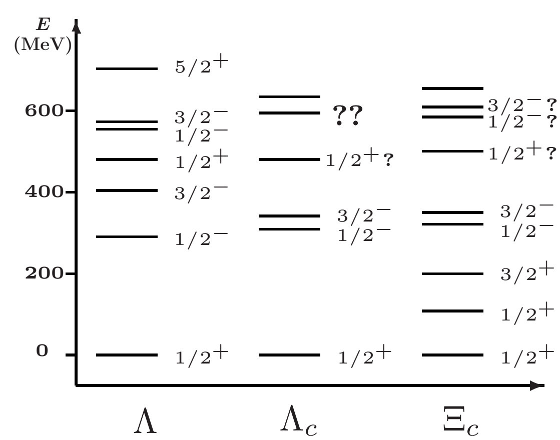

FIG. 2. Excitation spectrum of Λ, Λ_c^+, and Ξ_c. Between $\Lambda_{3/2^-}(1690)$ and $\Lambda_{5/2^+}(1690)$ there are two further states which are omitted for clarity. The quantum number assignments of Λ_c and Ξ_c follow Amsler *et al.* (2008), those with question marks are our tentative assignments. The $\Lambda_c(2880)$ marked ?? is suggested to have $J^P=5/2^+$. From Abe *et al.*, 2007.

ductive solenoid providing a magnetic field of 1.5 T. The tracking system is composed of a silicon vertex tracker and a drift chamber. A 40-layer drift chamber is used to measure particle momenta and the ionization loss dE/dx. Particle identification is provided by the dE/dx measurement and a ring-imaging detector. The electromagnetic calorimeter is a finely segmented array of CsI(Tl) crystals with energy resolution of $\sigma_E/E \approx 2.3\% \times E^{-1/4} + 1.9\%$ (E in GeV). The iron return yoke is instrumented with resistive plate chambers and limited streamer tubes for detection of muons and neutral hadrons.

Tracking, identification, and calorimetric systems of the BELLE detector (Iijima and Prebys, 2000) at KEKB are placed inside a 1.5 T superconducting solenoid magnet. Tracking and vertex measurements are provided by a silicon vertex detector and a central drift chamber. The central drift chamber has 50 layers of anode wires for tracking and dE/dx measurements. Particle identification is achieved using the central drift chamber, time-of-flight counters, and aerogel Cherenkov counters. The electromagnetic calorimeter consists of CsI(Tl) crystals of projective geometry. The flux return is instrumented with 14 layers of resistive plate chambers for muon identification and detection of neutral hadrons.

We mention results obtained by the ARGUS and SELEX Collaborations without introducing the detectors here and refer the reader interested in their performance to Albrecht *et al.* (1989) and Engelfried *et al.* (1998). Also some early bubble chamber results and results from the CERN ISR and SPS will be mentioned. At Fermilab, the photoproduction experiments E687, E691, E791, and Focus and SELEX using a hadron beam produced interesting results on charmed baryons.

So far, only a few baryons with beauty have been discovered. The energy of the B factories operating at the $\Upsilon(4S)$ is obviously not sufficient to produce beauty baryons. These are, however, produced abundantly by the Tevatron at Fermilab, in which antiprotons and protons collide at 1.96 TeV center-of-mass energy. Two major experiments, CDF and DØ, exploit the physics; the discovery of the top quark, the measurement of its mass to a precision of nearly 1%, and the study of B_s oscillations belong to the highlights of the Tevatron results. Earlier important results on beauty baryons were achieved at the CERN ISR and at LEP.

The CDF detector (Acosta *et al.*, 2005) consists of multiple layers of silicon microstrip detectors, providing for a precise measurement of a track's impact parameter with respect to the primary vertex, and a large open-cell drift chamber enclosed in a 1.4 T superconducting solenoid, which in turn is surrounded by calorimeters. The electromagnetic calorimeters use lead-scintillator sampling, the hadron calorimeters iron-scintillator sampling.

The inner tracking of DØ (Abazov *et al.*, 2006) is composed of a silicon microstrip tracker for vertexing and a central fiber tracker, both located within a 2 T superconducting solenoidal magnet. Calorimetry relies on liquid-argon and uranium detectors. An outer muon system consists of a layer of tracking detectors and scintillation trigger counters in front of and behind 1.8 t iron toroids.

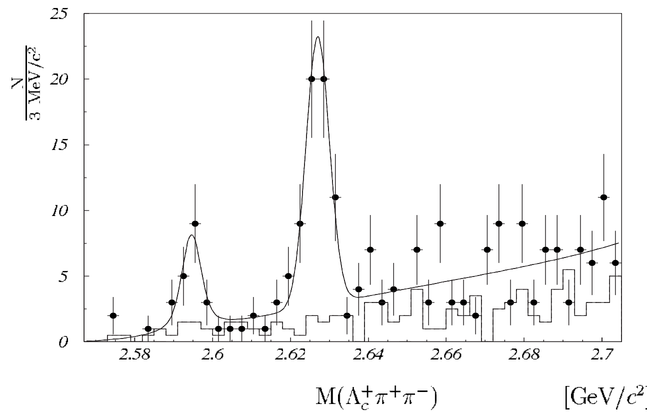

FIG. 3. The $\Lambda_c^+\pi^+\pi^-$ invariant mass distribution after a cut on the Λ_c^+ (reconstructed from five decay modes) and using side bins (dashed line). From Albrecht *et al.*, 1997.

D. Charmed baryons

1. The Λ_c states

a. Λ_c^+

The first observation of a charmed baryon, of Λ_c^+, was reported two years after the J/ψ discovery (Knapp *et al.*, 1976). Now, Λ_c^+ is the best known charmed baryon. Due to its high mass, it has a large number of decay modes. Among these, $\Lambda_c^+ \to p\bar{K}\pi, p\bar{K}\pi\pi$ and $\Lambda\pi^+\pi, \Lambda\pi^+\pi\pi$ have the largest decay fractions, summing up to about 20%. The most precise mass measurement was made by the BABAR Collaboration (Aubert *et al.*, 2005), finding

$$M_{\Lambda_c} = 2286.46 \pm 0.14 \text{ MeV}. \qquad (3)$$

The lifetime was measured by E687, CLEO, Focus, and SELEX. The lifetimes of all heavy baryons stable against hadronic decays are collected in Table I.

b. $\Lambda_c(2593)^+$ and $\Lambda_c(2625)^+$

The $\Lambda_c(2625)^+$ was discovered by the ARGUS Collaboration at the e^+e^- storage ring DORIS II at DESY (Albrecht *et al.*, 1993). Figure 3 shows the $\Lambda_c^+\pi^+\pi^-$ invariant mass distribution with increased statistics (Albrecht *et al.*, 1997) in which the $\Lambda_c(2593)^+$ is observed as well. The latter state was first observed by CLEO (Edwards *et al.*, 1995). Table III compares the results on both states from the ARGUS (Albrecht *et al.*, 1997), CLEO (Edwards *et al.*, 1995), and E687 (Frabetti *et al.*, 1994, 1996) Collaborations.

The $\Lambda_c(2593)^+$ decays with a large fraction (>70%) via $\Sigma_c\pi$; the small phase space favors vanishing orbital angular momentum. The Σ_c is the lowest-mass charmed isovector state and is thus expected to have $J^P = 1/2^+$. Then, $J^P = 1/2^-$ follows for the $\Lambda_c(2593)^+$. Most likely,

TABLE III. Mass and width of the $\Lambda_c(2593)^+$ and $\Lambda_c(2625)^+$ measured at CLEO, BABAR, and BELLE.

		M (MeV/c^2)	Γ (MeV/c^2)
ARGUS	$\Lambda_c(2593)$	$2596.3\pm0.9\pm0.6$	$2.9^{+2.9+1.8}_{-2.1-1.4}$
CLEO	$\Lambda_c(2593)$	$2594.0\pm0.4\pm1.0$	$3.9^{+1.4+2.0}_{-1.2-1.0}$
E687	$\Lambda_c(2593)$	$2581.2\pm0.2\pm0.4$	
ARGUS	$\Lambda_c(2625)$	$2628.5\pm0.5\pm0.5$	<3.2
CLEO	$\Lambda_c(2625)$	$2629.5\pm0.2\pm0.5$	<1.9
E687	$\Lambda_c(2625)$	$2627.7\pm0.6\pm0.3$	

the $\Lambda_c(2625)^+$ is its $J^P=3/2^-$ companion and the two states correspond to $\Lambda_{1/2^-}(1405)$ and $\Lambda_{3/2^-}(1520)$. See Sec. IV.F for further discussion.

c. $\Lambda_c(2765)^+$ [or $\Sigma_c(2765)^+$], $\Lambda_c(2880)^+$, and $\Lambda_c(2940)^+$

The CLEO Collaboration reported two peaks in the $\Lambda_c^+\pi^+\pi^-$ final state (Artuso *et al.*, 2001), which could be Λ_c^+ or Σ_c^+ excitations. One of them is found 480 MeV above the Λ_c^+ baryon and is rather broad, $\Gamma\approx 50$ MeV; the other one is narrow, $\Gamma<8$ MeV, and its mass lies $596\pm1\pm2$ MeV above the Λ_c^+.

The BABAR Collaboration observed two peaks in the D^0p invariant mass distribution (see Fig. 4) (Aubert *et al.*, 2007). It is the first observation of a heavy baryon disintegration into a heavy-quark meson and a light-quark baryon. Due to the kinematics, the larger part of the released energy is carried away by the baryon. The D^+p final state shows no peaks; thus the isospin of the heavy baryon must be zero which identifies the peaks as $\Lambda_c(2880)^+$ and $\Lambda_c(2940)^+$ (and not belonging to the Σ_c^+ series). The former one coincides with the narrow state observed by Artuso *et al.* (2001), called $\Lambda_c(2880)^+$.

The BELLE Collaboration confirmed the $\Lambda_c(2940)^+$ in $\Lambda_c^+\pi^+\pi^-$. The decay proceeds via formation of $\Sigma_c(2455)^{++}$ or $\Sigma_c(2455)^0$ resonances in the intermediate state (Abe *et al.*, 2007). The $\Lambda_c(2880)^+$ and $\Lambda_c(2940)^+$ mass and width measured by BABAR and BELLE are consistent (see Table IV).

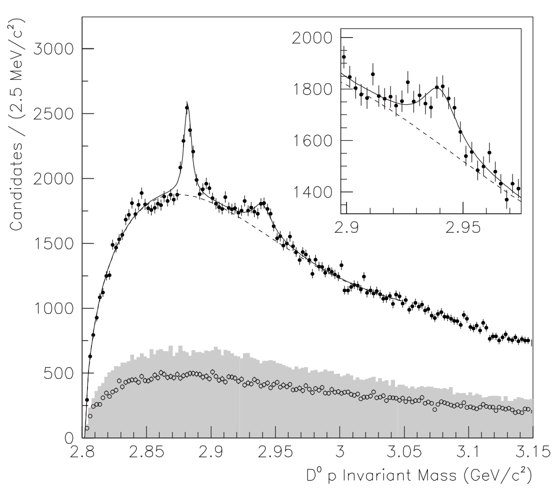

FIG. 4. Invariant mass distribution for D^0p candidates at BABAR. Also shown are the contributions from D^0 sidebands (gray) and wrong-sign combinations (open dots). From Aubert *et al.*, 2007.

TABLE IV. Mass and width of the $\Lambda_c(2880)$ and $\Lambda_c(2940)$ measured at CLEO (Artuso *et al.*, 2001), BABAR (Aubert *et al.*, 2007), and BELLE (Abe *et al.*, 2007).

		M (MeV/c^2)	Γ (MeV/c^2)
CLEO	$\Lambda_c(2880)$	$2882.5\pm1\pm2$	<8
BABAR	$\Lambda_c(2880)$	$2881.9\pm0.1\pm0.5$	$5.8\pm1.5\pm1.1$
BELLE	$\Lambda_c(2880)$	$2881.2\pm0.2\pm0.4$	$5.8\pm0.7\pm1.1$
BABAR	$\Lambda_c(2940)$	$2939.8\pm1.3\pm1.0$	$17.5\pm5.2\pm5.9$
BELLE	$\Lambda_c(2940)$	$2938.0\pm1.3^{+2.0}_{-4.0}$	13^{+8+27}_{-5-7}

The two sequential decay modes improve the sensitivity to study the quantum numbers of the resonance. As shown in Abe *et al.* (2007), the angular distribution of the $\Lambda_c(2880)^+\to\Sigma_c(2455)\pi$ decay favors high spin and is compatible with $J=5/2$ (see Fig. 5). The experimental ratio of the $\Lambda_c(2880)^+$ partial widths $\Gamma[\Sigma_c(2520)\pi]/\Gamma[\Sigma_c(2455)\pi]=0.23\pm0.06\pm0.03$ is calculated in the framework of heavy-quark symmetry to be 1.45 for $J^P=5/2^-$ and 0.23 for $J^P=5/2^+$ (Isgur and Wise, 1991; Cheng and Chua, 2007). Thus the spin-parity assignment $5/2^+$ is favored over $5/2^-$. Note that this assignment requires angular momentum $L=3$ between $\Sigma_c(2455)$ and π at a decay momentum 370 MeV/c while $L=1$ is sufficient for the suppressed $\Sigma_c(2520)\pi$ decay mode. The D^0p decay mode of $\Lambda_c(2880)^+$ poses a further problem. Again, $L=3$ is required for $J^P=5/2^+$, now at 320 MeV decay momentum. When $J^P=1/2^-$ is assigned to $\Lambda_c(2880)^+$, the $\Sigma_c(2455)\pi$ and D^0p decay mode proceed via S wave while the suppressed $\Sigma_c(2520)\pi$ decay requires D wave.

Based on the spin-parity assignment $5/2^+$ for the $\Lambda_c(2880)^+$ and on the mass load flux tube model (LaCourse and Olsson, 2008), the series of Λ_c^+ states in the first line of Table II is suggested to have quantum num-

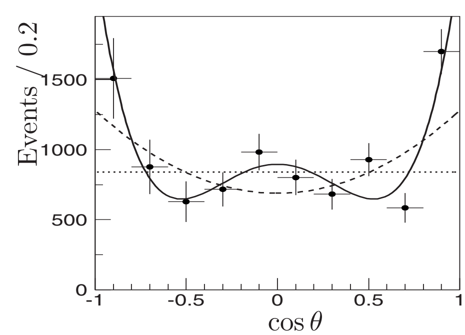

FIG. 5. The yield of $\Lambda_c(2880)^+\to\Sigma_c(2455)^0\pi^+$ and $\Sigma_c(2455)^{++}\pi^-$ decays as a function of the helicity angle. The fits correspond to $\Lambda_c(2880)^+$ spin hypotheses $j=1/2$ (dotted line), 3/2 (dashed curve), and 5/2 (solid curve), respectively. From Abe *et al.*, 2007.

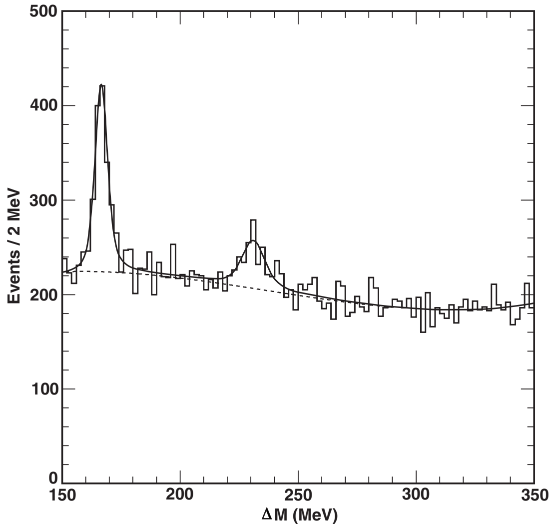

FIG. 6. Mass difference spectrum $M(\Lambda_c^+\pi^0)-M(\Lambda_c^+)$ from CLEO. The solid line fit is to a third-order polynomial background shape and two P-wave Breit-Wigner functions smeared by Gaussian resolution functions for the two signal shapes. The dashed line shows the background function. From Ammar *et al.*, 2001.

bers $1/2^+$, $1/2^-$, $3/2^-$, $3/2^+$, $5/2^+$, and $5/2^-$ (Cheng *et al.*, 2009). The spin-parity assignment $5/2^+$ for the $\Lambda_c(2880)^+$ is constitutive for this interpretation of the spectrum.

Finally, we notice that the mass of the $\Lambda_c(2940)^+$ is at the D^*p threshold, a fact which invites interpretations of this state as a D^*p molecule (He *et al.*, 2007).

2. The Σ_c states

a. Σ_c(2455) and Σ_c(2520)

These two states have been observed in a large number of experiments; here we show only the recent results of the CLEO Collaboration. Σ_c^+ and Σ_c^{*+} were observed in their $\Lambda_c^+\pi^0$ decay (Ammar *et al.*, 2001), and Σ_c^{*++} and Σ_c^{*0} in their decay into $\Lambda_c^+\pi^\pm$ (Athar *et al.*, 2005). The data of Athar *et al.* (2005) cover the e^+e^- energy range 9.4–11.5 GeV while Ammar *et al.* (2001) used data at the $\Upsilon(4S)$. But B decays were suppressed by kinematic cuts and in both cases, the Σ_c^* baryons are likely produced from the $e^+e^-\to q\bar{q}$ continuum. Figure 6 shows the momentum of pions recoiling against the Λ_c^+, which defines the mass gap between Σ_c or Σ_c^* and Λ_c^+. From the angular distribution of the $B^-\to\Sigma_c(2455)^0\bar{p}$ decays, the spin of the $\Sigma_c(2455)^0$ baryon is determined to be 1/2 (Aubert *et al.*, 2008b), while the Σ_c(2520) quantum numbers $J^P=3/2^+$ are quark-model assignments. The numerical results on masses and widths are reproduced in Table V.

TABLE V. Mass and width of the Σ_c(2455) and Σ_c(2520) measured at CLEO.

		M (MeV/c^2)	Γ (MeV/c^2)
Σ_c(2455)	$M(\Sigma_c^{+})-M(\Lambda_c^+)$	$167.4\pm0.1\pm0.2$	$2.3\pm0.2\pm0.3$
	$M(\Sigma_c^{+})-M(\Lambda_c^+)$	$166.4\pm0.2\pm0.3$	<4.6
	$M(\Sigma_c^{0})-M(\Lambda_c^+)$	$167.2\pm0.1\pm0.2$	$2.5\pm0.2\pm0.3$
Σ_c(2520)	$M(\Sigma_c^{*+})-M(\Lambda_c^+)$	$231.5\pm0.4\pm0.3$	$14.4^{+1.6}_{-1.5}\pm1.4$
	$M(\Sigma_c^{*+})-M(\Lambda_c^+)$	$231.0\pm1.1\pm2.0$	<17
	$M(\Sigma_c^{*0})-M(\Lambda_c^+)$	$231.4\pm0.5\pm0.3$	$16.6^{+1.9}_{-1.7}\pm1.4$

b. $\Sigma_c(2800)^+$

The BELLE Collaboration observed an isotriplet of charmed baryons decaying to the $\Lambda_c^+\pi$ final state at 2800 MeV (Mizuk *et al.*, 2005). An additional peak at $\Delta M\sim0.42$ GeV/c^2, visible in the $\Lambda_c^+\pi^+$ and $\Lambda_c^+\pi^-$ invariant mass distributions, was identified as a reflection from the $\Lambda_c(2880)^+\to\Sigma_c(2455)\pi\to\Lambda_c^+\pi^+\pi^-$ decays. The parameters of all isospin partners are consistent (see Table VI). Based on the mass and width, the $3/2^-$ assignment for these states was proposed (Mizuk *et al.*, 2005). Aubert *et al.* (2008b) observed the state at $2846\pm8\pm10$ MeV and with a width of $86^{+33}_{-22}\pm12$ MeV.

3. The Ξ_c states

a. Ξ_c and Ξ_c'

The Ξ_c^+ was discovered by Biagi *et al.* (1983) at the CERN SPS hyperon beam in Σ^- nucleon collisions, $\Sigma^-+\text{Be}\to(\Lambda K^-\pi^+\pi^+)+X$, its isospin partner Ξ_c^0 by the CLEO Collaboration (Avery *et al.*, 1989) through its decay to $\Xi^-\pi^+$. Both states were studied in different production and decay modes. The PDG quotes

$$\begin{aligned} &\Xi_c^+ \quad M=2467.9\pm0.4\text{ MeV}, \quad \tau=442\pm26\text{ fs},\\ &\Xi_c^0 \quad M=2471.0\pm0.4\text{ MeV}, \quad \tau=112^{+13}_{-10}\text{ fs}. \end{aligned} \tag{4}$$

i. The Ξ_c (2645). The spin wave function of the isospin doublet Ξ_c^+ and Ξ_c^0 contains a pair of light quarks, $[su]$ and $[sd]$, mostly in a spin $S=0$ state. There should exist a second doublet in which the light-quark pair is mostly in spin triplet $S=1$. This pair is denoted $\Xi_c^{0,+\prime}$.

The latter two states were discovered by the CLEO Collaboration (Jessop *et al.*, 1999). In a first step, the two ground-state Ξ_c baryons were reconstructed using several decay modes (see Fig. 7). The ground-state Ξ_c baryons were observed jointly with a low-energetic photon. The $\Xi_c^+\gamma$ and $\Xi_c^0\gamma$ invariant masses show signals which were interpreted as the missing $\Xi_c^{+,0\prime}$ partners of the

TABLE VI. Mass and width of the Σ_c(2800) measured at CLEO.

		M (MeV/c^2)	Γ (MeV/c^2)
Σ_c(2800)	$M(\Sigma_c(2800)^{++})-M(\Lambda_c^+)$	$514.5^{+3.4+2.8}_{-3.1-4.9}$	75^{+18+12}_{-13-11}
	$M(\Sigma_c(2800)^{+})-M(\Lambda_c^+)$	$505.4^{+5.8+12.4}_{-4.6-2.0}$	62^{+37+52}_{-23-38}
	$M(\Sigma_c(2800)^{0})-M(\Lambda_c^+)$	$515.4^{+3.2+2.1}_{-3.1-6.0}$	61^{+18+22}_{-13-13}

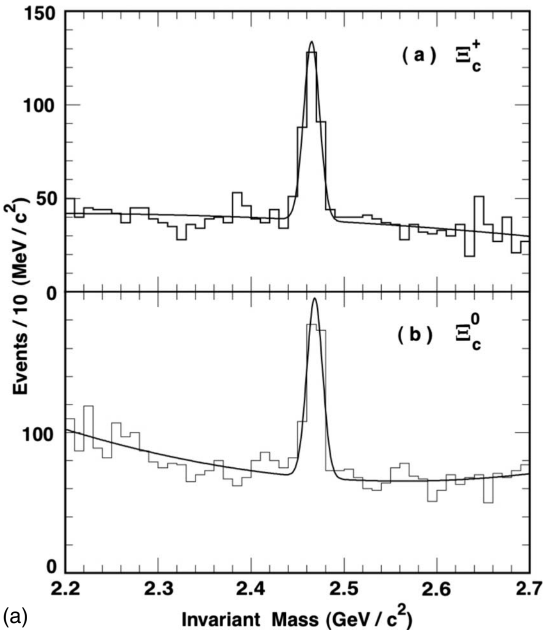

(a)

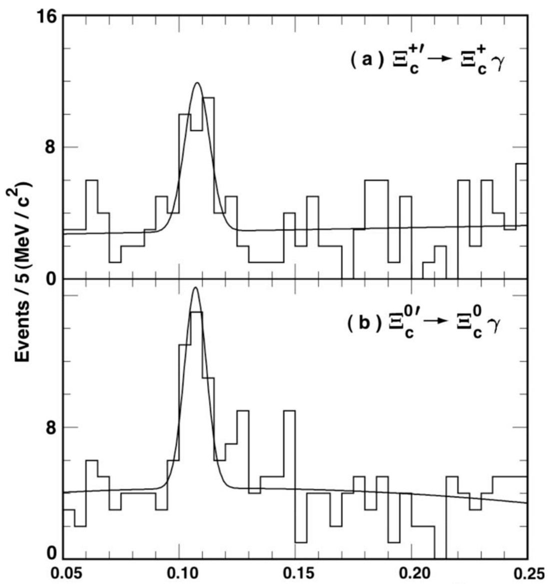

(b)

FIG. 7. The Ξ_c and Ξ_c'. Upper panel: (a) Summed invariant mass distributions for $\Xi^-\pi^+\pi^+$ and $\Xi^0\pi^+\pi^0$ combinations with $x_p>0.5$ and 0.6, respectively, and (b) for $\Xi^-\pi^+$, $\Xi^-\pi^+\pi^0$, Ω^-K^+, and $\Xi^0\pi^+\pi^-$ combinations. Lower panel: Invariant mass difference $\Delta M(\Xi_c\gamma-\Xi_c)$ distributions for $\Xi_c^+\gamma$ and $\Xi_c^0\gamma$, where contributions from the different Ξ_c decay modes have been summed in each case. From Jessop *et al.*, 1999.

ground-state $\Xi_c^{+,0}$ baryons. The mass differences $M(\Xi_c^{+\prime})-M(\Xi_c^+)$ and $M(\Xi_c^{0\prime})-M(\Xi_c^0)$ were measured to be $107.8\pm1.7\pm2.5$ and $107.0\pm1.4\pm2.5$ MeV/c^2, respectively.

BABAR confirmed the existence of the Ξ_c' and found that the rate of Ξ_c' production over Ξ_c is about 18% in the e^+e^- continuum but about 1/3 in B decays. The angular distribution of $\Xi_c'\to\Xi_c\gamma$ decays was found to be consistent with the prediction for $J^P=1/2^+$ even though higher spins cannot yet be ruled out (Aubert *et al.*, 2006b). BELLE determined the $\Xi_c(2645)^+$ mass to be $2645.6\pm0.2^{+0.6}_{-0.8}$ and the $\Xi_c(2645)^0$ to be $2645.7\pm0.2^{+0.6}_{-0.7}$, respectively (Lesiak *et al.*, 2008).

TABLE VII. Mass and width of the $\Xi_c(2790)$ and $\Xi_c(2815)$ measured at CLEO.

		M (MeV/c^2)	Γ (MeV/c^2)
$\Xi_c(2790)$	$M(\Xi_c^0\gamma\pi^+)-M(\Xi_c^0)$	$318.2\pm1.3\pm2.9$	<15
	$M(\Xi_c^+\gamma\pi^-)-M(\Xi_c^+)$	$324.0\pm1.3\pm3.0$	<12
$\Xi_c(2815)$	$M(\Xi_c^0\pi^+\pi^-)-M(\Xi_c^0)$	$347.2\pm0.7\pm2.0$	<6.5
	$M(\Xi_c^+\pi^+\pi^-)-M(\Xi_c^+)$	$348.6\pm0.6\pm1.0$	<3.5

b. Ξ_c(2790) and Ξ_c(2815)

Csorna *et al.* (2001) observed decays of Ξ_c resonances to Ξ_c' plus a pion. Mass differences for the two states to the $\Xi_c^{+,0}$ ground states are given in Table VII. The precision for the $\Xi_c(2815)$ mass was improved by Lesiak *et al.* (2008) to $2817.0\pm1.2^{+0.7}_{-0.8}$ and $2820.4\pm1.4^{+0.9}_{-1.0}$ for the neutral and charged state, respectively. These observations complement an earlier observation of the CLEO Collaboration (Alexander *et al.*, 1999) in which a doublet of Ξ_c resonances was observed, one decaying into $\Xi_c^+\pi^+\pi^-$ via an intermediate Ξ_c^{*0}, and its isospin partner decaying into $\Xi_c^0\pi^+\pi^-$ via an intermediate Ξ_c^{*+}. Mass differences and widths are collected in Table VII. These resonances are interpreted as the $J^P=1/2^-$ and $3/2^-$ Ξ_c particles, the charmed-strange analogs of the $\Lambda_c^+(2593)$ and $\Lambda_c^+(2625)$, or of the light-quark $\Lambda_{1/2^-}(1405)$ and $\Lambda_{3/2^-}(1520)$ pair.

c. Ξ_c(2980) and Ξ_c(3080)

The BELLE Collaboration observed two new Ξ_c states, the $\Xi_c(2980)$ and $\Xi_c(3080)$, decaying to $\Lambda_c^+K^-\pi^+$ and $\Lambda_c^+K_S\pi^-$ (Chistov *et al.*, 2006); see Figs. 8(a) and 8(b). In contrast to other Ξ_c decay modes, the c and s quark separate, thus forming a charmed baryon and a strange meson. (Likewise, decays into ΛD^+ are allowed above 3 GeV and could be searched for.) The broader of the two states was measured to have a mass of $2978.5\pm2.1\pm2.0$ MeV/c^2 and a width of $43.5\pm7.5\pm7.0$ MeV/c^2. The mass and width of the narrow state are measured to be $3076.7\pm0.9\pm0.5$ MeV/c^2 and $6.2\pm1.2\pm0.8$ MeV/c^2, respectively. A search for the isospin partner decaying into $\Lambda_c^+K_S^0\pi^-$ yielded evidence for a signal at the mass of $3082.8\pm1.8\pm1.5$ MeV/c^2; the broader low-mass baryon is just visible.

The BABAR Collaboration confirmed observations of the $\Xi_c(2980)$ and $\Xi_c(3080)$ (Aubert *et al.*, 2006a) by studying the $\Lambda_c^+K_S^0$, $\Lambda_c^+K^-$, $\Lambda_c^+K^-\pi^+$, $\Lambda_c^+K_S^0\pi^-$, $\Lambda_c^+K_S^0\pi^-\pi^+$, and $\Lambda_c^+K^-\pi^+\pi^-$ mass distributions [see Fig. 8(c)]. In addition, BABAR studied the resonant structure of the $\Lambda_c^+K^-\pi^+$ final state (Aubert *et al.*, 2008a); see Fig. 8(d). The $\Xi_c(3080)$ was found to decay through the interme-

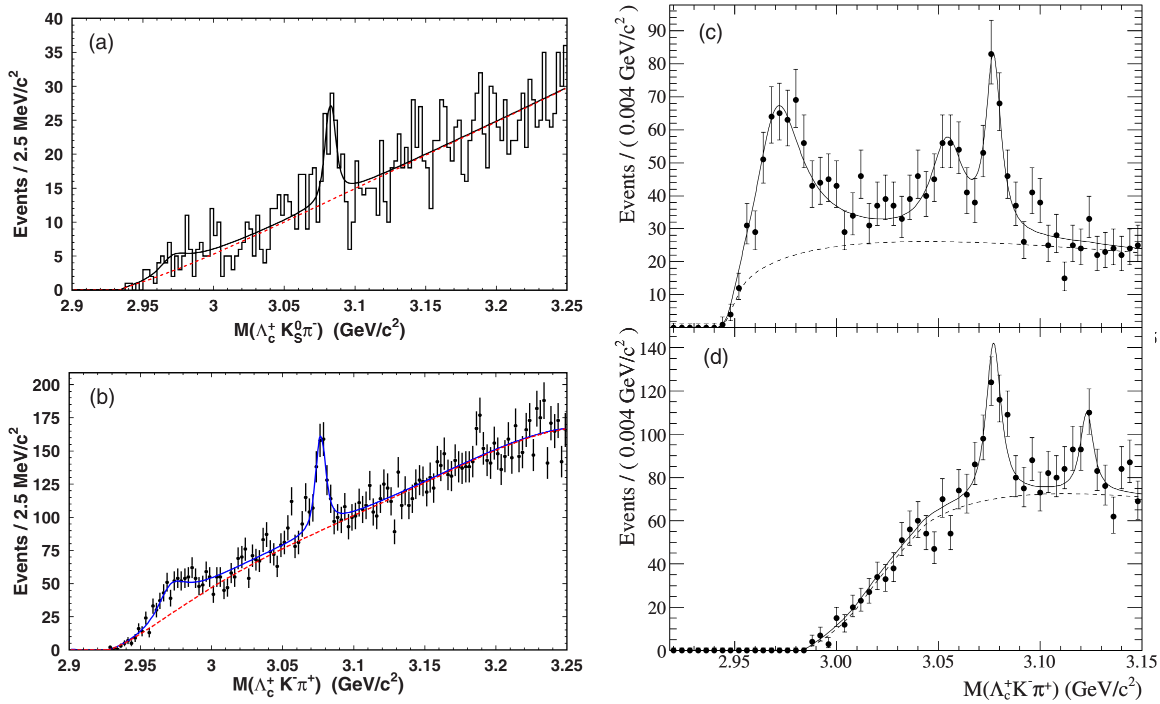

FIG. 8. (Color online) Ξ_c spectroscopy. (a) $M(\Lambda_c^+ K^- \pi^+)$ and (b) $M(\Lambda_c^+ K_S^0 \pi^-)$ distribution at BELLE (Chistov *et al.*, 2006). (c) The $\Lambda_c^+ K^- \pi^+$ invariant mass distribution for $M(\Lambda_c^+ \pi^+)$ consistent with the $\Sigma_c(2455)$ and (d) with the $\Sigma_c(2520)$, measured at BABAR (Aubert *et al.*, 2006a, 2008a).

diate $\Sigma_c(2455)$ and $\Sigma_c(2520)$ states, with roughly equal probability. The $\Xi_c(2980)$ was found to decay through the intermediate $\Sigma_c(2455)\bar{K}$; the $\Sigma_c(2455)\bar{K}$ mass distribution shows an additional signal establishing $\Xi_c(3055)^+$. The $\Sigma_c(2455)\bar{K}$ mass distribution shows evidence for $\Xi_c(2980)$ as strong threshold enhancement, for $\Xi_c(3080)$ and for a third signal at $\Xi_c(3123)$. The BELLE and BABAR parameters for the new Ξ_c states are summarized in Table VIII.

Based on their mass and width, the $\Xi_c(3080)$ state is proposed to be a strange partner of the spin-parity $J^P = 5/2^+ \Lambda_c(2880)^+$ resonance, while the $\Xi_c(2980)$ should have $J^P = 1/2^+$ or $3/2^+$ (Cheng and Chua, 2007; Garcilazo *et al.*, 2007; Rosner, 2007; Ebert *et al.*, 2008).

TABLE VIII. Mass and width of the $\Xi_c(2790)$ and $\Xi_c(2815)$ measured at CLEO (Chistov *et al.*, 2006) and BABAR Aubert *et al.*, 2008a).

		M (MeV/c^2)	Γ (MeV/c^2)
BELLE	$\Xi_c(2980)^+$	$2978.5 \pm 2.1 \pm 2.0$	$43.5 \pm 7.5 \pm 7.0$
BABAR	$\Xi_c(2980)^+$	$2969.3 \pm 2.2 \pm 1.7$	$27 \pm 8 \pm 2$
BABAR	$\Xi_c(3055)^+$	$3054.2 \pm 1.2 \pm 0.5$	$17 \pm 6 \pm 11$
BELLE	$\Xi_c(2980)^0$	$2977.1 \pm 8.8 \pm 3.5$	43.5 (fixed)
BABAR	$\Xi_c(2980)^0$	$2972.9 \pm 4.4 \pm 1.6$	$31 \pm 7 \pm 8$
BELLE	$\Xi_c(3080)^+$	$3076.7 \pm 0.9 \pm 0.5$	$6.2 \pm 1.2 \pm 0.8$
BABAR	$\Xi_c(3080)^+$	$3077.0 \pm 0.4 \pm 0.2$	$5.5 \pm 1.3 \pm 0.6$
BELLE	$\Xi_c(3080)^0$	$3082.8 \pm 1.8 \pm 1.5$	$5.2 \pm 3.1 \pm 1.8$
BABAR	$\Xi_c(3080)^0$	$3079.3 \pm 1.1 \pm 0.2$	$5.9 \pm 2.3 \pm 1.5$
BABAR	$\Xi_c(3123)^+$	$3122.9 \pm 1.3 \pm 0.3$	$4.4 \pm 3.4 \pm 1.7$

4. The Ω_c states

a. Ω_c

The discovery of the Ω_c $(=csd)$ marked a milestone; it completed the number of stable single-charmed baryons. The first evidence for it was reported in Biagi *et al.* (1985) and confirmed in several experiments. We quote here its mass (Amsler *et al.*, 2008)

$$M_{\Omega_c} = 2697.5 \pm 2.6 \text{ MeV}. \tag{5}$$

The Ω_c lifetime (see Table I) was measured by the WA89 Collaboration at CERN and, recently, by the FOCUS and SELEX experiments at Fermilab. The SELEX (E781) experiment used 600 GeV/$c\Sigma^-$, π^- and p beams (Iori *et al.*, 2007) while WA89 and FOCUS are photoproduction experiments. All three experiments reconstructed about 75 Ω_c^0 in the $\Omega^-\pi^-\pi^+\pi^+$ and $\Omega^-\pi^+$ decay modes.

b. Ω_c^*

Recently, an excited Ω_c state has been suggested by the BABAR Collaboration; it was introduced as Ω_c^*. It was produced inclusively in the process $e^+e^- \to \Omega_c^* X$, where X denotes the remainder of the event. The Ω_c^* was observed in its radiative decay to the Ω_c ground state. The latter was constructed from one of the Ω_c decay sequences

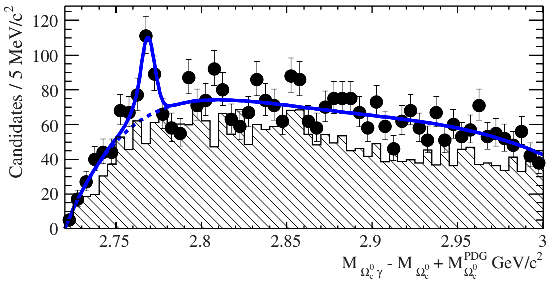

FIG. 9. (Color online) The invariant mass distributions of $\Omega_c^0\gamma$ candidates, with Ω_c^0 reconstructed in various decay modes. The $M_{\Omega_c^0\gamma}$ mass is corrected for the difference between the reconstructed Ω_c^0 mass and the nominal value $M_{\Omega_c^0}^{\mathrm{PDG}}$. The shaded histograms represent the mass distribution expected from the mass sideband of Ω_c^{*0}. From Aubert *et al.*, 2006c.

$$\Omega_c^0 \to \Omega^-\pi^+, \Omega^-\pi^+\pi^0, \Omega^-\pi^+\pi^+\pi^-, \Omega^- \to \Lambda K^- \\ \text{or } \Omega_c^0 \to \Xi^- K^-\pi^+\pi^+, \Xi^- \to \Lambda\pi^- \tag{6}$$

Figure 9 shows the $\Omega_c^0\gamma$ invariant mass after all Ω_c decay modes were added up. A significant enhancement (with 5.2σ) is observed above a smooth background. It is identified with the $J^P=3/2^+$ excitation of the Ω_c ground state. Its mass was found to be 70.8 ± 1.5 MeV above the ground state. The observation was confirmed by BELLE (Solovieva *et al.*, 2005), reporting a mass difference to the ground state of $70.7\pm0.9^{+0.1}_{-0.9}$ MeV.

5. Double-charm baryons

The SELEX Collaboration reported a statistically significant signal in the $\Lambda_c^+K^-\pi^+$ invariant mass distribution at 3519 ± 1 MeV, a lifetime of less than 33 fs at 90% confidence level (Mattson *et al.*, 2002), and produced in a 600 GeV/c charged hyperon beam. Due to its decay mode, the signal is assigned to production of a doubly-charmed baryon, Ξ_{cc}^+. The state was confirmed by SELEX in the $\Xi_{cc}^+ \to pD^+K^-$ decay mode (Ocherashvili *et al.*, 2005). In spite of intense searches, the state failed to be observed in the photoproduction experiment FOCUS (Ratti, 2003) although they observe 19 500 Λ_c^+ baryons, compared to 1.650 observed at SELEX. BABAR reports $\approx 600\times10^3$ reconstructed Λ_c^+ baryons but only upper limits for Ξ_{cc}^+ and Ξ_{cc}^+ (Aubert *et al.*, 2006d). Of course, SELEX starts with a hyperon beam which may be better suited to produce double-charm baryons. But doubts remain concerning the evidence reported by SELEX.

The lack of double-charm baryons at B factories is surprising. In these experiments, double-charm production is abundant, leading in particular to $e^+e^- \to J/\psi + X$ and the discovery of the η_c' in the missing-mass spectrum. One could thus expect double-charm production should hadronize also into baryon-antibaryon pairs, $\Xi_{cc}+\bar{\Xi}_{cc}$, or $\Xi_{cc}+\bar{\Lambda}_c+\bar{D}$, etc. In general, baryon production is suppressed by one order of magnitude as compared to mesons. In J/ψ decays, events with baryons in the final state constitute about 5% of all hadronic decays.

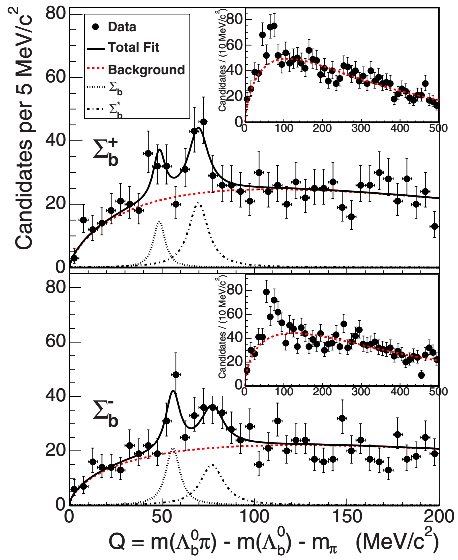

FIG. 10. (Color online) The invariant mass distributions for the $\Lambda_b^0\pi^+$ (top) and $\Lambda_b^0\pi^-$ (bottom) combinations at CDF. From Aaltonen *et al.*, 2007a.

E. Beautiful baryons

1. The Λ_b states

The Λ_b was discovered early at the CERN ISR (Bari *et al.*, 1991a, 1991b) and later reported by several collaborations. We give here only the PDG values for its mass (Amsler *et al.*, 2008)

$$M_{\Lambda_b} = 5620.2 \pm 1.6 \text{ MeV}; \tag{7}$$

its lifetime is given in Table I.

2. The Σ_b states

a. Σ_b and Σ_b^*

The Σ_b baryon with $J^P=1/2^+$ and a low-mass excitation identified as $J^P=3/2^+\Sigma_b^*$ were discovered recently at Fermilab (Aaltonen *et al.*, 2007a) by the CDF Collaboration in the $\Lambda_b^0\pi^+$ and $\Lambda_b^0\pi^-$ final states (see Fig. 10).

The signal region exhibits a clear excess of events even though the statistics is not sufficient to determine mass and widths of the expected Σ_b and Σ_b^*. Therefore, the $M(\Sigma_b^{*+})-M(\Sigma_b^+)$ and $M(\Sigma_b^{*-})-M(\Sigma_b^-)$ mass differences were assumed to the same and the widths of the Breit-Wigner resonances were fixed to predictions based on the heavy-quark symmetry (Körner *et al.*, 1994).

Both the shape and the normalization of the background were determined from Monte Carlo simulations. The results of the fit are given in Table IX. The significance of the four-peak structure relative to the background-only hypothesis is 5.2σ (for seven degrees of freedom). The significance of every individual peak is about 3σ.

TABLE IX. Results of the $\Sigma_b^{(*)}$ fit.

$m(\Sigma_b^+)-m(\Lambda_b^0)=188.1^{+2.0+0.2}_{-2.2-0.3}$ MeV$/c^2$
$m(\Sigma_b^-)-m(\Lambda_b^0)=195.5\pm1.0\pm0.2$ MeV$/c^2$
$m(\Sigma_b^*)-m(\Sigma_b)=21.2^{+2.0+0.4}_{-1.9-0.3}$ MeV$/c^2$

3. The Ξ_b states

a. Ξ_b

A further baryon with beauty, the Ξ_b, contains a b, s, and a d quark and thus a negatively charged quark from each family. It was discovered at Fermilab (Aaltonen *et al.*, 2007b; Abazov *et al.*, 2007). Its history will be outlined shortly.

Indirect evidence for the Ξ_b^- baryon based on an excess of same-sign $\Xi^-\ell^-$ events in jets was observed from experiments at the CERN LEP e^+e^- collider but no exclusively measured candidate was reported. The first direct observation of the strange b baryon Ξ_b^- ($\bar{\Xi}_b^+$) was achieved at Fermilab (Abazov *et al.*, 2007) by the DØ Collaboration by reconstruction of the decay sequence $\Xi_b^-\to J/\psi\Xi^-$, with $J/\psi\to\mu^+\mu^-$, and $\Xi^-\to\Lambda\pi^-\to p\pi^-\pi^-$ (Fig. 11, top). The CDF Collaboration reported a more precise mass value. Their $J/\psi\Xi^-$ invariant mass distribution exhibits a significant peak (Aaltonen *et al.*, 2007b) at a mass of

$$M_{\Xi_b}=5792.9\pm2.5\pm1.7\ \text{MeV}, \tag{8}$$

which is shown in Fig. 11, bottom. The mass and number of Ξ_b^- events observed by Aaltonen *et al.* (2007b) and Abazov *et al.* (2007) are given in Table X, with the lifetime in Table I. The results of DØ and CDF are consistent.

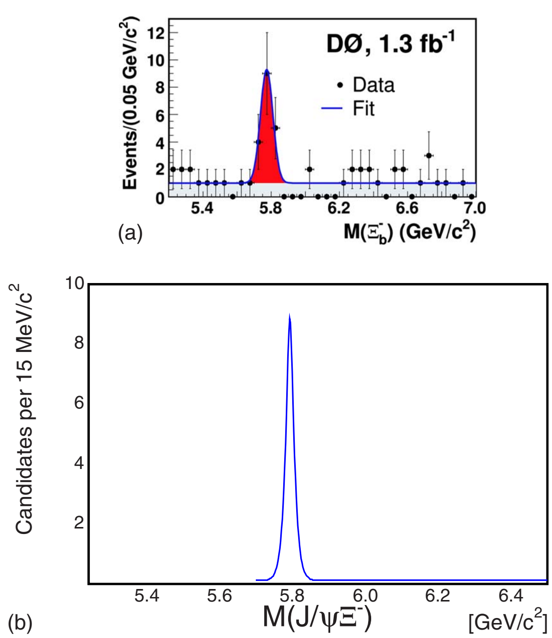

FIG. 11. (Color online) The invariant mass distributions of the $J/\psi\Xi^-$ combinations at DØ (top) (Abazov *et al.*, 2007) and CDF (bottom) (Aaltonen *et al.*, 2007b).

TABLE X. The parameters of the Ξ_b^- measured by DØ and CDF.

	Yield	Mass (MeV$/c^2$)	Significance
DØ	$15.2\pm4.4^{+1.9}_{-0.4}$	$5774\pm11\pm15$	5.5σ
CDF	17.5 ± 4.3	$5792.9\pm2.5\pm1.7$	7.7σ

4. The Ω_b

Figure 12 (top) shows evidence for the Ω_b^- baryon reported by the DØ Collaboration. It was reconstructed from the decay sequence $\Omega_b^-\to J/\psi\Omega^-$, with $J/\psi\to\mu^+\mu^-$, $\Omega^-\to\Lambda K^-$, and $\Lambda\to p\pi^-$. The signal has a statistical significance exceeding 5σ. Its mass was reported to be (Abazov *et al.*, 2008)

$$M_{\Omega_b}=6.165\pm0.010\pm0.013\ \text{GeV}. \tag{9}$$

It is unexpectedly high, see Sec. IV.C. Recently, the Ω_b has been seen (Fig. 12, bottom) by the CDF Collaboration (Aaltonen *et al.*, 2009); their result is

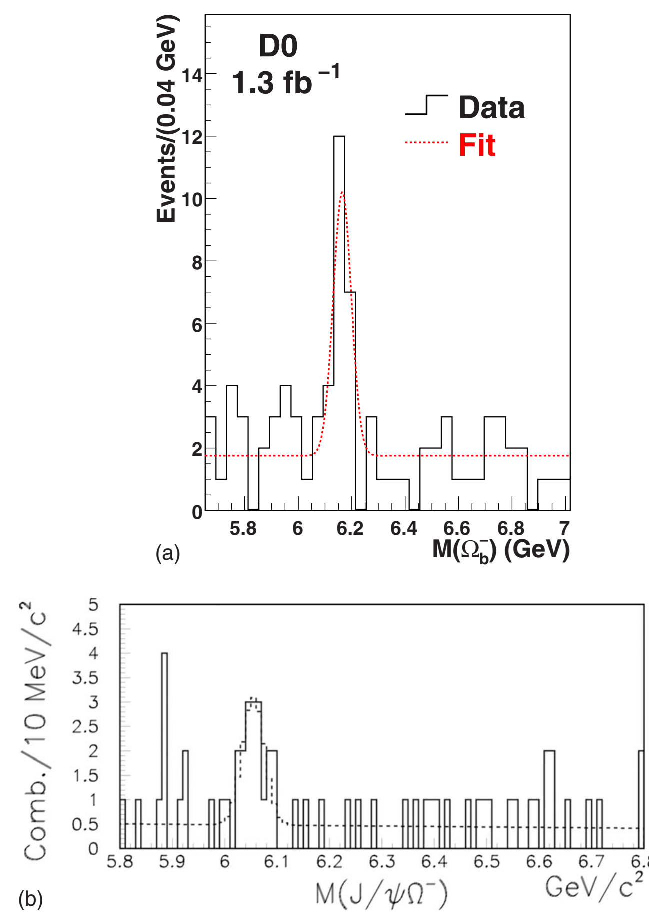

FIG. 12. (Color online) The search for the Ω_b^-. Top: DØ data. The $M(\Omega_b^-)$ distribution of the Ω_b^- candidates after all selection criteria. The dotted curve is an unbinned likelihood fit to the model of a constant background plus a Gaussian signal. From Abazov *et al.*, 2008. Bottom: CDF data. $J/\Psi\Omega^-$ mass distribution. From Aaltonen *et al.*, 2009.

$$M_{\Omega_b} = 6.054 \pm 0.007 \pm 0.013 \text{ GeV}, \tag{10}$$

closer to most theoretical predictions. For the Ω_b^- lifetime, see Table I.

F. A future at LHC

The CDF and DØ experiments have demonstrated the potential of hadron machines for the discovery of new baryon resonances. At LHC, double-charmed baryons should be produced abundantly, a total number of 10^9 is estimated by Berezhnoi *et al.* (1998), and one may even dream of (ccc) baryons. Baryons and mesons with b quarks and their excitations will also be produced; such events should not be thrown away at the trigger level.

III. LIGHT-QUARK BARYON RESONANCES

In this section we give a survey of data which have been reported in recent years and an outline of partial-wave analysis methods used to extract the physical content from the data. The light-baryon excitation spectrum is also discussed.

A. Pion- (kaon-) nucleon elastic and charge exchange scattering

1. Cross sections

The dynamical degrees of freedom of three quarks bound in a baryon lead to a rich excitation spectrum. It is impossible to observe them all as individual resonances but a sufficiently large number of states should be known to identify the proper degrees of freedom and their effective interactions. First insight into the experimental difficulties can be gained by inspecting, in Fig. 13, the total cross section for elastic $\pi^\pm$ scattering off protons. The π^+p cross section is dominated by the well known $\Delta_{3/2^+}(1232)$ resonance. A faint structure appears at 1.7 GeV, slightly better visible in the elastic cross section, a second bump can be identified at 1.9–2 GeV in mass, and a small enhancement is seen at 2.4 GeV. Above this mass, the spectrum becomes structureless. The total cross section for π^-p scattering exhibits three distinctive peaks at the $\Delta_{3/2^+}(1232)$, at 1.5 GeV, and at 1.7 GeV; a fourth enhancement at 1.9 GeV is faint, a further peak at 2.2 GeV leads into the continuum.

The gradual disappearance of the resonant structures suggests that at least part of the problem is due to the increasingly smaller elastic width of resonances when their masses increase: more and more inelastic channels open, and the resonances decouple from the elastic scattering amplitude. A second problem are overlapping resonances and their large widths. The peaks in Fig. 13 may contain several resonances. Hence a partial-wave decomposition is required to determine the amplitudes which contribute to a particular energy bin. Very high statistics and polarization data are required to disentangle the different partial waves. At present, it is an open issue up to which mass baryon resonances can be identified. A second and even more exciting question is whether QCD really supports the full spectrum of three-quark models. In the literature, diquark models are popular; the experimental resonance spectrum has features which are easily understood assuming quasistable diquark configurations within a baryon; however, there are also resonances—albeit with one or two star classification—which require three quarks to participate in the dynamics. Less familiar in this context are two dynamical arguments: an extended object has three axes but the object rotates only around the two axes having minimal or maximal moments of inertia. And, surprisingly, a series of coupled resonators with approximately equal resonance frequencies resonate coherently after some swinging-in period even if the oscillators start with random phases and amplitudes. Hence there may be restrictions concerning the observable spectrum of baryon resonances.

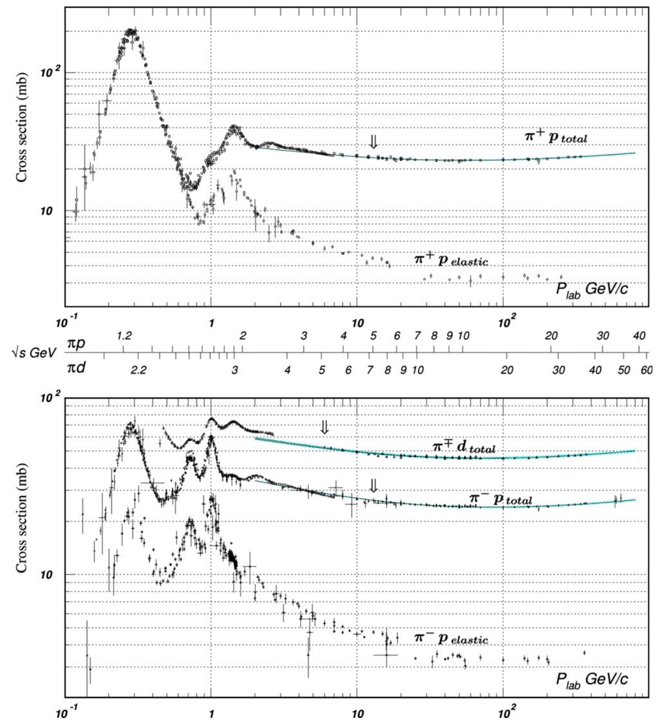

FIG. 13. (Color online) The total and elastic cross sections for $\pi^\pm$ scattering off protons. From http://pdg.lbl.gov/current/xsect/, courtesy of the COMPAS group, IHEP, Protvino.

2. Angular distributions

Most of the peaks in Fig. 13 contain several resonances with similar masses but different angular momenta. The differential cross sections $d\sigma/d\Omega$ in Fig. 14 allow for insight into the dynamics of the scattering process.

The first striking effect seen from the data is the preference for forward angles ($\theta \lesssim 40°$) of the scattered pion. The preference for forward pion scattering at low energies reflects the role of background processes like t-channel exchange with a ρ meson (or a ρ Regge trajec-

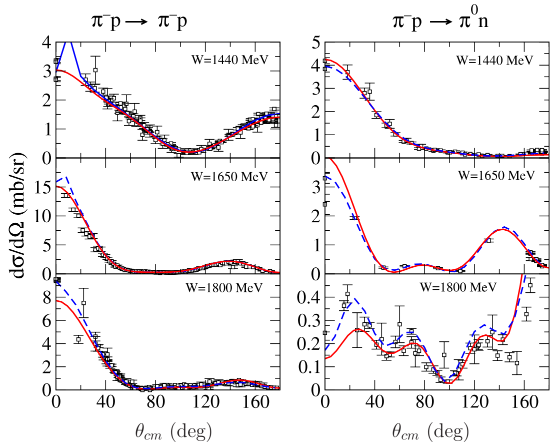

FIG. 14. (Color online) Differential cross section for several different center-of-mass energies. Solid and dashed curves correspond to different SAID (http://gwdac.phys.gwu.edu/ solutions).

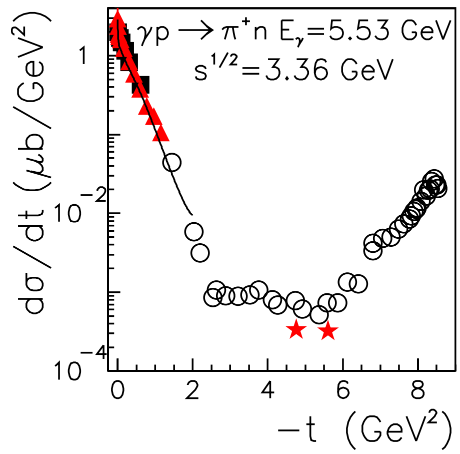

FIG. 16. (Color online) The $\gamma p \to n\pi^+$ differential cross section as a function of $-t$ for E_γ=5.53 GeV (Sibirtsev *et al.*, 2007). The data are from Anderson *et al.* (1969, 1976) and Zhu *et al.* (2005).

tory) transmitting four-momentum from pion to proton. Formation of resonances produces a symmetry between forward and backward scattering, at least at the amplitude level; interference between amplitudes can of course lead to forward-backward asymmetries. Here it is useful to compare the Clebsch-Gordan coefficients for different reactions,

	$\pi^- p \to \pi^- p$	$\pi^- p \to \pi^0 n$
s,u channel N	2/3	$-\sqrt{2}/3$
s,u channel Δ	1/3	$+\sqrt{2}/3$
t channel ρ	1/2	$1/\sqrt{2}$

The forward cross section for elastic and CEX have nearly the same size and the interpretation of the forward peak is supported. The backward peak at 1440 MeV is stronger in elastic than in charge exchange scattering suggesting strong isospin 1/2 contribution in the s channel [via $N(1440)P_{11}$ formation] and/or u-channel nucleon exchange. At W=1800 MeV, there is no CEX forward peak; a complex distribution evolves, indicating contributions from high-spin s-channel resonances. The elastic cross section continues to exhibit a strong forward peak due to the exchange of isoscalar mesons, e.g., of the Pomeron. The three processes s-, t-, and-u-channel exchange are shown in Fig. 15. The data were obtained through the scattering analysis interactive dial-in (SAID) online applications (http://gwdac.phys.gwu.edu/).

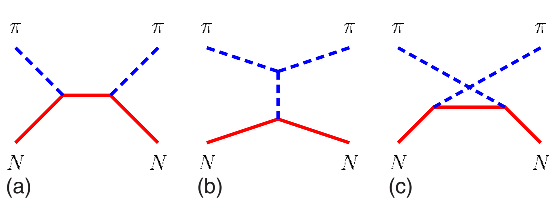

FIG. 15. (Color online) Pion-nucleon scattering: (a) s-channel exchange, (b) t-channel exchange, and (c) u-channel exchange.

An example illustrating the effect of t- and u-channels exchanges is shown in Fig. 16. For forward pions, the four-momentum transfer $t=-q^2$ to the proton is small; a diffractivelike decrease of the cross section as a function of t is observed. The peak is due to meson exchange in the t channel, mostly of ρ and ω; in analyses, the exchange is Reggeized to include higher mass ρ and ω excitations. The slope corresponds to the ρ/ω mass. For very large (negative) $t=-2k^2(1-\cos\theta)$, $u=-2k^2(1+\cos\theta)$ becomes a small number. The slope is smaller and corresponds to the nucleon mass.

The differential cross sections σ are related to the transversity scattering amplitudes

$$\sigma = |f^+|^2 + |f^-|^2, \tag{11}$$

which can be decomposed into the nucleon spin-flip amplitude g and the nonflip amplitude h, $f^+=g+ih$, $f^-=g-ih$. The latter amplitudes can be expanded into the partial waves

$$g(k,\theta) = \frac{1}{k}\sum_l [(l+1)a_{l^+} + l a_{l^-}]P_l(\cos\theta), \tag{12a}$$

$$h(k,\theta) = \frac{1}{k}\sum_l [a_{l^+} - a_{l^-}]\sin\theta P_l'(\cos\theta), \tag{12b}$$

where k is the momentum and θ is the scattering angle in the center-of-mass system. The expansion into Legendre polynomials extends over all angular momenta l, the $\pm$ sign indicates that the total angular momentum is $J=l\pm 1/2$. The dimensionless partial-wave amplitudes $a_{l\pm}=[\eta_{l\pm}\exp(2i\delta_{l\pm})]/2i$ are related to the inelasticities $\eta_{l\pm}$ and the phase shifts $\delta_{l\pm}$.

It is obvious that the two amplitudes cannot be deduced from the differential cross sections alone. Polarization observables need to be measured. We discuss the polarization P and the two spin rotation parameters A and R.

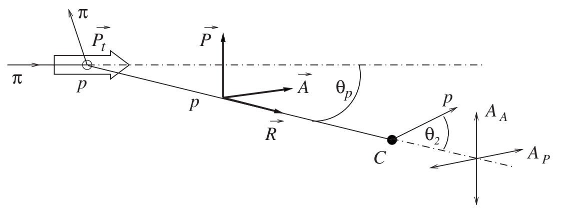

FIG. 17. Definition of polarization variables. From Alekseev *et al.*, 2006.

3. Polarization variables

The polarization variable P can be measured using a polarized target. If the proton polarization vector is parallel to the decay-plane normal, there is, at any laboratory scattering angle θ, a left-right asymmetry of the number of scattered pions which defines P. The polarization of the scattered proton does not need to be known. Thus large data sets exist where P was determined, from Rutherford (Cox *et al.*, 1969; Martin *et al.*, 1975; Brown *et al.*, 1978) and from CERN (Albrow *et al.*, 1970, 1972), among other places. P constrains the amplitudes but does not yet yield a unique solution,

$$P\sigma_{\rm tot} = |f^{+}|^2 - |f^{-}|^2. \tag{13}$$

Further variables need to be measured. Figure 17 shows the definitions of polarization variables which can be deduced in πN elastic scattering off longitudinally polarized protons. The proton is deflected by an angle θ_p in the laboratory system. The proton polarization vector now has a component P which is perpendicular to the scattering plane, a component R along its direction of flight, and a component A along the third orthogonal direction. The components A and P can be measured by scattering the recoil proton off a carbon foil as shown in Fig. 17. The analyzing power of the π carbon scattering process leads to a left-right asymmetry of the proton count rate A_P in the scattering plane; analogously, the A_A parameter can be determined by measuring the up-down asymmetry of proton count rate. The relation between R,A and the scattering amplitudes are given by

$$(R + iA)\sigma_{\rm tot} = f^{+}f^{-}\exp[-i(\theta_{\rm cm} - \theta_p)]. \tag{14}$$

The polarization parameters obey the relation

$$P^2 + A^2 + R^2 = 1. \tag{15}$$

As can been seen from Eqs. (11) and (13), a measurement of the differential cross section and polarization P are not sufficient to reconstruct the complex amplitudes f^{+} and f^{-} but only their absolute values. Recoil polarization data require a secondary interaction of the scattered nucleon. Such experiments have been performed at Gatchina (Alekseev *et al.*, 1991, 1995, 1997, 2000, 2006), at Los Alamos (Mokhtari *et al.*, 1985, 1987; Seftor *et al.*, 1989) and a few other laboratories but only over a limited energy range. An unbiased energy-independent partial-wave analysis is therefore not possible. Constraints from dispersion relations are necessary to extract meaningful partial-wave amplitudes. For baryon masses and widths, the PDG refers mostly to five analyses which we call the reference analyses. Other results are mostly not used to calculate averages.

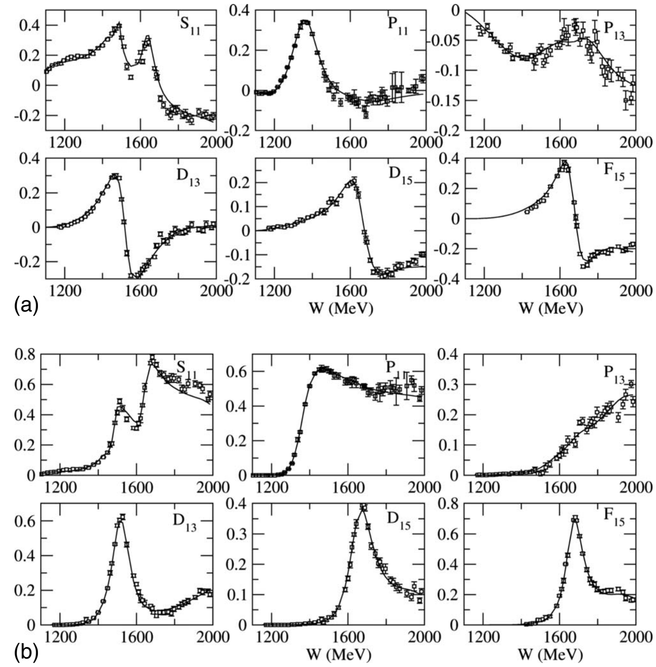

FIG. 18. Fit to the $I=\frac{1}{2}$ Re$(T_{\pi N,\pi N})$ and Im$(T_{\pi N,\pi N})$ of SAID (http://gwdac.phys.gwu.edu/).

The analyses of the Karlsruhe-Helsinki (KH) and Carnegie-Mellon (CM) groups were published in 1979 and 1980, respectively; still today, they contain the largest body of our knowledge on N^* and Δ^* as listed by the PDG. The Kent group made a systematic study of the inelastic reactions $\pi N \to N\pi\pi$. Hendry presented data taken on elastic πN scattering at 14 momenta in the range from 1.6 to 10 GeV and extracted resonance contributions. The Virginia Tech Partial-Wave Analysis Facility (SAID) (which moved to the George Washington University ten years ago) included more data on πN scattering, in particular from Gatchina, Los Alamos, PSI, and TRIUMF, and publishes regularly updated solutions. In a first step, energy-independent partial-wave amplitudes are constructed, and then energy-dependent partial-wave fits are performed using a coupled-channel Chew-Mandelstam K matrix. The results may not yet satisfy all of the requirements imposed by analyticity and crossing symmetry. These requirements are then addressed at fixed four-momentum transfer t by a complete set of fixed-t dispersion relations, which are handled iteratively with the data fitting. Figure 18 shows the reconstructed amplitudes for some partial waves.

4. *K*-nucleon elastic scattering

Kaon-nucleon scattering remains at a standstill since 1980; a survey of achievements up to 1980 was presented by Gopal (1980). For this reason, we do not elaborate on hyperon spectroscopy in this review. We mention a few recent results from a low-momentum kaon beam at

BNL in which differential and total cross sections and the induced hyperon polarization have been measured.

B. Inelastic pion and kaon nucleon scattering and other reactions

Inelastic reactions like $\pi^- p \to n\pi^+\pi^-$ and $\pi^- p \to p\pi^0\pi^-$ and similar kaon-induced reactions require large solid-angle coverage of the detector. The Large Aperture Superconducting Solenoid (LASS) spectrometer at SLAC was the last experiment having an intense 11 GeV/c kaon beam at its disposal. The main results are reviewed by Aston *et al.* (1990). The experiment had a significant impact on the spectroscopy of mesons with open or hidden strangeness. At that time the focus of the community was on glueballs and hybrids, and the LASS data were important as reference guide for quarkonium states. The data contained information on strange baryons as well (Wright *et al.*, 1995). Lack of interest and shortage of manpower prevented an analysis of this unique data set. Only evidence for one baryon resonance was reported, an Ω^* at 2474 ± 12 MeV mass and 72 ± 33 MeV width (Aston *et al.*, 1988), in its $\Omega\pi^+\pi^-$ decay.

The absence of appropriate beams and detectors gave a long scientific lifetime to results obtained by the use of bubble chambers in the sixties and seventieth. The most important results were reviewed by Manley *et al.* (1984), who fitted data and provided amplitudes for the most important isobars. At low energies, data were recorded by the OMICRON Collaboration at the CERN synchrocyclotron (Kernel *et al.*, 1989a, 1989b, 1990) and TRIMF and Los Alamos (Lowe *et al.*, 1991; Sevior *et al.*, 1991; Pocanic *et al.*, 1994).

1. Experiments at BNL

The Crystal Ball detector has an animated history. It started operation in 1978 at SPEAR with studies of radiative transitions between charmonium states (Gaiser *et al.*, 1986). In 1982 it was moved to DESY for spectroscopy of the Υ family and two-photon physics (Bienlein and Bloom, 1981). In the late 1990s it was transferred to BNL where it was exposed to π^- and K^- beams, and is presently installed at MAMI for photoproduction experiments (see Sec. III.C). The ball consists of 672 NaI detectors covering $\approx 94\%$ of 4π. The main results from BNL will be summarized in this section.

a. $\pi^- p \to n\pi^0$ and $n\eta$

The Crystal Ball Collaboration measured the reaction $\pi^- p \to n\eta$ from threshold to 747 MeV/c pion momentum (Kozlenko *et al.*, 2003; Prakhov *et al.*, 2005) (see Fig. 19). Angular distributions with nearly full angular coverage were reported for seven π^- momenta. The total cross section $d\sigma_{\mathrm{tot}}$ was obtained by integration of $d\sigma/d\Omega$. The rapid increase of the cross section and the rather flat angular distributions indicate that $N_{1/2^-}(1535)$ is formed as an intermediate state. A small quadratic term reveals contributions from the $N\eta$ D wave due to $N_{3/2^-}(1520)$ (Arndt *et al.*, 2003a; Arndt, Briscoe, Morrison, *et al.*, 2005). The effect of the η production threshold can be seen in pion charge exchange $\pi^- p \to n\pi^0$ (Starostin *et al.*, 2005) in the form of a small cusp. For the latter reaction, the Crystal Ball Collaboration measured precise differential cross section in the momentum interval $p_\pi = 649 - 752$ MeV/c. The cusp is rather weak and not as dramatic as in pion photoproduction. The Δ region was studied with full solid angle coverage using eight different momenta (Sadler *et al.*, 2004).

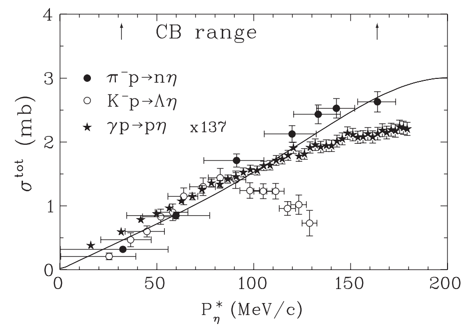

FIG. 19. Total cross section for $\pi^- p \to n\eta$, $K^- p \to \Lambda\eta$, and $\gamma p \to p\eta$. The later cross section is scaled by a factor of 137. From Prakhov *et al.*, 2005.

b. $K^- p \to \Lambda\pi^0$, $\Sigma^0\pi^0$, and $\Lambda\eta$

The reaction $K^- p \to \Lambda\pi^0$ was studied in the mass range from 1565 to 1600 MeV (Olmsted *et al.*, 2004). Differential cross sections and induced Λ polarization were reported for three K^- momenta. The data were shown to be incompatible with the claimed existence of $\Sigma_{3/2^-}(1580)$, a one-star candidate with properties not fitting into expectations based on $SU(3)_f$ symmetry. An interpretation of the hyperon spectrum including this state is proposed by Melde *et al.* (2008).

Differential distributions and hyperon recoil polarization were also reported for the reaction $K^- p \to \Sigma^0\pi^0$ at eight beam momenta between 514 and 750 MeV/c. The forthcoming partial-wave analysis could have a significant impact on low-mass Λ states (Manweiler *et al.*, 2008).

Particularly interesting is the reaction $K^- p \to \Lambda\eta$ (Manley *et al.*, 2002). The cross section rises steeply from threshold and reaches a maximum of about 1.4 mb at $W \sim 1.675$ GeV/c^2. The data show a remarkable similarity to the $SU(3)_f$ flavor-related $\pi^- p \to p\eta$ cross section. The latter is dominated by $N_{1/2^-}(1535)$, the former by formation of the intermediate $\Lambda_{1/2^-}(1670)$ state, for which mass and width, of $M = 1673 \pm 2$ MeV, $\Gamma = 23 \pm 6$ MeV, respectively, and an elasticity $x = 0.37 \pm 0.07$ were measured. The fraction with which $\Lambda_{1/2^-}(1670)$ decays to $\Lambda\eta$ is determined to $(16 \pm 6)\%$. Resonance parameters and decay modes were found in good agreement with the quark-model predictions of Koniuk and Isgur (1980a) but disagree with the results of an analysis using a Bethe-Salpeter coupled-channel for-

TABLE XI. Decay branching ratios to baryon plus η of spin-1/2 negative-parity baryons.

Decay mode	Fraction	Decay mode	Fraction
$N_{1/2^-}(1535)\to N\eta$	45–60 %	$N_{1/2^-}(1650)\to N\eta$	3–10 %
$\Lambda_{1/2^-}(1670)\to \Lambda\eta$	10–25 %	$\Lambda_{1/2^-}(1800)\to \Lambda\eta$	not seen
$\Sigma_{1/2^-}(1620)\to \Sigma\eta$	not seen	$\Sigma_{1/2^-}(1750)\to \Sigma\eta$	15–55 %

malism incorporating chiral symmetry (García-Recio *et al.*, 2003). The latter analysis finds a $\Lambda\eta$ decay fraction of $(68\pm1)\%$ and an inelasticity of $(24\pm1)\%$.

In both cases, the branching ratio of $\Lambda_{1/2^-}(1670)$ for decays into $\Lambda\eta$ is much larger than that of other resonances. In Table XI we list the branching ratios of negative-parity spin-1/2 resonances for decays into η mesons. We notice that for $N_{1/2^-}$ the lower mass state (mainly $S=1/2$) has a strong coupling the $N\eta$ while it is smaller by about one order of magnitude for the higher-mass state (mainly $s=3/2$). The situation is similar for $\Lambda_{1/2^-}$ but opposite for $\Sigma_{1/2^-}$. We note that in $\Lambda_{1/2^-}$ the ud diquark has isospin zero while for $\Sigma_{1/2^-}$ $I=1$. The connection is not yet understood.

c. $\pi^-p\to n2\pi^0$, $K^-p\to\Lambda2\pi^0$ and to $\Sigma2\pi^0$

Three reactions leading to $2\pi^0$ in the final state were studied; $\pi^-p\to n2\pi^0$ from threshold to 750 MeV/c (Craig *et al.*, 2003; Prakhov *et al.*, 2004b), $K^-p\to\pi^0\pi^0\Lambda$ and $K^-p\to\pi^0\pi^0\Sigma^0$ for $pK^-=514$ to 750 MeV/c (Prakhov *et al.*, 2004a, 2004c). The cross sections for the three reactions reveal a few interesting patterns (Nefkens *et al.*, 2002); see Fig. 20. The cross section for $K^-p\to\Lambda2\pi^0$ is smaller than that for $\pi^-p\to n2\pi^0$ by a factor of 2. A reduction due to strangeness production is not unexpected. But the cross section for $K^-p\to\Sigma2\pi^0$ is much smaller than the other ones. This requires a dynamical interpretation.

If the reactions would produce $\sigma\,[=f_0(600)]$ at a sizable rate, one should expect similar cross sections for all

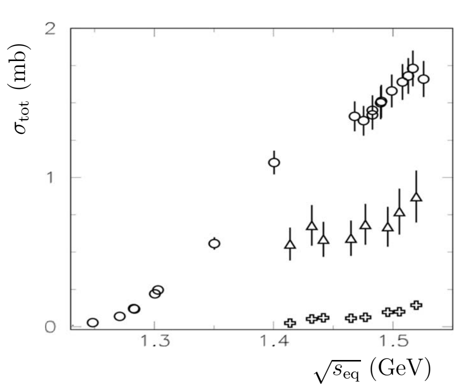

FIG. 20. The total cross sections as functions of the equivalent total energy $\sqrt{s_{\rm eq}}$, defined as the standard s for pions and as $\sqrt{s_{\rm eq}}\equiv\sqrt{s}-(m_s-m_d)$ for incident kaons (Nefkens *et al.*, 2002). Circles: $\sigma_{\rm tot}(\pi^-p\to\pi^0\pi^0n)$. Triangles: $\sigma_{\rm tot}(K^-p\to\pi^0\pi^0\Lambda)$. Crosses: $\sigma_{\rm tot}(K^-p\to\pi^0\pi^0\Sigma^0)$.

TABLE XII. J/ψ and ψ' branching ratios for decays into final states containing mesons and baryons.

	J/ψ		ψ'	
$N\bar{N}\pi$	(9.7 ± 0.6)	10^{-3}	(7.6 ± 0.6)	10^{-4}
$p\bar{p}\pi^+\pi^-$	(6.0 ± 0.5)	10^{-3}	(7.6 ± 0.6)	10^{-4}
$N\bar{N}\eta$	(4.18 ± 0.36)	10^{-3}	(0.58 ± 0.13)	10^{-4}
$\Lambda\bar{\Lambda}\eta$	(0.26 ± 0.08)	10^{-3}	<1.2	10^{-4}
$pK^-\bar{\Lambda}$	(0.9 ± 0.2)	10^{-3}		
$pK^-\bar{\Sigma}^0$	(0.29 ± 0.08)	10^{-3}		
$\Sigma\bar{\Lambda}\pi$	(0.23 ± 0.03)	10^{-3}		

three reactions. This is not the case; at least the two reactions $\pi^-p\to n2\pi^0$ and $K^-p\to\Lambda2\pi^0$ must be dominated by production of baryon resonances. A partial-wave analysis of the former data revealed a large contribution of $N_{1/2^+}(1440)$ interfering with $N_{1/2^-}(1535)$ and $N_{3/2^-}(1520)$ (Sarantsev *et al.*, 2008), where $N_{1/2^+}(1440)$ decays via $\Delta\pi$ and via $N\sigma$. The broad shoulder in the $K^-p\to\Lambda2\pi^0$ cross section is tentatively interpreted as evidence for $\Lambda_{1/2^+}(1600)$ decaying via $\Sigma^0_{3/2^+}(1385)\pi^0$ as intermediate state (Prakhov *et al.*, 2004c). A partial-wave analysis of the data has not been performed.

2. Baryon excitations from J/ψ and ψ' decays

Baryon resonances can be searched for in final states from J/ψ and ψ' decays into a baryon, an antibaryon, and at least one meson. In Table XII, relevant branching fractions are given, demonstrating the discovery potential of J/ψ decays for baryon spectroscopy. In particular resonances recoiling against Λ, Σ, $\Sigma_{3/2^+}(1385)$, Ξ, $\Xi_{3/2^+}(1530)$ are rewarding. In other reactions, there is no real means to decide if $\Sigma_{1/2^-}(1750)$ belongs to an SU(3)$_f$ octet or decuplet, or if it is a mixture. Observation of $\Sigma_{1/2^-}(1750)$ recoiling against Σ and/or $\Sigma_{3/2^+}(1385)$ in ψ' decays would identify its SU(3)$_f$ nature.

As example for the use of J/ψ decays in baryon spectroscopy we show in Fig. 21 the Dalitz plot $M^2_{n\pi}$ vs $M^2_{p\pi}$ for $J/\psi\to p\pi^-\bar{n}$ decays, and the $p\pi^-$ mass projection (Ablikim *et al.*, 2006). Four peaks can be identified. A partial-wave analysis (Li *et al.*, 2009) assigns the first

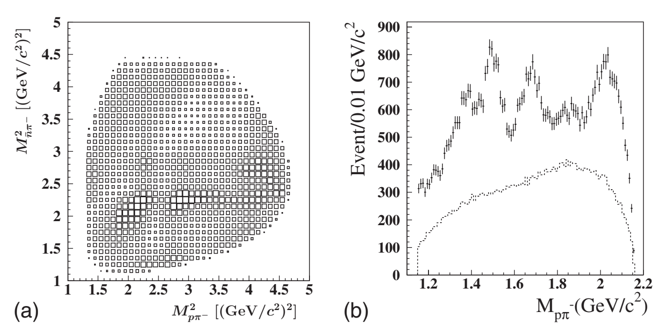

FIG. 21. Dalitz plots of $M^2_{n\pi}$ vs $M^2_{p\pi}$ for $J/\psi\to p\pi^-\bar{n}$ and $p\pi^-$ invariant mass spectrum. From Li *et al.*, 2009.

peak to $N(1440)P_{11}$ with Breit-Wigner mass and width of $1358\pm6\pm16$ MeV and $179\pm26\pm50$ MeV; the N^* peaks at 1500 and 1670 MeV are identified with the well-known second and third resonance regions, and the fourth peak is interpreted as a new N^* resonance with $2040^{+3}_{-4}\pm25$ MeV mass and width of $230\pm8\pm52$ MeV. The fit prefers P_{13} quantum numbers.

C. Photoproduction experiments, a survey

1. Aims of photoproduction experiments

a. How many baryon resonances are known?

Baryon spectroscopy defined by πN elastic scattering is at a bifurcation point. The listings of the PDG give a large number of baryon resonances which were reported by the analyses of the Karlsruhe-Helsinki group (Höhler *et al.*, 1979) and the Carnegie-Mellon group (Cutkosky *et al.*, 1980), with ratings from one-star to four-stars. In the most recent analysis of the George Washington (GWU) group (Arndt *et al.*, 2006) including a large number of additional data sets from pion factories (even though mostly at low energy), practically only the four-star resonances are confirmed. A decisive question is therefore if Höhler is right in his critique of the GWU analysis that the method used by the GWU group suppresses weak higher-mass resonances (Höhler, 2004). The confirmation of a few resonances found by Höhler *et al.* (1979) and Cutkosky *et al.* (1980) and questioned by Arndt *et al.* (2006) would already help to give credit to the old analyses.

b. How many baryon resonances are expected?

Quark models predict a large number of baryon resonances. Experimentally, the density of states in the mass region above 1.8 GeV is much smaller than expected. A reason might be (Koniuk and Isgur, 1980b) that these *missing resonances* decouple from the πN channel. Then they escape detection in πN elastic scattering. These resonances are expected to have no anomalously low helicity amplitudes; then they must show up in photoproduction of multiparticle final states.

c. What is the structure of baryon resonances?

Electroproduction of baryon resonances provides additional information, inaccessible to πN scattering. Helicity amplitudes, form factors, and generalized polarizabilities can be extracted. Intense experimental and theoretical efforts have been devoted to determinations of the E_2/M_1 (electric quadrupole versus magnetic dipole) and C_2/M_1 (longitudinal electric quadrupole versus magnetic dipole) ratio for the $N\to\Delta(1232)$ transition amplitude. For a review of the hadron structure at low Q^2, see Drechsel and Walcher (2008).

2. Experimental facilities

a. Bubble chambers

In the late 1960s, photoproduction was studied in bubble chamber experiments. Results at DESY were summarized by Erbe *et al.* (1968), and those from SLAC by Ballam *et al.* (1972, 1973).

b. NINA

The electron synchrotron NINA at Daresbury was used to study photoproduction reactions. We quote here only two of their late publications (Barber *et al.*, 1982, 1984), where references to earlier work can be found.

c. Bonn synchroton

In Bonn, a 2.5 GeV electron synchrotron started operation in 1967 and was used for photoproduction experiments. The latest publication reported on production of positive pions at large angles (Dannhausen *et al.*, 2001). The accelerator is now used to feed ELSA.

d. ELSA

The electron stretcher ring ELSA, in operation since 1987, serves either as storage ring producing synchrotron radiation or as postaccelerator and pulse stretcher delivering a continuous electron beam (1 nA, duty factor $\approx$70%) with up to 3.5 GeV energy. A few detectors were installed at ELSA: PHOENICS (Bock *et al.*, 1998), ELAN (Kalleicher *et al.*, 1997), GDH (Naumann *et al.*, 2003), SAPHIR, and CBELSA in different configurations. SAPHIR was a magnetic detector with a central drift chamber (CDC), with a magnetic field perpendicular to the beam axis and the target placed in the center of the CDC. Forward hodoscopes in coincidence with the tagging system gave a fast trigger and provided particle identification by measuring the time of flight (Schwille *et al.*, 1994). It was dismantled in 1999. The CBELSA experiment is based on the 4π photon detector Crystal Barrel (Aker *et al.*, 1992), which had been moved in 1997 from LEAR CERN to Bonn. An inner scintillating fiber detector is used for charged-particle detection and trigger purposes (van Pee *et al.*, 2007). Later, the forward direction was covered (Elsner *et al.*, 2007) by the TAPS (Gabler *et al.*, 1994) or a MiniTaps detector.

e. Jlab

The continuous electron beam accelerator facility at the Department of Energy's Thomas Jefferson National Accelerator Facility (Jlab) delivers a 6 GeV primary electron beam into three different experimental areas, Halls A, B, and C, for simultaneous experiments. Halls A and C both have two spectrometers; in Hall A, two identical high-resolution spectrometer covering a maximum momentum of 4 GeV/c are installed, while in Hall C one is dedicated to analyze high-momentum particles, the other has a short path length for the detection of decay particles. Hall B houses the Jlab Large Acceptance Spectrometer (CLAS), the detector most relevant for baryon spectroscopy. The CLAS detector is based on a six-coil toroidal magnet which provides a largely azimuthal field distribution. Particle trajectories are reconstructed, using drift chambers, with a momentum resolution of 0.5% at forward angles. Cherenkov counters, time-of-flight scintillators, and electromagnetic calorimeters provide good particle identification (Mecking *et al.*, 2003).

f. ESFR

The GRAAL experiment was installed at the European Synchrotron Radiation Facility (ESRF) in Grenoble (France). The tagged and polarized γ-ray beam was produced by Compton scattering of laser photons off the 6 GeV electrons circulating in the storage ring. The shortest UV wavelength of 351 nm yielded a maximal γ-ray energy of 1.5 GeV. The tagging system used 128 silicon microstrips with a pitch of 300 μm. The proton track was measured by two cylindrical multiwire proportional chambers with striped cathodes and two forward planar chambers. Charged particles were identified by dE/dx and time-of-flight measurement. Photons coming from neutral decay channels of π^0 and η were detected in 480 21-radiation-lengths BGO crystals supplemented by a lead-scintillator sandwich time-of-flight wall in the forward direction (Bartalini *et al.*, 2005).

g. SPring-8

The LEPS (laser electron photons at SPring-8) detector uses backscattered photons from the 8 GeV stored electron beam producing a tagged γ-ray beam of up to 2.4 GeV. The LEPS spectrometer consists of a wide-gap dipole magnet with charged-particle tracking detectors. An array of scintillator bars 4 m downstream of target and scintillators just behind the target provided a time-of-flight information. Electron-positron pairs are vetoed by an aerogel Cherenkov detector.

h. MAMI

The electron accelerator MAMI consists of three cascaded racetrack microtrons and a harmonic double-sided microtron for final acceleration (Blomqvist *et al.*, 1998). A linear accelerator provides a 4 MeV beam with the racetrack microtrons of 15, 180, and 855 MeV, respectively. The maximum energy at the end of the new fifth stage is 1.5 GeV, with a beam current of up to 100 μA. Photons can be provided with linear or circular polarization. The development of a polarized target is finalized.

A major installation for baryon spectroscopy is the Crystal Ball detector (see *Experiments at BNL* in Sec. III.B). The detector capabilities are strengthened by a forward-wall TAPS consisting of 510 hexagonally shaped BaF_2 detectors.

3. Total cross sections for photoinduced reactions

The total photoabsorption cross section shown in Fig. 22 exhibits a large peak ($\approx$500 μb) due to $\Delta(1232)$ production, shows some structures in the second and third resonance regions, and levels off at about 150 μb at a few GeV. At very high energies, the photon splits into a $q\bar{q}$ pair with vector-meson quantum numbers and the interaction between proton and photon is dominated by Pomeron exchange exhibiting the typical relativistic rise in the multi-GeV energy range. The structure of the photon and its interaction with protons, a central issue at H1 and ZEUS, is beyond the scope of this article; see the review by Butterworth and Wing (2005).

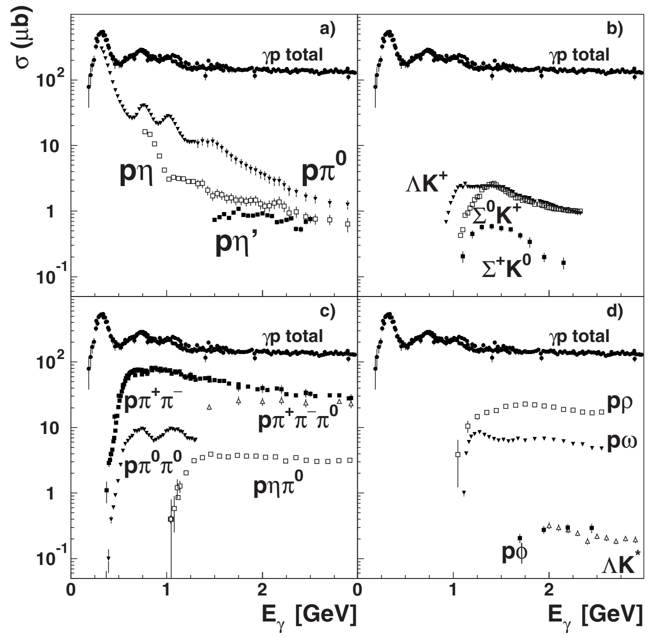

FIG. 22. Total photoabsorption cross section and exclusive cross sections for single-meson and multimeson production. (a) Total, $p\pi^0$, $p\eta$, $p\eta'$; (b) total, ΛK^+, Σ^0K^+, Σ^+K^0; (c) $p\rho$, $p\omega$, $p\phi$, ΛK^{*+}, Σ^+K^{*0}, Σ^0K^{*+}; (d) $p\pi^+\pi^-$, $p\pi^0\pi^0$, $p\pi^0\eta$, $p\pi^+\pi^-\pi^0$, pK^+K^-.

4. The GDH sum rule

The photoproduction cross section depends on the helicity of proton and photon. The total helicity may be 3/2 or 1/2; the fractional difference

$$E = \frac{\sigma_{3/2} - \sigma_{3/2}}{\sigma_{3/2} + \sigma_{3/2}} \tag{16}$$

is an important quantity. Such measurements require circularly polarized photons and a target of polarized protons.

The development of techniques to produce polarized targets and photons has a long history. The most recent driving force for this development was the chance to test the Gerasimov-Drell-Hearn sum rule (Drell and Hearn, 1966; Gerasimov, 1966)

$$\int_0^\infty \frac{dE_\gamma}{E_\gamma}[\sigma_{3/2}(E_\gamma) - \sigma_{1/2}(E_\gamma)] = \frac{2\pi^2\alpha}{M_p^2}\kappa_p^2, \tag{17}$$

which relates the integrated helicity-difference cross section to the anomalous magnetic moment κ_p.

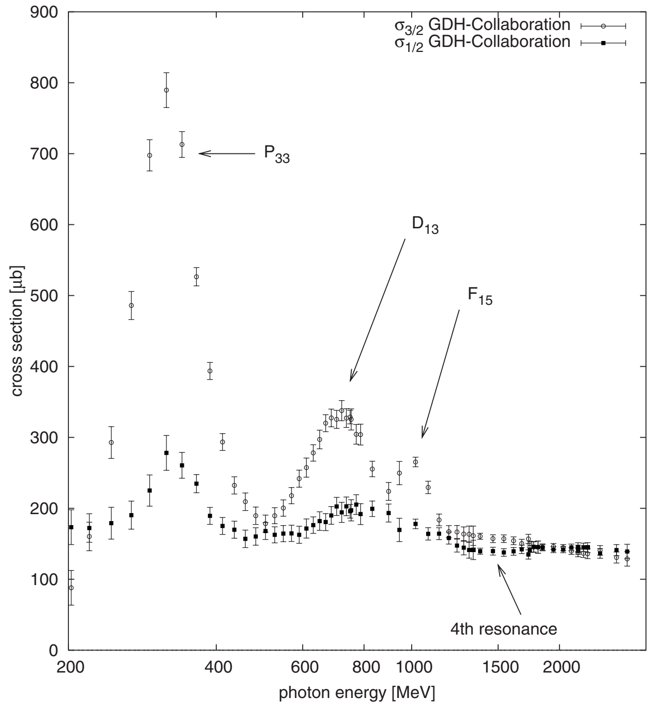

FIG. 23. Separate helicity state total cross sections $\sigma_{3/2}$ and $\sigma_{1/2}$ of the proton (Ahrens *et al.*, 2000, 2001, 2006a; Dutz *et al.*, 2003).

Figure 23 shows the separate helicity contributions to the total cross section, measured at ELSA (Dutz *et al.*, 2003) and MAMI (Ahrens *et al.*, 2000, 2001, 2006a). Most of the resonance strength of the first three resonances originates from the 3/2 helicity channel. The integrated difference, weighted with $1/E_\gamma$, needs to be corrected for the unmeasured regions. The low-energy part can be estimated using Mainz analysis interactive dial-in (MAID) predictions, with the integral from 2.9 GeV up to ∞ using deep inelastic scattering data. Comparison of the calculated 205 μb and measured $212\pm6\pm16$ μb value shows remarkable agreement (Helbing, 2006).

First measurements of the helicity difference on exclusive final states have been published recently (Ahrens *et al.*, 2006b, 2007); these measurements provide an important input to partial-wave analyses.

D. Photoproduction of pseudoscalar mesons

1. Polarization observables

The differential cross section for electroproduction of pseudoscalar mesons off nucleons is given by the product of the flux of the virtual photon field—with longitudinal (L) and transverse (T) polarization—and the virtual differential cross section, which depends on six response functions ($R_i{=}R_T,R_L,R_{TL},R_{TT},R_{TL'},R_{TT'}$). The response functions depend on two additional indices characterizing the target polarization and the recoil polarization of the final-state baryon. The response functions can be written as CGNL (Chew, Goldberger, Low, and Nambu, 1957) or helicity amplitudes. The formalism is tedious; a derivation of formulas and a comprehensive compendium of the relations between the different schemes can be found in Knöchlein *et al.* (1995). In photoproduction, the longitudinal component of the photon polarization vector vanishes, and the problem is easier to handle. From the four CGNL amplitudes, *sixteen* bilinear products can be formed which define the measurable quantities. The differential cross sections can be divided into three classes, for experiments with polarized photons and polarized target (BT, 18a) and experiments measuring the baryon recoil polarization and using either polarized photons (BR, 18b) or a polarized target (TR, 18c),

$$\begin{aligned}\sigma = \sigma_0\{&1 - p_\perp\Sigma\cos 2\varphi + t_x(-p_\perp H\sin 2\varphi + p_\odot F)\\ &- t_y(-T + p_\perp P\cos 2\varphi) - t_z(-p_\perp G\sin 2\varphi\\ &+ p_\odot E)\},\end{aligned} \tag{18a}$$

$$\begin{aligned}\sigma = \sigma_0\{&1 - p_\perp\Sigma\cos 2\varphi + \sigma_{x'}(-p_\perp O_{x'}\sin 2\varphi - p_\odot C_{x'})\\ &- \sigma_{y'}(-P + p_\perp T\cos 2\varphi) - \sigma_{z'}(p_\perp O_{z'}\sin 2\varphi\\ &+ P_\odot C_{z'})\},\end{aligned} \tag{18b}$$

$$\begin{aligned}\sigma = \sigma_0\{&1 + \sigma_{y'}P + t_x(\sigma_{x'}T_{x'} + \sigma_{z'}T_{z'}) + t_y(T + \sigma_{y'}\Sigma)\\ &- t_z(\sigma_{x'}L_{x'} - \sigma_{z'}L_{z'})\}.\end{aligned} \tag{18c}$$

We use $\sigma{=}2\rho_f d\sigma/d\Omega$, where ρ_f denotes the density matrix for the final state baryon, σ_0 the unpolarized differential cross section, $p_\perp$ the degree of linear photon polarization, and φ the angle between photon polarization vector and reaction plane, and $p_\odot$ the circular photon polarization. The target polarization vector is represented by (t_x,t_y,t_z) with z chosen as photon beam direction and y as normal of the reaction plane. The Pauli matrices $(\sigma'_x,\sigma'_y,\sigma'_z)$ referring to the recoiling baryon are defined in a frame with the momentum vector of the outgoing meson as the z' axis and where the y' axis is the same as the y axis. The x and x' axes are defined by orthogonality.

The quantities defined by capital letters (and, of course, the differential cross section σ_0) are those to be determined. Some have traditional names; we mention the beam and target asymmetries Σ and T, the recoil polarization P, and the helicity difference of the cross section $E\sigma{=}\sigma_{1/2}{-}\sigma_{3/2}$. The spin correlation coefficients $C_{x'},C_{z'}$ $(L_{x'},L_{z'})$ define the transfer of circular (oblique) polarization to a recoiling baryon.

Not all 16 observables need to be measured to arrive at a unique solution (up to an overall phase); relations between the observables reduce the number of required experiments. Seven appropriately chosen experiments can be sufficient but may lead to discrete ambiguities of the solution. Hence a minimum of up to eight functions need to be measured (Barker *et al.*, 1975; Chiang and Tabakin, 1997). The minimum contains experiments with polarization of photons, target, and recoiling baryon. This number may be smaller due to inequalities among observables (Artru *et al.*, 2009). If $|A|^2+|B|^2 \leqslant 1$, and if a first measurement gives $A \approx -1$, then a measurement of B is not anymore needed.

A set of data which allows for an energy-independent full reconstruction of the amplitude is commonly referred to as a "complete" experiment. Of course, a complete experiment requires the measurement of isospin related channels, and it remains open if the goal can be reached in practice (Workman, 1999).

2. Photoproduction of pions

The structures observed in the total photoabsorption cross section are much more pronounced in single-π^0 photoproduction [Fig. 22(a)]; the cross section reaches 400 μb at the $\Delta(1232)$ position, 40 μb at the second, and 26 μb at the third resonance peak. There are indications for the fourth resonance region; then, the cross section decreases rapidly. The cross section for π^0 production has been derived by integration over differential cross sections $d\sigma/d\cos\theta$, where θ is the angle of the π^0 meson with respect to the direction of the photon in the γp rest frame. Most recent data from Jlab (Dugger *et al.*, 2007) and ELSA (Bartholomy *et al.*, 2005; van Pee *et al.*, 2007) cover a large energy and angular range. References to earlier data are listed in van Pee *et al.* (2007). The agreement between the data is remarkable; at high energy, small discrepancies in the forward direction show up between the ELSA data (which are shown in Fig. 24) and the Jlab data. The Crystal Barrel Collaboration has new data in the extreme forward angle which will hopefully resolve this discrepancy.

The beam asymmetry is available from MAMI in the low-energy region (Beck, 2006) (shown in Fig. 25), from GRAAL (Bartalini *et al.*, 2005) and from ELSA (Elsner *et al.*, 2009). Some data on target and proton recoil polarization and a few data on double polarization can be found at the GWU Data Analysis Center (http://gwdac.phys.gwu.edu/). Data on the related reaction $\gamma p \to n\pi^+$ for the low-energy region are given in MacCormick *et al.* (1996); angular distributions and beam asymmetry in Bartalini *et al.* (2002). Recently, differential cross sections for $\gamma p \to n\pi^+$ have been measured by the CLAS Collaboration for energies from 0.725 to 2.875 GeV (Dugger *et al.*, 2009). The results are consistent with previously published results. For the photon energies in the range from 1.1 to 5.5 GeV, cross sections for $\gamma n \to p\pi^-$ and $\gamma p \to n\pi^+$ were measured at Jlab (for selected scattering angles) with the aim to test ideas in perturbative QCD (Zhu *et al.*, 2003). Further details and references to earlier data can be found in Zhu *et al.* (2005). The beam asymmetry for photoproduction of neutral pions from quasifree nucleons in a deuteron target was measured with the GRAAL detector for photon energies between 0.60 and 1.50 GeV (Di Salvo *et al.*, 2009). The asymmetries for quasifree protons and quasifree neutrons were found to 0.8 GeV and substantially different at higher energies.

Electroproduction of pions is sensitive to the Q^2 dependence of electromagnetic transition operators and

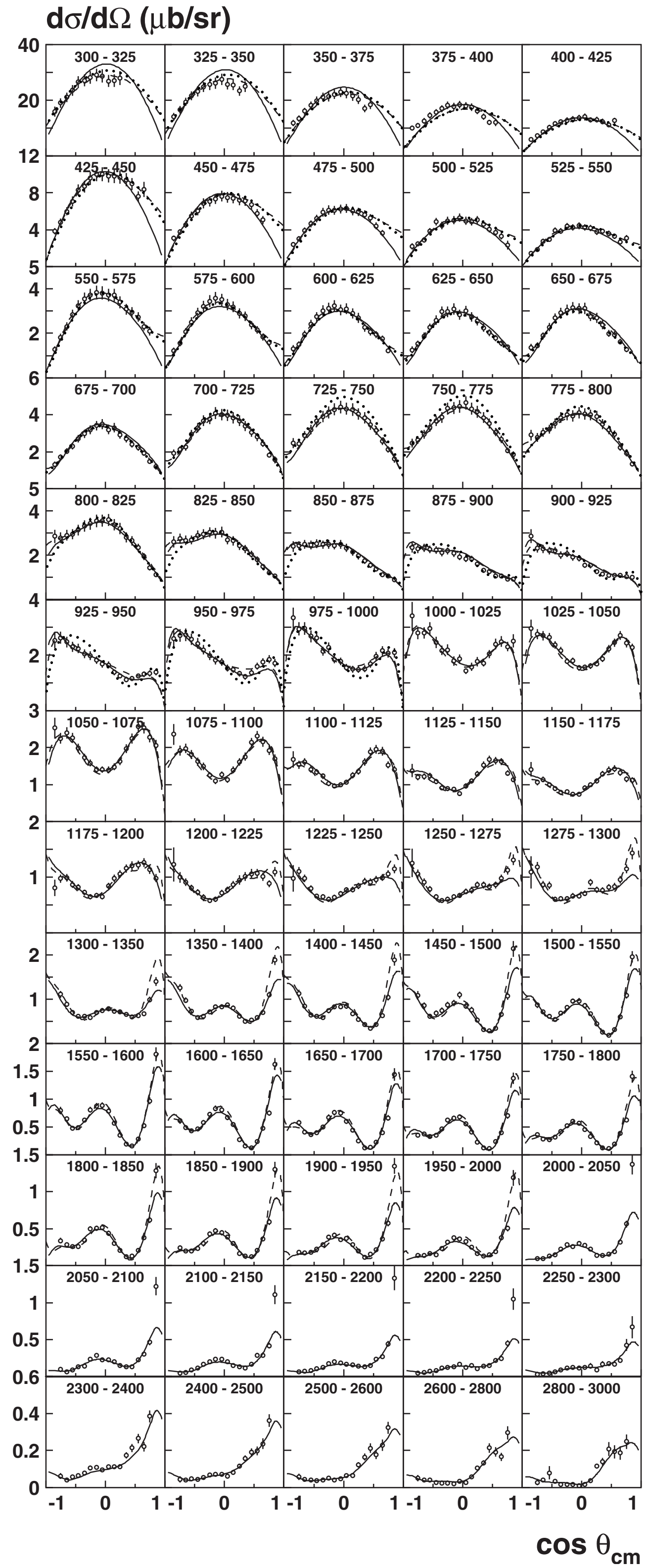

FIG. 24. Differential cross sections for $\gamma p \to p\pi^0$. The solid line represents the BnGa, the dashed line the SAID (SM05), and the dotted line the MAID model.

provides the possibility to determine additional amplitudes; in particular, the interference between real and imaginary amplitudes can be determined. The longitudinal amplitude $L_{l\pm}$ and the scalar amplitude $S_{l\pm}$ are re-

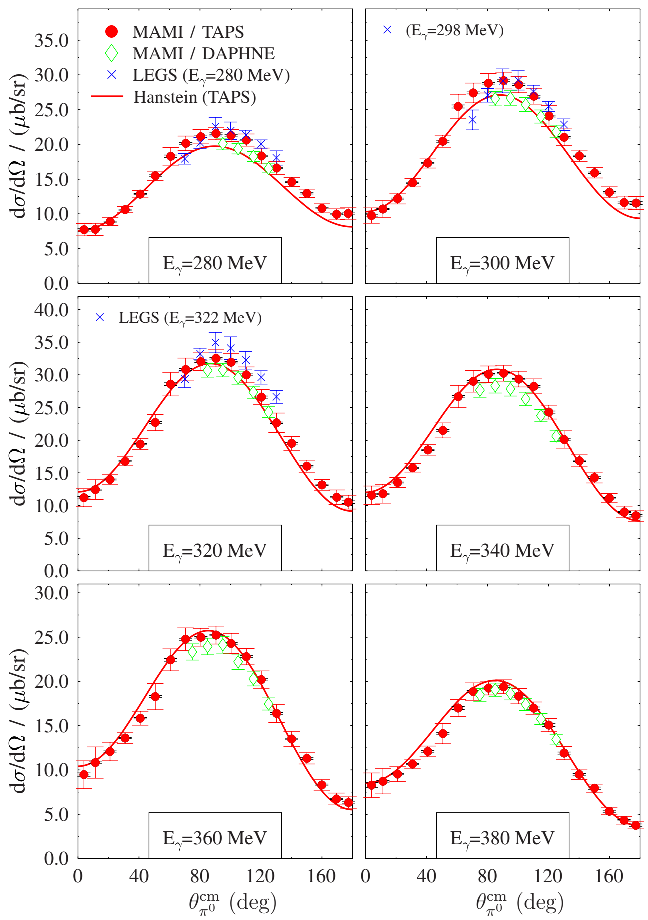

FIG. 25. (Color online) Photon asymmetry Σ in the Δ resonance region for $\gamma p \to p\pi^0$. The solid line is the MAID model. From Beck, 2006.

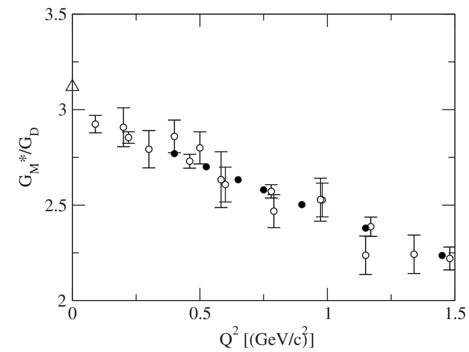

FIG. 26. G_M^* normalized by the dipole factor $G_D=[1+Q^2/0.71\ (\mathrm{GeV}/c)^2]^{-1}$.

lated due to gauge invariance and only $S_{l\pm}$ needs to be determined. The reaction $e^-p \to e^-p\pi^0$ was studied in the Δ region at four-momentum transfers $Q^2=0.2$ (Elsner *et al.*, 2006), 2.8, and 4.0 GeV^2 (Frolov *et al.*, 1999), and the ratios of multipoles S_{0+}/M_{1+}, S_{1+}/M_{1+}, and E_1+/M_{1+} were extracted from decay angular distributions. The related $e^-p \to e^-n\pi^+$ reaction was investigated in the first and second nucleon resonance regions in the $0.25 < Q^2 < 0.65$ GeV^2 range (Joo *et al.*, 2002, 2003, 2005; Egiyan *et al.*, 2006). The data were used by Excited Baryon Analysis Center (EBAC) (Julia-Diaz *et al.*, 2009) to extract the dependence of the helicity amplitudes on the (squared) momentum transfer Q^2, and "dressed form factors" were determined. Figure 26 shows the resulting magnetic transition form factor G_M^* normalized to the conventional dipole form factor for the $N \to \Delta$ transition. The Q^2 dependence serves as fix point for comparison of higher-mass excitations.

At higher invariant masses, electroproduction of single pions can be discussed within the frame of generalized parton distributions or by extending the Regge formalism to high photon virtualities (Avakian *et al.*, 2004; Ungaro *et al.*, 2006; De Masi *et al.*, 2008). Recently, electroproduction of pions was studied using a polarized ($^{15}NH_3$) target. The data, recorded in the first and second nucleon resonance regions in a Q^2 range from 0.187 to 0.770 GeV^2 (Biselli *et al.*, 2008), are expected to place strong constraints on the electrocoupling amplitudes $A_{1/2}$ and $S_{1/2}$ for the $N_{1/2^+}(1440)$, $N_{1/2^-}(1535)$, and $N_{3/2^-}(1520)$ resonances. The CLAS Collaboration also performed a measurement of semi-inclusive π^+ electroproduction in the Q^2 range from 1.4 to 5.7 (GeV$/c)^2$ with broad coverage in all other kinematic variables (Osipenko *et al.*, 2009). The results suggest a similarity between the spectator diquark fragmentation in $\gamma^* p \to n\pi^+$ and the antiquark fragmentation in e^+e^- collisions.

Electroproduction of π^0 mesons in the threshold region, including the π^+ production threshold, was studied at very low Q^2 at MAMI (Weis *et al.*, 2008).

3. Photoproduction of η and η' mesons

The cross section for photoinduced production of η mesons is sizable reaching 16 μb just above its threshold; see Fig. 22(a). The most recent data can be found in Dugger *et al.* (2002), Crede *et al.* (2005), Bartalini *et al.* (2007), and Bartholomy *et al.* (2007). Bartholomy *et al.* (2007) provided a survey of older data. At 1 GeV photon energy, a small dip is observed but otherwise, the cross section does not show any significant structures. (The anomaly in the GRAAL data at 1 GeV does not show up when the angular distributions are fitted with the BnGa amplitudes; hence the anomaly is likely due to the polynomial extrapolation of the angular distribution into an uncovered region.) At E_γ=2 GeV, the η cross section is smaller than the π^0 cross section by a factor of 3. The GRAAL beam asymmetry (Bartalini *et al.*, 2007) is confirmed and extended in range by Elsner *et al.* (2007). Recently, the CLAS (Williams *et al.*, 2009a) and the CB-ELSA/TAPS (Crede *et al.*, 2009) Collaborations reported new data on η and η' photoproduction. In the high-energy region and for forward angles, the CB-ELSA/TAPS cross section is significantly larger than CLAS (Fig. 27). We note that CB-ELSA/TAPS data are based on two fully reconstructed η decay modes; both with very little background and a high detection efficiency.

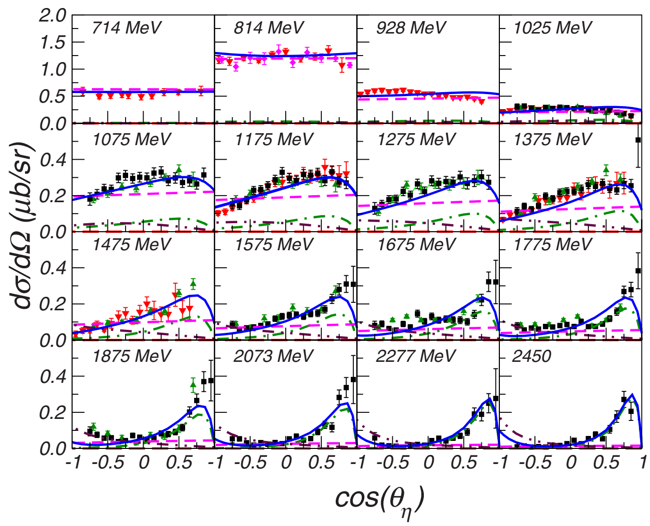

FIG. 27. (Color online) Differential cross sections for the reaction $\gamma p \to p\eta$ from CBELSA (Bartholomy *et al.*, 2007) and CLAS (Dugger *et al.*, 2002) for different invariant masses and fit results (Nakayama *et al.*, 2008). The dashed line represents the S_{11}, the dash-dot-dotted line the D_{13}, and the dash-dotted line the meson-exchange contribution; their sum is given as solid line.

Photoproduction of η mesons off neutrons gives access to the helicity amplitudes $A^n_{1/2}, A^n_{3/2}$ of $N_{1/2^-}(1535)$ coupling to $N\eta$. The reaction has recently attracted considerable additional interest due to the possibility that a narrow $J^P=1/2^+$ nucleon resonance at ≈ 1680 MeV may have been found (Kuznetsov, 2007, 2008). For a more detailed discussion, see Sec. IV.G.1 below. Recently, precise angular distributions (Jaegle *et al.*, 2008) and beam asymmetries (Fantini *et al.*, 2008) have been reported.

Electroproduction of η mesons was reported in Denizli *et al.* (2007) for total center-of-mass energy $W = 1.5$–2.3 GeV and invariant squared momentum transfer $Q^2 = 0.13$–3.3 GeV^2, and photocouplings and ηN coupling strengths of baryon resonances were deduced. A structure was seen at $W \sim 1.7$ GeV. The shape of the differential cross section is indicative of the presence of a P-wave resonance that persists to high Q^2. The data are extended by Dalton *et al.* (2009) to $Q^2 \sim 5.7$ and 7.0 GeV^2 for center-of-mass energies from threshold to 1.8 GeV. A first double polarization experiment on η electroproduction was reported by Merkel *et al.* (2007).

The photoproduction cross section for η' mesons, reported by Dugger *et al.* (2006), rises slowly from threshold and reaches a maximum of about 1 μb at $E_\gamma = 1.9$ MeV; at large energies, its cross section falls below the η cross section by a factor of ≈ 2, likely because of the twice smaller $u\bar{u}+d\bar{d}$ component in the η' wave function.

4. The reactions $\gamma p \to K^+\Lambda$, $K^+\Sigma^0$, and $K^0\Sigma^+$

Figure 22(b) show cross sections for photoproduction of final states with strangeness. For ΛK^+ and $\Sigma^0 K^+$ the cross sections reach about 2.5 μb; for $\Sigma^+ K^0$, it is a factor of 4 smaller. The ratio for decays of nucleon resonances into $\Sigma^+ K^0$ or $\Sigma^0 K^+$ is 1/2, for Δ resonances it is 2. The $\Sigma^0 K^+$ cross section is larger than that for $\Sigma^+ K^0$; the former reaction receives contributions from kaon exchange which is forbidden for the latter reaction. In partial-wave analyses (Castelijns *et al.*, 2008), the $N_{1/2^+}(1880)$ resonance is seen to make a significant contribution to final states with open strangeness.

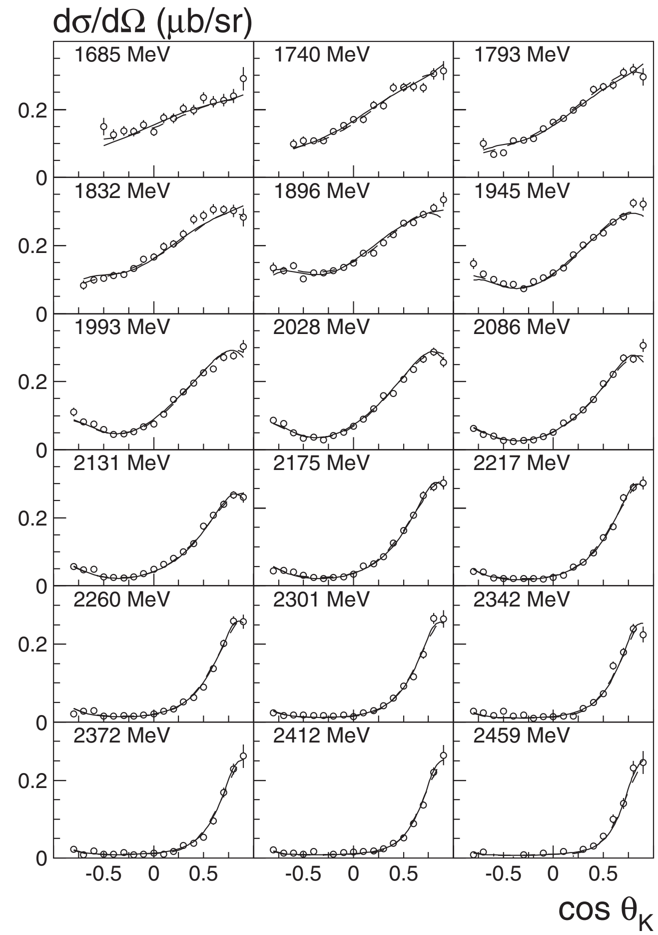

FIG. 28. Differential cross sections for $\gamma p \to K^+\Lambda$. The solid curves represent a Bonn-Gatchina fit. From Bradford *et al.*, 2006.

Differential distributions for $\gamma p \to K^+\Lambda$, $K^+\Sigma^0$, and $K^0\Sigma^+$ have been measured at ELSA with SAPHIR (Glander *et al.*, 2004; Lawall *et al.*, 2005) and CBELSA/TAPS (Castelijns *et al.*, 2008), GRAAL (Lleres *et al.*, 2007), at Jlab with the CLAS detector (Bradford *et al.*, 2006), and by LEPS at SPring-8 (Zegers *et al.*, 2003; Sumihama *et al.*, 2006; Hicks *et al.*, 2007). The data of Bradford *et al.* (2006) are shown in Fig. 28. The reconstruction of the hyperon decay defines its polarization status. At GRAAL and SPring-8, the γ-ray beam is created by rescattering of optical photons which are easily polarized; in these measurements, the beam asymmetry is determined as well.

Recently, spin transfer from linearly and circularly polarized photons to final-state hyperons has been measured at GRAAL (Lleres *et al.*, 2009); see Fig. 29 and

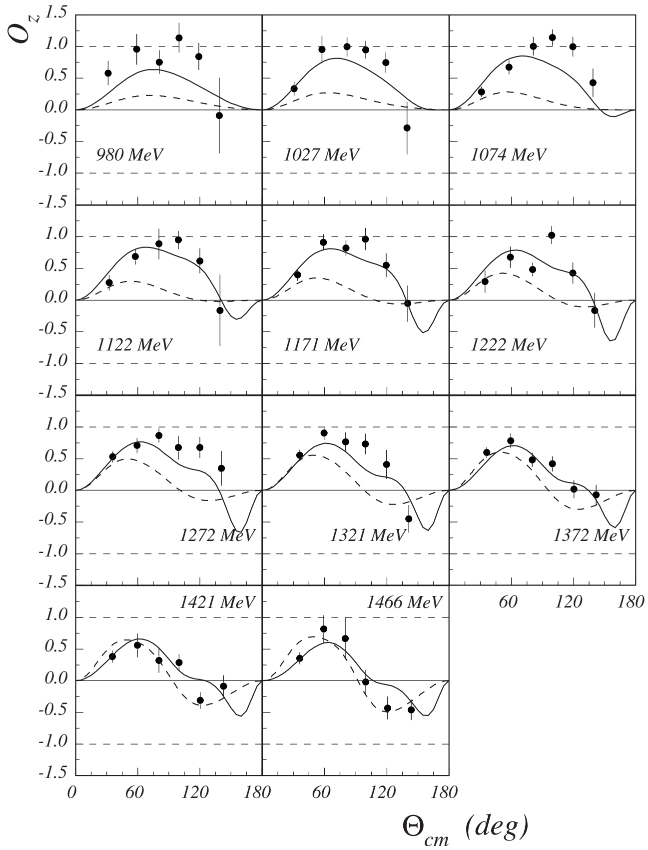

FIG. 29. Angular distributions of the beam recoil observable O_z (Lleres *et al.*, 2009). Data are compared with predictions of the Bonn-Gatchina (solid line, private communication from the GRAAL Collaboration) and the Regge-plus-resonance model of Corthals, Van Cauteren, *et al.* (2007).

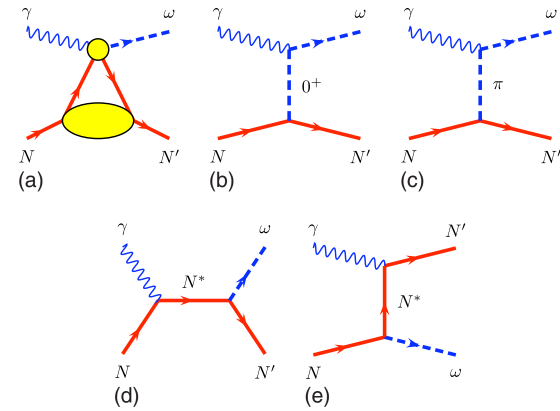

FIG. 30. (Color online) Contributions to ω photoproduction. (a) The handbag diagram for hard photoproduction and electroproduction. The large blob represents the generalized parton distribution of the nucleon. At lower energies, processes (b), (c), (d) are more appropriate to describe the reaction. (b) Natural parity t-channel exchange and (c) t-channel exchange via the pion trajectory. (d) s-channel intermediate resonance excitation. The same diagrams contribute to ρ production while ϕ are produced dominantly via (b). For K^* production, a kaon trajectory is exchanged, the outgoing N' is replaced by a hyperon. (d), (e) Baryon pole in the s and u channel.

Bradford *et al.* (2007). The data exhibit a striking transfer of the photon polarization to the Λ (Schumacher, 2008); the data mark an important step towards a complete experiment.

Electroproduction of $K^+\Lambda$ and $K^+\Sigma^0$ final states from a proton target was studied at Jlab using the CLAS detector. The separated structure functions σ_T, σ_L, σ_{TT}, and σ_{LT} were extracted for momentum transfers in the range $0.5 \leq Q^2 \leq 2.8$ GeV^2 and invariant energy in the range $1.6 \leq W \leq 2.4$ GeV, while spanning nearly the full center-of-mass angular range of the kaon (Ambrozewicz *et al.*, 2007). The polarized structure function $\sigma_{LT'}$ was measured for the reaction $p(\vec{e}, e'K^+)\Lambda$ in the nucleon resonance region from threshold up to $W = 2.05$ GeV for central values of Q^2 of 0.65 and 100 GeV^2 (Nasseripour *et al.*, 2008). The separated structure functions reveal clear differences between the production dynamics for the Λ and Σ^0 hyperons.

The polarization transferred from virtual photons to Λ and Σ^0 hyperons was measured using the CLAS spectrometer at beam energies of 2.567, 4.261, and 5.754 GeV (Carman *et al.*, 2003, 2009) spanning momentum transfers up to 5.4 GeV^2. The data suggest that the Λ polarization is maximal along the virtual photon direction. The large polarization effects—as also observed in photoproduction (Bradford *et al.*, 2007; Lleres *et al.*, 2009)—call for a simple interpretation accounting for the dynamics of quarks and gluons in a domain thought to be dominated by meson or baryon degrees of freedom. Two possible scenarios are discussed in Carman *et al.* (2009).

E. Photoproduction of multimesonic final states

1. Vector mesons

Photons and unflavored vector mesons share the same quantum numbers. In soft vector-meson production by real photons, natural-parity (Pomeron) exchange provides the leading term to the cross section. The cross section falls off exponentially with the squared recoil momentum t characteristic for "diffractive" production. At low energies, a significant pion (kaon) exchange contribution is expected because of the large $(\rho, \omega) \to \pi^0\gamma$ $(K^* \to K\gamma)$ coupling. Most interesting in the context of this review are contributions from N^* production since quark models predict for some N^* resonances large couplings to $N\omega$ and to $N\rho$. Figure 30 shows the different reaction mechanisms.

Photoproduction of ρ mesons was studied by the CLAS (Battaglieri *et al.*, 2001) and SAPHIR (Wu *et al.*, 2005) Collaborations, ω mesons by CLAS (Battaglieri *et al.*, 2003), SAPHIR—these data are shown in Fig. 31—(Barth *et al.*, 2003a), GRAAL (Ajaka *et al.*, 2006), and CBELSA/TAPS (Klein *et al.*, 2008). Large statistics data on differential cross sections and spin density matrix elements for $\gamma p \to p\omega$ have been reported recently by CLAS (Williams *et al.*, 2009c), for energies from threshold up to $W = 2.84$ GeV. $N_{5/2^+}(1680)$ and $N_{3/2^-}(1700)$ near

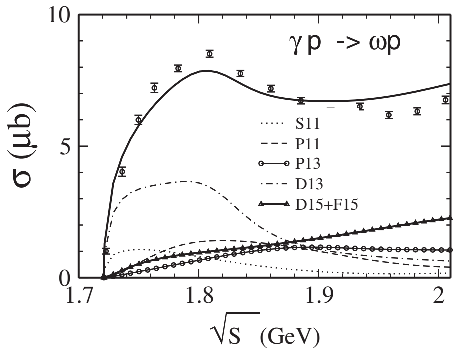

FIG. 31. The total cross section for ω photoproduction (Barth *et al.*, 2003a) and decomposition into partial waves by Shklyar, Lenske, *et al.* (2005).

threshold, $N_{7/2^-}(2190)$, and possibly a $N_{5/2^+}$ around 2 GeV were determined as leading contributions in an event-based partial-wave analysis (Williams *et al.*, 2009b).

Photoproduction of ϕ mesons was reported by CLAS (Anciant *et al.*, 2000), SAPHIR (Barth *et al.*, 2003b), and LEPS (Mibe *et al.*, 2005); the reactions $\gamma p \to K^{*0}\Lambda$ and $\gamma p \to K^{*0}\Sigma$ were reported by CLAS (Hleiqawi *et al.*, 2007); $\gamma p \to K^{*0}\Sigma^+$ by CBELSA/TAPS (Nanova *et al.*, 2008). The size of the cross section is about 24 μb for ρ, 8 μb for ω, and 0.2 μb for ϕ production [see Fig. 22(c)], while ratios 9:1:2 would be expected from the direct photon-vector-meson couplings. For pion exchange, the ω cross sections should exceed the ρ cross section while ϕ production would vanish.

In the multi-GeV range, electroproduction is sensitive to the transition between the low-energy hadronic and high-energy partonic domains; at sufficiently large energies, generalized parton distributions can be determined [see, e.g., Goloskokov (2008)]. However, there is so far no attempt to use the data for baryon spectroscopy. Here we provide reference to recent CLAS papers on electroproduction of ρ (Morrow *et al.*, 2009), ω (Morand *et al.*, 2005), and ϕ mesons (Santoro *et al.*, 2008).

2. $\gamma N \to N\pi\pi$ and $N\pi\eta$

Multimeson production collects an increasing fraction of the cross section; see Fig. 22(d). The most important channels are $\gamma p \to p\pi^+\pi^-$ (Wu *et al.*, 2005); above 2 GeV, $\gamma p \to p\pi^+\pi^-\pi^0$ reaches a similar strength (Barth *et al.*, 2003a). In the low-energy region, the different isospin channels of two-pion photoproduction (Zabrodin *et al.*, 1999) can be used to study chiral dynamics (Gomez Tejedor and Oset, 1996; Nacher *et al.*, 2001). Differences in $\pi^+\pi^0$ and $\pi^0\pi^0$ invariant mass distributions were assigned to a $N\rho$ decay branch of the $N_{3/2^-}(1520)$ nucleon resonance (Langgärtner *et al.*, 2001). In the resonance region, photoproduction of two charged pions is dominated by diffractive ρ production and the direct production $\gamma p \to \pi^-\Delta(1232)^{++}$; $\gamma p \to \pi^+\Delta(1232)^0$ plays a less important role. The CLAS Collaboration reported a study of the moments of the di-pion decay angular distributions and extracted S, P, and D waves in the 0.4–1.4 GeV $\pi\pi$ mass range (Battaglieri *et al.*, 2008, 2009).

Intermediate baryon resonances are much stronger in photoproduction of two neutral pions (Assafiri *et al.*, 2003; Ahrens *et al.*, 2005; Thoma *et al.*, 2008). The helicity dependence of the $\gamma p \to p\pi^+\pi^-$ total cross section was measured at MAMI for photon energies from 400 to 800 MeV (Ahrens *et al.*, 2007; Krambrich *et al.*, 2009). At higher energies, beam-helicity asymmetries were studied at Jlab (Strauch *et al.*, 2005). Two-pion electroproduction from Jlab was reported by Ripani *et al.* (2003), Hadjidakis *et al.* (2005) and, with very high statistics, Fedotov *et al.* (2009). The pion pair was produced at photon virtualities ranging in Q^2 from 0.2 to 0.6 GeV^2 and invariant mass W from 1.3 to 1.57 GeV. A phenomenological analysis found nonresonant mechanisms to provide the most significant part of the cross section. Within the EBAC model, electrocouplings of the $N(1440)P_{11}$ and $N(1520)D_{13}$ states can be extracted. The present state of art of the fits is described in Mokeev *et al.* (2009). A fraction of the data and the most significant isobar contributions are shown in Fig. 32.

The reaction $\gamma p \to p\pi^0\eta$ gives access to resonances in the $\Delta\eta$ system. The reaction was studied at SPring-8 (Nakabayashi *et al.*, 2006), at GRAAL (Ajaka *et al.*, 2008), at ELSA (Gutz *et al.*, 2008; Horn *et al.*, 2008a, 2008b), and at MAMI (Kashevarov, 2009). The $p\pi^0\eta$ Dalitz plots for two different photon energy ranges are shown in Fig. 33, with $\Delta(1232)$ and $N(1535)$ as intermediate resonances in $\gamma p \to [\Delta(1232)\eta; N(1535)\pi] \to p\pi^0\eta$ cascade decays. Likewise, $\gamma p \to p\pi^0\omega$ can be used to study the $\Delta\omega$ system. However, so far data are scarce (Junkersfeld *et al.*, 2007).

3. Hyperon resonances and the $\Theta(1540)^+$

In 2003, evidence for a narrow baryon resonance with positive strangeness $\Theta(1540)^+$, i.e., with a constituent $\bar{s}$ quark, was reported by four different laboratories (Barmin *et al.*, 2003; Barth *et al.*, 2003c; Nakano *et al.*, 2003; Stepanyan *et al.*, 2003) with properties as predicted in a chiral soliton model (Diakonov *et al.*, 1997). A broad search was initiated to confirm or disprove these findings, including the search for related phenomena such as $\Phi(1860)$ ($=ssdd\bar{u}$) (Alt *et al.*, 2004) and $\Theta_c(3100)$ ($=uudd\bar{c}$) (Chekanov *et al.*, 2004). The evidence for pentaquarks has now faded away (Danilov and Mizuk, 2008) even though some evidence persists (Nakano *et al.*, 2009); remarks on the coherence of experimental findings and results from lattice QCD and QCD sum rules can be found in Tariq (2007).

Our knowledge of excited strange baryons rests nearly entirely on KN scattering data which are not reviewed here. The $\Lambda_{3/2^-}(1520)$ hyperon was studied in photoproduction by LEPS (Kohri *et al.*, 2009) in the threshold region, by SAPHIR (Wieland *et al.*, 2010) for photon energies below 2.65 GeV, and in electroproduction by

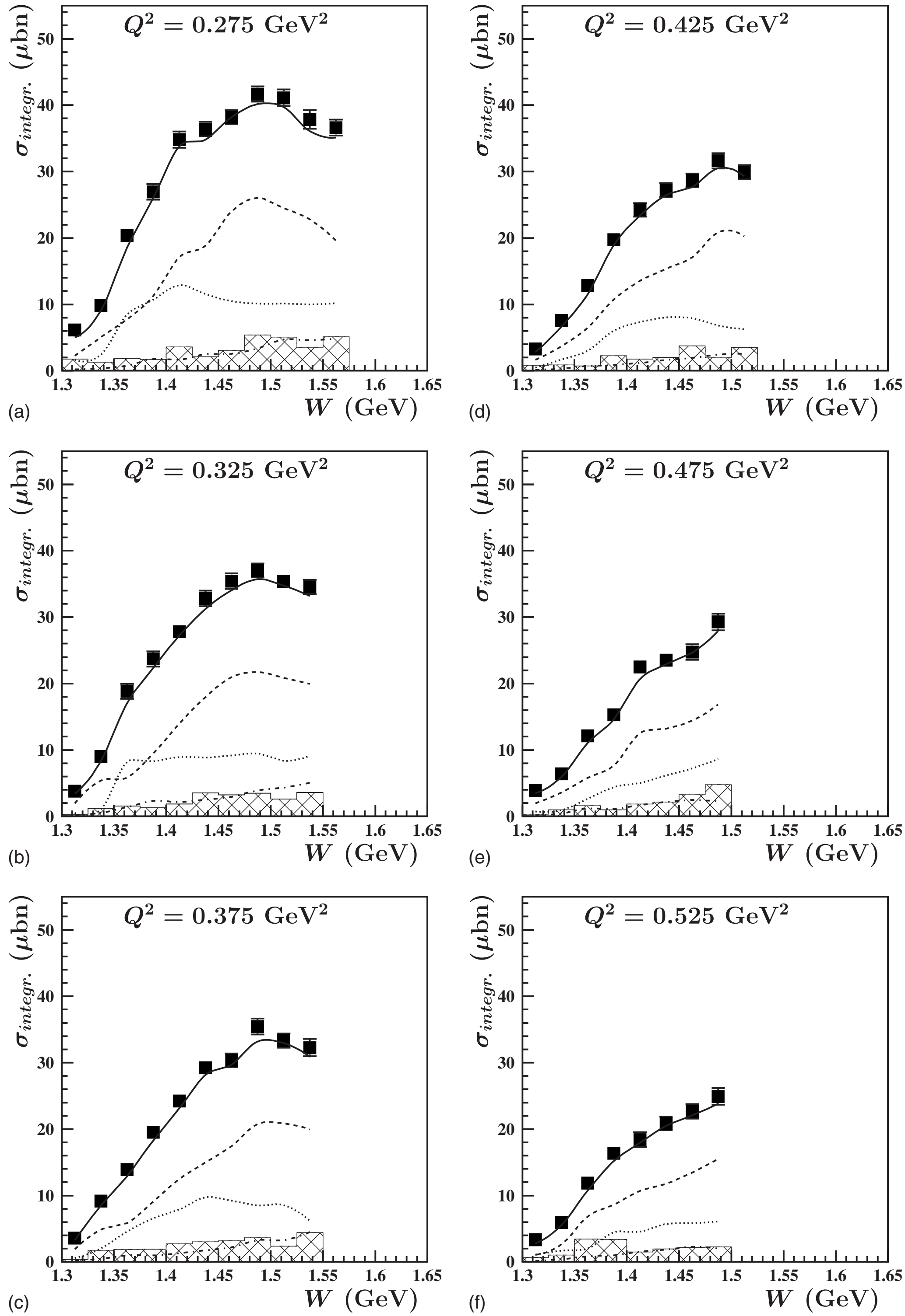

FIG. 32. Electroproduction of $p\pi^+\pi^-$ after integration over the full dynamics. The cross sections are decomposed into the dominant isobar channels. The recent CLAS data (Fedotov *et al.*, 2009) are shown by full symbols. Shadowed areas represent the systematical uncertainties. The solid lines correspond to an EBAC fit (JM06) to the six one-fold differential cross sections (Mokeev *et al.*, 2009). The contributions from $\pi^-\Delta^{++}$, $\pi^+\Delta^0$ channels are shown by dashed and dot-dashed lines and the contributions from direct 2π production by dotted lines, respectively.

CLAS at electron beam energies of 4.05, 4.25, and 4.46 GeV (Barrow *et al.*, 2001). The decay angular distributions suggest resonant contributions at low energies, and at high-energy dominance of t-channel diagrams with either K^+ exchange or longitudinal coupling to an exchanged K^*. The Q^2 dependence of the $\Lambda_{3/2^-}(1520)$ production cross section is similar to the one observed for photoproduction and electroproduction of the Λ hyperon. The reaction $\gamma p \to K^{*0}\Sigma^+$ provides hints for a significant role of $K_0(900)$ exchange (Hleiqawi *et al.*, 2007).

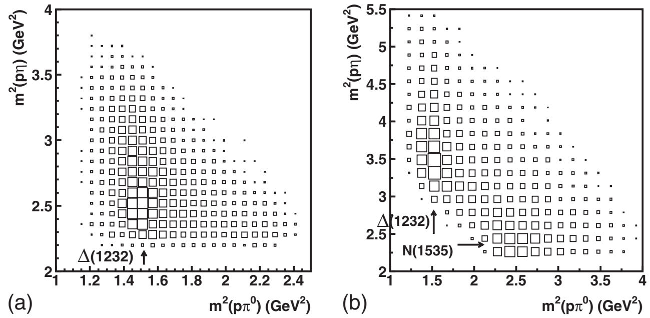

FIG. 33. Dalitz plot (Crystal Barrel at ELSA) for the reaction $\gamma p \to p\pi^0\eta$ for (a) $E_\gamma < 1.9$ GeV and (b) $E_\gamma > 1.9$ GeV. $\Delta(1232)$ is seen in both Dalitz plots; $N(1535)$ is visible only for high photon energies even though the $N(1535)\pi$ production threshold (~ 1.0 GeV) is lower than the $\Delta(1232)\eta$ production threshold (~ 1.2 GeV).

Differential cross sections for $\gamma p \to K^+\Lambda_{1/2^-}(1405)$ and $\gamma p \to K^+\Sigma^0(1385)$ for forward K^+ scattering angles have been reported for photon energies ranging from 1.5 to 2.4 GeV (Hicks *et al.*, 2009). The $\Lambda_{1/2^-}(1405)$ to $\Sigma^0(1385)$ production ratio decreased with increasing photon energy possibly suggesting different internal structures (Niiyama *et al.*, 2008). Cross sections and beam asymmetries for $K^+\Sigma^{*-}$ photoproduction from the deuteron at 1.5–2.4 GeV were reported by Hicks *et al.* (2009).

F. Partial-wave analyses

A discussion of problems, principles, and achievements of partial-wave analysis goes beyond the scope of this paper, which concentrates on a review of the data which have been gathered and the physical significance of the results. Partial-wave analyses are performed at a number of places, using different methods. Even though small groups or individuals have made significant contributions to the field, most partial-wave analyses are performed at a few places only.

1. SAID and MAID

The longest continuous tradition is held by the SAID group (Arndt *et al.*, 2003b). A recent review can be found in Arndt *et al.* (2008). The group maintains and updates analyses of the elastic πN (including πd), KN, NN databases and on photoproduction and electroproduction of pseudoscalar mesons. The web page http://gwdac.phys.gwu.edu/ provides access to the data, to partial-wave amplitudes, and to current energy-dependent predictions for observable quantities. A similar page is found at Mainz (http://www.kph.uni-mainz.de/MAID/). The most recent solutions for πN elastic scattering were obtained by Arndt *et al.* (2006), for KN elastic scattering by Hyslop *et al.* (1992), for photoproduction of pions, jointly with the most recent CLAS data by Dugger *et al.* (2007). Amplitudes for photoproduction of η and η' were determined by Chiang *et al.* (2003) and Briscoe *et al.* (2005) and those for kaon photoproduction by Mart and Sulaksono (2006). Principles of multichannel analyses are discussed by Vrana *et al.* (2000). The latter results differ significantly from those of single-channel fits emphasizing the need to include inelasticity explicitly. Electroproduction amplitudes (MAID-07) were reported by Drechsel *et al.* (2007). The MAID and SAID databases provide indispensable tools for physicists working in the field. Both groups determine masses, widths, and quantum numbers mostly from πN scattering; photoproduction data complement the information by providing helicity amplitudes (Arndt *et al.*, 2005b; Pasquini *et al.*, 2006).

2. EBAC

The EBAC has developed a model to study nucleon resonances pion- and photon-induced reactions (Matsuyama *et al.*, 2007). The model is based on an energy-independent Hamiltonian derived from an interaction Lagrangian. The main results on $\pi N \to N\pi$ were given by Julia-Diaz *et al.* (2007), on $\pi N \to N\eta$ (Durand *et al.*, 2008), and on $\pi N \to N\pi\pi$ by Kamano *et al.* (2009a). Photoproduction of pions was studied by Sibirtsev *et al.* (2007) and Julia-Diaz *et al.* (2008, 2009) and electroproduction of η and η' by Julia-Diaz *et al.* (2009) and pion pairs by Mokeev *et al.* (2009). A common analysis of single- and double-pion photoproduction is presented in Kamano *et al.* (2009a, 2009b). A review of the method and recent achievements was presented by Lee (2007).

3. The Giessen model

The Giessen group analyzes simultaneously pion- and photon-induced data on γN and πN to πN, $2\pi N$, ηN, $K\Lambda$, $K\Sigma$, and ωN for energies from the nucleon mass up to $\sqrt{s}=2$ GeV. The method is based on a unitary coupled-channel effective Lagrangian model. The results of the partial-wave analyses were reported by Feuster and Mosel (1998, 1998b), Penner and Mosel (2002a, 2002b), Shklyar *et al.* (2005, 2007), Shklyar, Lenske, *et al.* (2005) and Shyam, *et al.* (2010).

4. The Bonn-Gatchina model

The Bonn-Gatchina group analyzes large data sets, including recent results from photoproduction of kaons and multiparticle final states such as $p\pi^0\pi^0$ and $p\pi^0\eta$. The latter data are included in event-based likelihood fits which fully exploit the information contained in the correlations between the different variables. The methods are described by Anisovich *et al.* (2005, 2007a) and Klempt *et al.* (2006) and results by Anisovich *et al.* (2005, 2007b, 2009), Sarantsev *et al.* (2005, 2008), Nikonov *et al.* (2008), and Thoma *et al.* (2008). Data on meson and baryon spectroscopy as well as the BnGa πN partial-wave amplitudes, photoproduction multipoles, and predictions for observables can be found on the web page http://pwa.hiskp.uni-bonn.de/.

5. Other approaches

We mention further the analysis of the Gent group which describes photoproduction and electroproduction of hyperons in a Regge-plus-resonance approach (Corthals *et al.*, 2006, 2007; Corthals, Van Cauteren, *et al.*, 2007).

A few words should be added as general remarks. Partial-wave amplitudes are constrained by a number of theoretical considerations. First, amplitudes need to be analytical functions in the complex s plane; left-hand cuts due to threshold singularities can be treated using the N/D formalism. Amplitudes should obey crossing symmetry; ideally, amplitudes should be defined as functions of s, t, and u. In elastic πN scattering, these requirements are met approximately by forcing amplitudes to satisfy fixed-t dispersion relations. Amplitudes should respect chiral symmetry. This requirement can be enforced in models using a chiral Lagrangian or by including the πN scattering amplitudes in the fits. Finally, amplitudes have to preserve unitarity; the number of incoming particles in a given partial wave, e.g., πN in the $J^P=3/2^+$ wave, has to be preserved. This requirement can be met using a K matrix in which background amplitudes and resonances can be added in a unitarity-preserving way.

Even when the scattering amplitudes are known, the extraction of resonance parameters from meson-nucleon and photoinduced reactions is not easy. The physical quantity which should not depend on the reaction mechanism is supposedly the pole position. Masses and widths can be determined, e.g., in the πN elastic scattering, by the speed-plot or the time-delay method (Suzuki *et al.*, 2009), methods which may be more stable than parameters deduced from Breit-Wigner parametrizations. An alternative method to define Breit-Wigner parameters (Thoma *et al.*, 2008) is to construct a Breit-Wigner amplitude as a function of s which reproduces the pole position of the scattering amplitude. Ceci *et al.* (2008) suggested to derive the resonance parameter from the trace of K and T matrices.

Coupling constants for decays of a resonance into $A+b$ can be determined as residues of pole of the $A+b \to A+b$ scattering amplitude in the complex s plane. The partial decay width is usually defined as $\Gamma_{Ab}=\rho_{Ab}g^2_{Ab}$, where ρ_{Ab} is the phase space [including centrifugal barrier and Blatt-Weisskopf corrections (Anisovich *et al.*, 2005)], calculated at the nominal mass and g^2_{Ab} the squared coupling constant at the nominal mass. The definition has the nonintuitive consequence that the partial decay width of a subthreshold resonance vanishes identically even though the decay is possible via the tails of the mother (and/or daughter) resonance. More intuitive, but in practice less well defined, is a definition where the ratio of partial to total width is given by the ratio of the intensity in one channel to the intensity in all channels. One particular case are the $N\gamma$ decays or the $A_{1/2}$ and $A_{3/2}$ helicity amplitudes, describing the nucleon-photon coupling for a total spin 1/2 and 3/2, respectively. A thorough discussion of these amplitudes, including the longitudinal helicity amplitude $S_{1/2}$ is given in Aznauryan *et al.* (2008). With the definition of a partial decay width as residue of a pole in the $\gamma N \to N\gamma$ amplitude, helicity amplitudes become complex quantities.

The coupling of a resonance to a decay channel has an impact on its mass. Quark-model calculations usually give masses of "stable" baryons, of baryons before they are "dressed with a meson cloud." The EBAC group makes the attempt to determine bare baryon masses, masses a resonance might have before it dresses itself with a meson cloud. In meson spectroscopy, the Gatchina group (Anisovich *et al.*, 2008) identified the undressed states with the K-matrix poles. However, Workman and Arndt (2009) did not find a simple association between K- and T-matrix poles. We believe bare masses to be highly model-dependent quantities; the determination of the T-matrix poles is easy once the amplitudes are known, and they should be given, at least in addition. Finally, it is the T-matrix pole position which is given by the PDG and which can be compared to other analyses. The future will have to decide if dressing of quark-model states or undressing of observed resonances may become a useful concept.

G. Summary of N^* and Δ^* resonances

The Review of Particle Properties of the PDG (Amsler *et al.*, 2008) is indispensable for any physicist working in nuclear and particle physics, and also in this review frequent use has been made of it. In baryon spectroscopy, listings of main properties of resonances are given and a selection is made which data are used to define the properties, which data are listed but not used for averaging, and which results to not warrant to be mentioned. Based on these results, a status is defined, with four stars given to a resonance with certain existence and fairly well-defined properties and three-star resonances are almost certain but some parameters are less well defined. A resonance is given two stars if the evidence for its existence is fair and one star if it is poor. The judgement is dominantly based on analyses from Cutkosky *et al.* (1979) and Höhler *et al.* (1979)—updated in Cutkosky *et al.* (1980)—Manley and Saleski (1992), and Arndt *et al.* (2006).

We suggest here "our own" version of the PDG listings by including the results of the Bonn-Gatchina analysis (Anisovich *et al.*, 2009). So far, results from photoproduction were not yet used to estimate the status of a resonance or to determine mass or width. The reason for this decision is the following: unlike πN elastic scattering, it is—at least so far—not possible to derive energy-independent partial-wave amplitudes from photoproduction data. For an independent observer, it is difficult to judge how reliable a fit to data is, and if alternative solutions exists in which a particular resonance is not needed. However, in the recent analysis of the Bonn-Gatchina group, the same amplitudes are used as in Arndt *et al.* (2006). The BnGa differs by constraining the amplitudes of the SM06 solution by data on photoproduction. In previous analyses, the inelasticity of baryon resonances are mostly unknown and are fitted as free unconstrained parameters of the fit. Constraining the SM06 amplitudes by known inelasticities can only improve our knowledge.

In Table XIII we list the N^* and Δ^* resonances, give our estimate for mass and width, and our rating. Results from five analyses are given. Four new resonances are suggested which are underlined.

(1) The $N_{3/2^-}(1860)$ is found in the PDG listings under the entry $N(2080)D_{13}$ [$N_{3/2^-}(2080)$]. It is observed at this mass in the KH analysis; CM suggest two states, here we list both under the two headings. Kent confirmed the lower-mass state at 1804 MeV. In the BnGa analysis, it assumes a mass of 1875 MeV. $N_{3/2^-}(1860)$ is not seen by KH nor by GWU and we give it a two-star status.

(2) A second newly introduced resonance is $N_{1/2^+}(1880)$. Evidence comes from the Kent and BnGa analyses.

(3) $N_{5/2^+}(1870)$ replaces the PDG entry $N(2000)F_{15}$ [$N_{5/2^+}(2000)$]. It is seen in all but the CM analysis and we rate it with three stars.

(4) $N_{1/2^-}(1905)$ was reported by KH and Kent. In PDG, the two results are combined with the CM result (2180 MeV) to give $N(2090)S_{11}$.

The five analyses listed in Table XIII are used to determine our rating. Resonances get four stars if seen in four experiments, including the GWU analysis. One star is subtracted if it is not seen in the GWU analysis; two stars are assigned if seen in three and one star if seen by two analyses. Resonances included in the PDG which are seen only by one of the five analyses are kept in Table XIII but with no star. For those, no mass or width estimate is given, and they are not considered in Sec. IV. In some cases, the ratings differ from PDG; in case of up- (down-) graded resonances, the star rating is over (under) lined. The mass region above 2.5 GeV was studied in the KH and Hendry analysis only; we keep their PDG rating.

The mass and width are estimated from the spread of results rather than from the quoted errors. As a rule, we do not give extra weight to analyses quoting smaller errors. Mostly small errors indicate that correlations with other variables are not sufficiently explored. For two-star resonances we give a minimum error of ±3% on the mass and for one-star resonances of ±5%. The width error we assign is minimally about twice larger than the error in mass.

IV. MODELS AND PHENOMENOLOGY

A. Historical perspectives

1. SU(3) symmetry

The main concern of baryon spectroscopy in the late 1960s was to analyze the meson-baryon interaction and to understand the pattern of the many nucleon and Δ resonances, and the relation between these baryons and the strange baryons, Λ, Σ, Ξ, and their excitations. The dynamical mechanism proposed to generate these resonances was the meson-nucleon interaction: it accounted for the Δ resonance in the π-N system, but failed to predict most of the other states.

Then came flavor symmetry, based on the group SU(3), from now on called $SU(3)_f$, and its "eightfold way" version. The lowest-mass baryons, with spin $S=1/2$, form an octet (N,Λ,Σ,Ξ). The baryons with $S=3/2$ are in a decuplet which, in 1962, included $\Delta(1232)$, $\Sigma_{3/2^+}(1385)$ and $\Xi_{3/2^+}(1530)$ (named Σ^* and Ξ^* at that time). One state was missing. The regular mass spacing between $\Delta(1232)$, $\Sigma_{3/2^+}(1385)$, and $\Xi_{3/2^+}(1530)$ was used to predict the existence and the mass of the $\Omega(1672)$ baryon (Gell-Mann, 1962), with strangeness $S=-3$. Its experimental discovery (Barnes *et al.*, 1964) was a triumph for $SU(3)_f$.

It was then realized that if $SU(3)_f$ is taken seriously, there are three states in the fundamental representation, 3, named quarks, and the actual baryons correspond to the flavor representations found in the $3\times3\times3$ product. This was the beginning of the quark model, first a tool for building the $SU(3)_f$ representations, and then becoming a dynamical model.

Today, $SU(3)_f$ is understood from the universal character of the quark interaction (flavor independence) and the approximate equality of the masses of light and strange quarks. $SU(3)_f$ remains a valuable tool to correlate data in different flavor sectors and organize the hadron multiplets.

2. SU(6) symmetry

The group SU(6) combines $SU(3)_f$ with the spin group SU(2). For instance, the octet baryons with $S=1/2$ and the decuplet baryons with $S=3/2$ form a 56 representation of SU(6). This SU(6) symmetry emerges automatically in potential models with flavor-independent forces, in the limit where the strange quark mass m_s is equal to that or ordinary quarks, and the spin-dependent forces are neglected.

Further symmetry schemes have been proposed to analyze the baryon spectrum and properties; see, e.g., Bijker *et al.* (1994, 2000) and Kirchbach *et al.* (2001).

3. Early models

The harmonic oscillator model, as well as some of its many refinements, enables one to account explicitly for $SU(3)_f$ and SU(6) symmetry and their violation, and was crucial to assess the quark model not only as a mathematical tool to generate the actual representation out of the fundamental ones, but to understand the pattern of radial and orbital excitations. More refined constituent models were proposed later. Recently attempts were made to derive the baryon masses and properties directly from QCD, by sum rules or lattice simulations: the results are encouraging, but often restricted to the lowest levels.

TABLE XIII. Breit-Wigner masses W_R and widths Γ (in MeV) of N and Δ resonances.

Resonance	Our estimate	Our rating	KH	CM	Kent	GWU	BnGa
$N_{1/2^+}(1440)$	1450 ± 32; 300 ± 100	****	1410 ± 12; 135 ± 10	1440 ± 30; 340 ± 70	1462 ± 10; 391 ± 34	1485 ± 1; 284 ± 18	1440 ± 12; 335 ± 50
$N_{3/2^-}(1520)$	1522 ± 4; 115 ± 10	****	1519 ± 4; 114 ± 7	1525 ± 10; 120 ± 15	1524 ± 4; 124 ± 8	1516 ± 1; 99 ± 3	1524 ± 4; 117 ± 6
$N_{1/2^-}(1535)$	1538 ± 10; 175 ± 45	****	1526 ± 7; 120 ± 20	1550 ± 40; 240 ± 80	1534 ± 7; 151 ± 27	1547 ± 1; 188 ± 4	1535 ± 20; 170 ± 35
$N_{1/2^-}(1650)$	1660 ± 18; 165 ± 25	****	1670 ± 8; 180 ± 20	1650 ± 30; 150 ± 40	1659 ± 9; 170 ± 12	1635 ± 1; 115 ± 3	1680 ± 40; 170 ± 45
$N_{5/2^-}(1675)$	1675 ± 5; 153 ± 22	****	1679 ± 8; 120 ± 15	1675 ± 10; 160 ± 20	1676 ± 2; 159 ± 7	1674 ± 1; 147 ± 1	1678 ± 5; 177 ± 15
$N_{5/2^+}(1680)$	1683 ± 3; 126 ± 9	****	1684 ± 3; 128 ± 8	1680 ± 10; 120 ± 10	1684 ± 4; 139 ± 8	1680 ± 1; 128 ± 1	1685 ± 5; 117 ± 12
$N_{3/2^-}(1700)$	1725 ± 50; 190 ± 110	***	1731 ± 15; 110 ± 30	1675 ± 25; 90 ± 40	1737 ± 44; 250 ± 230		1730 ± 40; 310 ± 60
$N_{1/2^+}(1710)$	1713 ± 12; 220 ± 180	***	1723 ± 9; 120 ± 15	1700 ± 50; 90 ± 30	1717 ± 28; 480 ± 330		1725 ± 25; 200 ± 35
$N_{3/2^+}(1720)$	1730 ± 30; 320 ± 210	****	1710 ± 20; 190 ± 30	1700 ± 50; 125 ± 70	1717 ± 31; 380 ± 180	1750 ± 5; 256 ± 22	1770 ± 100; 650 ± 120
$N_{3/2^-}(1860)$	1850 ± 40; 260 ± 170	**		1880 ± 100; 180 ± 60	1804 ± 55; 450 ± 185		1870 ± 25; 150 ± 40
$N_{5/2^+}(1870)$	1880 ± 40; 270 ± 180	~~**~~	1882 ± 10; 95 ± 20		1903 ± 87; 490 ± 310	1818; 118	1910 ± 50; 360 ± 80
$N_{1/2^+}(1880)$	1890 ± 50; 210 ± 100	*			1885 ± 30; 113 ± 44		1900 ± 30; 300 ± 40
$N_{3/2^+}(1900)$	1940 ± 50; 340 ± 150	*			1879 ± 17; 498 ± 78		1960 ± 30; 185 ± 40
$N_{1/2^-}(1905)$	1905 ± 50; 250 ± 150	*	1880 ± 20; 95 ± 30		1928 ± 59; 414 ± 157		
$N_{7/2^+}(1990)$	2020 ± 60; 410 ± 110	**	2005 ± 150; 350 ± 100	1970 ± 50; 350 ± 120	2086 ± 28; 535 ± 120		
$N_{3/2^-}(2080)$	2100 ± 55; 310 ± 110	~~**~~	2080 ± 20; 265 ± 40	2060 ± 80; 300 ± 100			2160 ± 35; 370 ± 50
$N_{1/2^-}(2090)$				2180 ± 80; 350 ± 100			
$N_{1/2^+}(2100)$	2090 ± 100; 230 ± 200	*	2050 ± 20; 200 ± 30	2125 ± 75; 260 ± 100			
$N_{5/2^-}(2200)$	2160 ± 85; 350 ± 50	**	2228 ± 30; 310 ± 50	2180 ± 80; 400 ± 100			2065 ± 25; 340 ± 40
			KH	CM	Kent	GWU	Hendry
$N_{7/2^-}(2190)$	2150 ± 30; 440 ± 110	****	2140 ± 12; 390 ± 30	2200 ± 70; 500 ± 150	2127 ± 9; 550 ± 50	2152 ± 2; 484 ± 13	2140 ± 40; 270 ± 50
$N_{9/2^+}(2220)$	2260 ± 60; 490 ± 115	****	2205 ± 10; 365 ± 30	2230 ± 80; 500 ± 150		2316 ± 3; 633 ± 17	2300 ± 100; 450 ± 150
$N_{9/2^-}(2250)$	2255 ± 50; 420 ± 150	****	2268 ± 15; 300 ± 40	2250 ± 80; 400 ± 120		2302 ± 6; 628 ± 28	2200 ± 100; 350 ± 100
$N_{11/2^-}(2600)$	2630 ± 120; 650 ± 250	**	2577 ± 50; 400 ± 100				2700 ± 100; 900 ± 100
$N_{13/2^+}(2700)$	2800 ± 160; 600 ± 300	**	2612 ± 45; 350 ± 50				3000 ± 100; 900 ± 150
			KH	CM	Kent	GWU	BnGa
$\Delta_{3/2^+}(1232)$	1232 ± 1; 118 ± 2	****	1232 ± 3; 116 ± 5	1232 ± 2; 120 ± 5	1231 ± 1; 118 ± 4	1233 ± 1; 119 ± 1	1230 ± 2; 112 ± 4
$\Delta_{3/2^+}(1600)$	1615 ± 80; 360 ± 120	***	1522 ± 15; 220 ± 40	1600 ± 50; 300 ± 100	1706 ± 10; 430 ± 73		1640 ± 40; 480 ± 100
$\Delta_{1/2^-}(1620)$	1626 ± 23; 130 ± 45	****	1610 ± 7; 139 ± 18	1620 ± 20; 140 ± 20	1672 ± 7; 154 ± 37	1614 ± 1; 71 ± 3	1625 ± 10; 148 ± 15
$\Delta_{3/2^-}(1700)$	1720 ± 50; 370 ± 200	****	1680 ± 70; 230 ± 80	1710 ± 30; 280 ± 80	1762 ± 44; 600 ± 250	1688 ± 3; 182 ± 8	1780 ± 40; 580 ± 120
$\Delta_{1/2^+}(1750)$					1744 ± 36; 300 ± 120		
$\Delta_{1/2^-}(1900)$	1910 ± 50; 190 ± 100	**	1908 ± 30; 140 ± 40	1890 ± 50; 170 ± 50	1920 ± 24; 263 ± 39		
$\Delta_{5/2^+}(1905)$	1885 ± 25; 330 ± 50	****	1905 ± 20; 260 ± 20	1910 ± 30; 400 ± 100	1881 ± 18; 327 ± 51	1856 ± 2; 321 ± 9	1870 ± 32; 340 ± 32

TABLE XIII. (*Continued.*)

Resonance	Our estimate	Our rating	KH	CM	Kent	GWU	BnGa
$\Delta_{1/2^+}(1910)$	1935 ± 90; 280 ± 150	****	1888 ± 20; 280 ± 50	1910 ± 40; 225 ± 50	1882 ± 10; 229 ± 25	2068 ± 2; 543 ± 10	
$\Delta_{3/2^+}(1920)$	1950 ± 70; 260 ± 100	***	1868 ± 10; 220 ± 80	1920 ± 80; 300 ± 100	2014 ± 16; 152 ± 55		1995 ± 40; 360 ± 50
$\Delta_{5/2^-}(1930)$	1930 ± 30; 350 ± 170	$\underline{\ast\ast}$	1901 ± 15; 195 ± 60	1940 ± 30; 320 ± 60	1956 ± 22; 530 ± 140		
$\Delta_{3/2^-}(1940)$	1995 ± 60; 340 ± 130	$\cancel{\ast\ast}$		1940 ± 100; 200 ± 100	2057 ± 110; 460 ± 320		1995 ± 40; 360 ± 50
$\Delta_{7/2^+}(1950)$	1930 ± 16; 285 ± 45	****	1913 ± 8; 224 ± 10	1950 ± 15; 340 ± 50	1945 ± 2; 300 ± 7	1921 ± 1; 271 ± 1	1928 ± 8; 290 ± 14
$\Delta_{5/2^+}(2000)$			2200 ± 125; 400 ± 125		1752 ± 32; 251 ± 93		
$\Delta_{1/2^-}(2150)$				2200 ± 100; 200 ± 100			
			KH	CM	Kent	GWU	Hendry
$\Delta_{7/2^-}(2200)$	2230 ± 50; 420 ± 100	**	2215 ± 10; 400 ± 100	2200 ± 80; 450 ± 100			2280 ± 80; 400 ± 150
$\Delta_{9/2^+}(2300)$	2360 ± 125; 420 ± 200	**	2217 ± 80; 300 ± 100	2400 ± 125; 425 ± 150			2450 ± 100; 500 ± 200
$\Delta_{5/2^-}(2350)$	2310 ± 85; 490 ± 250	***	2305 ± 26; 300 ± 70	2400 ± 125; 400 ± 150		2233 ± 53; 773 ± 187	
$\Delta_{7/2^+}(2390)$	2390 ± 100; 300 ± 200	*	2425 ± 60; 300 ± 80	2350 ± 100; 300 ± 100			
$\Delta_{9/2^-}(2400)$	2400 ± 190; 530 ± 300	**	2468 ± 50; 480 ± 100	2300 ± 100; 330 ± 100		2643 ± 141; 895 ± 432	2200 ± 100; 450 ± 200
$\Delta_{11/2^+}(2420)$	2462 ± 120; 490 ± 150	***	2416 ± 17; 340 ± 28	2400 ± 125; 450 ± 150		2633 ± 29; 692 ± 47	2400 ± 60; 460 ± 100
$\Delta_{13/2^-}(2750)$	2720 ± 100; 420 ± 200	**	2794 ± 80; 350 ± 100				2650 ± 100; 500 ± 100
$\Delta_{15/2^+}(2950)$	2920 ± 100; 500 ± 200	**	2990 ± 100; 330 ± 100				2850 ± 100; 700 ± 200

4. Heavier flavors

The discovery of charm and beauty significantly enriched the spectrum of hadrons. The quark model gained in credibility by the success of potentials fitting the J/ψ and Υ excitations. The problem was to combine these new states in the existing schemes.

The extension of $SU(3)_f$ to $SU(4)_f$ or beyond is straightforward but not useful, as the symmetry is largely broken. However, with the advent of QCD, the ideas have evolved. The basic coupling, that of gluons to quarks, is linked to the color, not to the flavor. Hence, at least in the static limit, the quark-quark interaction should be *flavor independent* in the same way as in the physics of exotic atoms, the same Coulomb potential binds electrons, muons, kaons, and antiprotons.

Flavor independence is probed in various ways: the same "funnel" potential (Coulomb+linear) simultaneously fits the charmonium and bottomonium spectrum in the meson sectors. For baryons, regularities are also observed, which supports a picture with a flavor-independent confinement and flavor symmetry broken through the quark masses entering the kinetic energy and spin-dependent corrections. For instance, there is a smooth evolution of hyperfine splittings from $\Delta-N$ to $\Sigma_b^*-\Sigma_b$.

It would, of course, be appealing to describe all baryons within in a universal model, the light quark requiring only relativistic corrections due to their light mass. This is the spirit of the work by Godfrey and Isgur (1985) and Capstick and Isgur (1986). The success of this model is almost embarrassing, as QCD guides our intuition toward drastic differences between heavy and light quarks. Heavy quarks interact by exchanging gluons. On the other hand, the dynamics of light quarks is dominated by chiral symmetry, which seems hardly reducible to a local potential.

5. The role of color

One of the main motivations for introducing color was to account for the antisymmetrization of the quarks in baryons (Greenberg, 1964). In the harmonic oscillator and its various developments, the quarks in N, Δ, Ω^-, etc., are in a symmetric overall S wave, and the spin-isospin part is also symmetric. An antisymmetric $3\times 3\times 3 \to 1$ coupling of color ensures Fermi statistics.

Then, in this color scheme, a quark in a baryon sees a color $\bar{3}$ set of two quarks, which is analogous to the antiquark seen by a quark in an ordinary meson. This is the beginning of the diquark idea which will be discussed below.

QCD gives a picture where the quarks interact moderately at short distances, according to "asymptotic freedom," and more strongly at large distances, where a linear confinement is suggested by many studies, though not yet rigorously proved. The question is whether a Coulomb plus linear potential mimics QCD well enough so that reliable predictions can be done. A related question is whether the interaction among quarks in baryons is of pairwise nature.

Another problem, raised in the late 1970s in dealing with "color chemistry" (Chan *et al.*, 1978), is whether the color representations used by hadrons are restricted to 3 (quarks, antidiquarks), $\bar{3}$ (antiquarks, diquarks), and 1 (hadrons). Namely is the octet, which corresponds to gluons, restricted to the crossed channel, i.e., used only to mediate the interaction, or does it play a constituent role (glueballs, hybrid mesons and baryons)? Are there multiquark states containing color-sextet or color-octet clusters? Experimental evidence for the existence of hadrons with "hidden color" in the pre-LEAR area was overruled in high-statistics experiments in the early phase of LEAR (Walcher, 1988).

B. Models of ground-state baryons

1. Potential models

The simplest model consists of

$$H=\sum_{i=1}^{3}\frac{\boldsymbol{p}_i^2}{2m_i}+V(\boldsymbol{r}_1,\boldsymbol{r}_2,\boldsymbol{r}_3)-\frac{\left(\sum_i \boldsymbol{p}_i\right)^2}{2\sum_i m_i}, \tag{19}$$

where V is a suitable translation-invariant interaction, the best known choice being the harmonic oscillator

$$V(\boldsymbol{r}_1,\boldsymbol{r}_2,\boldsymbol{r}_3)=\frac{2K}{3}\sum_{i<j} r_{ij}^2, \tag{20}$$

where $r_{ij}=|\boldsymbol{r}_j-\boldsymbol{r}_i|$. The ground state is the minimum of H, which can be reached for instance by variational methods. For equal masses $m_i=m$, one can introduce the Jacobi coordinates

$$\boldsymbol{\rho}=\boldsymbol{r}_2-\boldsymbol{r}_1,\quad \boldsymbol{\lambda}=\frac{2\boldsymbol{r}_3-\boldsymbol{r}_1-\boldsymbol{r}_2}{\sqrt{3}}, \tag{21}$$

and minimize approximately Eq. (19) with the Gaussian trial wave function

$$\Psi_0(\boldsymbol{\rho},\boldsymbol{\lambda})=\left(\frac{\alpha^2}{\pi^2}\right)^{3/4}\exp\left[-\frac{\alpha}{2}(\boldsymbol{\rho}^2+\boldsymbol{\lambda}^2)\right], \tag{22}$$

which is the exact solution for Eq. (20) provided $\alpha=\sqrt{Km}$.

For the spin $S=3/2$ baryons, this symmetric orbital wave function is associated with a symmetric isospin wave function and a symmetric spin state such as $|\uparrow\uparrow\uparrow\rangle$.

For the nucleon, a mixed-symmetric spin doublet (here for $S_z=+1/2$),

$$S_{\rho,\lambda}=\left\{\frac{|\uparrow\downarrow\uparrow\rangle-|\downarrow\uparrow\uparrow\rangle}{\sqrt{2}},\frac{2|\uparrow\uparrow\downarrow\rangle-|\downarrow\uparrow\uparrow\rangle-|\uparrow\downarrow\uparrow\rangle}{\sqrt{6}}\right\} \tag{23}$$

is combined to an isospin doublet (here for proton)

$$I_{\rho,\lambda}=\left\{\frac{(udu)-(duu)}{\sqrt{2}},\frac{2(uud)-(duu)-(udu)}{\sqrt{6}}\right\} \tag{24}$$

in a spin-isospin wave function

$$(S_\lambda I_\lambda + S_\rho I_\rho)/\sqrt{2} \tag{25}$$

which is symmetric under permutations. The extension to unequal masses is straightforward.

It is amazing that simple potential models provide a good survey of ground-state baryons with various flavor content. If the potential V is taken as flavor independent, as suggested by QCD, then the Schrödinger equation exhibits regularity and convexity properties (Richard, 1992; Nussinov and Lampert, 2002). For instance,

$$M_{QQq} + M_{qqq} < 2M_{Qqq} \quad \text{if } Q \neq q. \tag{26}$$

2. From mesons to baryons

In most papers dealing with potential models of baryons, a pairwise interaction is assumed,

$$V(\boldsymbol{r}_1,\boldsymbol{r}_2,\boldsymbol{r}_3) = \frac{1}{2}\sum_{i<j} v(r_{ij}), \tag{27}$$

for instance $v(r)=\sigma r - a/r + b$. It is then argued (Han and Nambu, 1965; Stanley and Robson, 1980; Greenberg and Lipkin, 1981; Richard, 1981) that the potential between two quarks in a baryon is half the quark-antiquark potential in a meson. This result is exact for the one-gluon-exchange potential, or, more generally, any color-octet exchange, which contains an explicit $\tilde{\lambda}_i \cdot \tilde{\lambda}_j$ color operator, with expectation values $-16/3$ for $3\times\bar{3}\to 1$ and $-8/3$ for $3\times 3\to\bar{3}$. This 1/2 rule also holds if two quarks are close together and seen by the third one as a localized $\bar{3}$ source, which is equivalent to an antiquark. More generally, the t-channel color structure of v contains a singlet and an octet. The singlet cannot contribute to confinement, otherwise all quarks of the universe would be tightly bound. The simplest ansatz is to assume a pure color octet exchange, and this is why a factor of 1/2 is introduced in Eq. (27).

With this 1/2 rule, Hall-Post type of inequalities can be derived between meson and baryon ground-state masses (Richard, 1992). The simplest is for spin-averaged mass values

$$M_{Q\bar{Q}}/2 \leqslant M_{QQQ}/3, \tag{28}$$

satisfied by $\phi(1020)$ and $\Omega^-(1672)$.

QCD suggests that the linear potential $v(r)=\sigma r$ acting on the quark-antiquark pair of mesons is not generalized as $\sigma\Sigma r_{ij}/2$ in baryons, but by the so-called Y-shape potential

$$V(\boldsymbol{r}_1,\boldsymbol{r}_2,\boldsymbol{r}_3) = \sigma \min(d_1+d_2+d_3), \tag{29}$$

where d_i is the distance of a junction to the ith quark. Adjusting the location of the junction corresponds to the problem of Fermat and Torriccelli, whose generalization to more than three terminals is called the minimal Steiner-tree problem. If an angle of triangle is larger than 120°, then the junction coincides with this vertex, otherwise it views each side under 120°, as shown in Fig. 34.

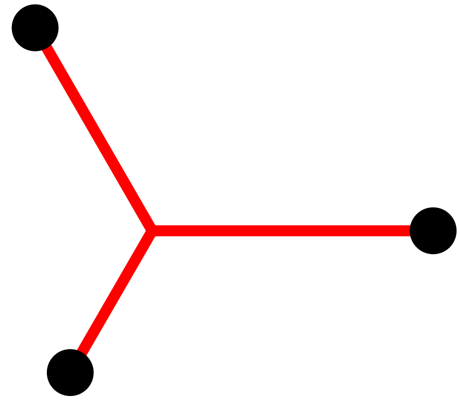

FIG. 34. (Color online) Three-quark confinement in the string limit.

Unfortunately, V given by the Y-shape potential (29) differs little from the result of the 1/2 rule, and one cannot probe this three-body dynamics from the baryon spectrum. The difference between the additive model $V \propto \Sigma\tilde{\lambda}_i\cdot\tilde{\lambda}_j v(r_{ij})$ and the minimal-path ansatz (Steiner tree) becomes more dramatic in the multiquark sector (Vijande *et al.*, 2007).

3. Hyperfine forces

To explain why the Δ with spin 3/2 is above the nucleon of spin 1/2, and similarly $\Sigma^* > \Sigma$, $\Xi^* > \Xi$, etc., the spin-independent potential V has to be supplemented by a spin-spin term, which is usually treated at first order, but sometimes nonpertubatively, after suitable regularization.

a. Chromomagnetism

The most popular model is the one-gluon exchange (De Rújula *et al.*, 1975), inspired by the Breit-Fermi term of QED. A slightly more general formulation involves a *chromomagnetic* interaction of the form

$$V_{\rm CM} = \sum_{i<j} \frac{\tilde{\lambda}_i^{(c)}\cdot\lambda_j^{(c)}\boldsymbol{\sigma}_i\cdot\boldsymbol{\sigma}_j}{m_i m_j} v_{ss}(r_{ij}), \tag{30}$$

where v_{ss} is short ranged. One of the most striking success of chromomagnetism is the explanation of the Σ-Λ splitting. For both states, $\Sigma_{i<j}\sigma_i\cdot\sigma_j = -3$ since we have an overall spin $S=1/2$. However, for the Λ, this strength is concentrated into the light-quark pair, and thus the downward shift is more important due to the $m_i^{-1}m_j^{-1}$ dependence of the operator (30).

Another success is the prediction of the hyperfine splittings when the strange quark is replaced by a quark with charm or beauty. While the Σ-Λ mass difference remains large, the Σ^*-Σ gap is much reduced. This is exactly the pattern observed for charm and beauty baryons; see Richard and Taxil (1983) for a study on how this effect depends on the assumed shape of the confining potential $v(r)$. The subtle interplay between the $m_i^{-1}m_j^{-1}$ dependence of the chromomagnetic operator and the short-range correlation induced by the central potential has been analyzed for beauty baryons, leading to successful predictions; see Karliner *et al.* (2009), and references therein.

b. Instantons, good diquarks

It has been stressed that chromomagnetism is not the unique solution. In particular, an *instanton-induced* interaction ('t Hooft, 1976) also accounts well for the hyperfine splittings; see Shuryak and Rosner (1989), Löring *et al.* (2001a), and Semay *et al.* (2001). It can be written as

$$V_{SS} = -4\sum_{i<j} g_{ij}\mathcal{P}^{[i,j]}\mathcal{P}^{S=0}\delta^{(3)}(\boldsymbol{r}_j - \boldsymbol{r}_j), \tag{31}$$

with the projection on the spin $S=0$ state and on the antisymmetric flavor state for each pair. The dimensionless coupling g_{ij} is stronger for light quarks than for $[ns]$. This explains the Σ-Λ mass difference, and other splittings within the ground states. Of course, the instanton-induced interaction differs more strikingly from chromomagnetism in the case of mesons, in particular for pseudoscalar and scalar mesons (Klempt *et al.*, 1995).

An interesting concept has been introduced (Wilczek, 2004; Jaffe, 2005), that of *good diquarks* with spin $S=0$, which is lower in mass than its vector counter part with $S=1$. For light quarks, the favored pair is in an antisymmetric isospin state $I=0$. Then the spectrum can be analyzed without referring to a specific dynamical model for the hyperfine interaction. However, this concept has been often associated to an extreme quark-diquark picture of baryon excitations, with many fewer levels than in the usual three-quark picture. Also, the concept of good diquark became rather sulfurous when associated to speculations about multiquark states which were neither supported by genuine few-body calculations nor confirmed by the data. We use here the concept of good diquark without endorsing its more extreme developments.

Note that the diquark model was discovered much earlier, and has been often rediscovered. For a historical survey, see Lichtenberg (1996).

c. Goldstone boson exchange

In conventional potential models, one starts with a degenerate ground state near 1100 MeV, and then a splitting between the N and Δ is introduced. Recently models have been developed where one starts from a unique state near 2 GeV, and then introduces a Goldstone-boson exchange (GBE) that reads (Glozman and Riska, 1996)

$$V_{\mathrm{OGE}} = \sum_{i<j} \frac{g^2}{4\pi}\frac{1}{4m_i m_j}\tilde{\lambda}_i^F \cdot \tilde{\lambda}_j^F \boldsymbol{\sigma}_i \cdot \boldsymbol{\sigma}_j \left[\frac{\mu^2 \exp(-\mu r_{ij})}{r_{ij}} - 4\pi\delta^{(3)}(\boldsymbol{r}_{ij})\right], \tag{32}$$

which pushes down both N and Δ but the former with larger strength.

This interaction is inspired by the one-pion-exchange potential in nuclear physics. However, in describing the nucleon-nucleon interaction, the contact term is usually neglected, as hidden by all uncertainties about the origin of the hard-core interaction at short distances. Here this is the reverse: the Yukawa tail plays a minor role, and the splitting of baryons is due to the contact term, which is regularized in explicit models exploiting this dynamics.

We note in this approach an important flavor dependence, as the pion does not couple to heavy quarks. It is not obvious how this interaction has to be adapted to the meson sector.

The GBE model has been studied by several groups, in particular Dziembowski *et al.* (1996), Valcarce *et al.* (1996), and Melde *et al.* (2008).

4. Improved pictures of ground-state baryons

The naive quark model, with its nonrelativistic kinematics, frozen number of constituents, instantaneous interaction, etc., is far from being fully satisfactory. Several improved pictured have been proposed. We review some of them. However, in a review devoted to baryon spectroscopy, we cannot set on the same footing constituent models giving predictions for the whole spectrum of excited states and sophisticated QCD-inspired studies, which are restricted to the ground state or at most to the first excitations.

a. Quark models with relativistic kinematics

It is now rather customary to replace the nonrelativistic contribution of constituent mass and kinetic energy, $m+p^2/2$, by the relativistic operator $(m^2+p^2)^{1/2}$. Examples are given in Basdevant and Boukraa (1986) and Capstick and Isgur (1986). This is more satisfactory, but does not solve the problems inherent to the choice of the dynamics. For instance, with a standard Coulomb-plus-linear interaction, the lowest nucleon excitation has negative parity.

b. Relativistic quark models

This is a more ambitious approach, aiming at a covariant formalism, even though some approximations are eventually unavoidable in the calculations. A recent example is given by Melde *et al.* (2008) and a benchmark is the work by the Bonn group (Löring, Kretzschmar, *et al.*, 2001; Löring *et al.* 2001a, 2001b; Metsch *et al.*, 2003; Migura *et al.*, 2006a), whose starting point is the Bethe-Salpeter equation. Here not only the masses and the static properties can be estimated, but also the form factors and quark distributions (Haupt *et al.*, 2006; Migura *et al.*, 2006b; Van Dyck *et al.*, 2008).

c. The MIT bag model

The MIT bag model stages massless or very light quarks moving freely inside of cavity of radius R, which is adjusted to minimize the bag energy. A good fit to the ground states of light baryons was achieved (De Grand *et al.*, 1975), and this model motivated a variety of developments. However, the model does not permit an easy estimate of the excitation spectrum. In particular, the center-of-mass motion cannot be removed explicitly.

d. The bag model for heavy quarks

The MIT bag model is not suited for heavy quarks. For heavy $(Q\bar{Q})$ or (QQQ), Hasenfratz and Kuti (1978) built a bag to confine the gluon field for any given quark configuration. The gluon energy is interpreted as the quark potential. Note that in the case of baryons (Hasenfratz *et al.*, 1980) this model leads to a Y-shape interaction, as discussed above. The case of hadrons with both heavy and light quarks is less easy; see Bernotas and Simonis (2008) for a recent update.

e. The cloudy bag

A problem with the MIT bag model is the discontinuity of the axial-vector current across the bag surface; or in a more empirical point of view, two nucleons do not interact once their separation exceeds twice the bag radius. Introducing a pion field around the nucleon (Brown and Rho, 1979) or even inside (Thomas *et al.*, 1981) restores a more physical picture.

Starting from a bag of large radius $R \sim 1$ fm, one ends with a smaller radius $R < 1$ fm for the three-quark domain, and a pion field extending beyond 1 fm. In fact R is not sharply determined, and the Stony Brook group got even variants with rather small radius.[1] In this limit, the details of the quark part become invisible: the quark core serves a source of the pion field, and carries the baryon number, and one recovers the skyrmion model and other soliton models.

f. Skyrmions and other soliton models

In this approach, the main emphasis is the coupling of meson to baryons. Hence the aim is less to perfectly reproduce the spectrum of high excitations than to account for the low-energy interactions. For a survey, references, and comparison with experimental data, see Karliner and Mattis (1986) and Weigel (2008). There are many variants, in particular in the way of treating strangeness and heavier flavors. For instance, Rho *et al.* (1992) considered the hyperons as bound states of a topological soliton and K, D, or B mesons.

g. Chiral perturbation theory and beyond

There is an idea by Weinberg and others that QCD is replaced at low energy by effective Lagrangians which share the same symmetries. The couplings are treated as free parameters and are used (consistently, i.e., at the same order in the expansion in powers of the momentum and quark masses) to calculate other properties. After fruitful developments in the physics of mesons (Donoghue *et al.*, 1989; Ecker *et al.*, 1989), this approach was also applied to nucleons (Bernard *et al.*, 1995) and became widely used. At small energies, chiral perturbation theory is exact. An extension to higher energies is possible by implementation of unitarity (Oller *et al.*, 2000). Further developments include strangeness, in particular to describe the $\Lambda_{1/2^-}(1405)$, and exact gauge invariance for photoproduction (Borasoy *et al.*, 2007); see Bernard (2008) for a recent survey.

[1]In an ideal scenario, there is a perfect duality between the three-quark and the pion field pictures, named the "Cheshire-cat principle" (Nadkarni and Nielsen, 1986).

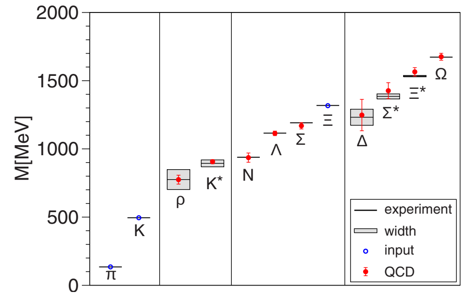

FIG. 35. (Color online) The light hadron spectrum of QCD. Horizontal lines and bands are the experimental values with their decay widths. The lattice results are shown by solid circles. Vertical error bars represent the combined statistical and systematic error estimates. π, K, and Ξ masses input quantities.

h. QCD sum rules

This approach to nonperturbative QCD was initiated by Shifman *et al.* (1979), and then developed by several groups. For a summary of early applications, see Reinders *et al.* (1985). The extension to baryons is nontrivial, since several operators can be chosen to describe a given state. After a pioneering paper (Ioffe, 1981), the situation was clarified in Chung *et al.* (1982), and subsequent papers devoted to various flavor combinations (Dosch *et al.*, 1989; Bagan *et al.*, 1993, 1994). Recently sum rules were extended to cover octet-decuplet splittings of heavy baryons (Albuquerque *et al.*, 2009).

The idea is to link, via analytical properties, the perturbative domain of QCD, where calculations can be done exactly, and the nonperturbative domain, which can be described in terms of a few basic constants. These can be adjusted forming a few physical quantities, which can be used to calculate other quantities.

i. Lattice QCD

Here QCD is reformulated as a field theory in a discretized phase space and solved using astute and powerful techniques which require, however, expensive computing means. In the domain of hadron spectroscopy, the best-known applications of lattice QCD are those dealing with glueballs and hybrid mesons, and also scalar mesons, but recently the physics of baryons has also been studied. Figure 35 shows the achievements of lattice QCD. Pion masses down to 190 MeV were used to extrapolate to the physical point and lattice sizes of up to 6 fm (Dürr *et al.*, 2008). Lattice techniques have also been applied to single-charm baryons (Lewis *et al.*, 2001) and even to double-charm baryons (Flynn *et al.*, 2003; Brambilla *et al.*, 2004).

C. Phenomenology of ground-state baryons

1. Missing states

Almost all ground-state baryons containing light or strange quarks and at most one heavy quark are now identified. Still missing are the isospin partners Σ_b^0 and Ξ_b^0 and the spin excitations ($S=3/2$) of the recently discovered Ξ_b and Ω_b.

The existence of $\Xi_{cc}^+(3519)$ is uncertain. Its predicted mass (Fleck and Richard, 1989; Körner *et al.*, 1994) is about 100 MeV larger and recent calculations give even larger mass values. As compared to a naive equal spacing for $p(940)$, $\Lambda_c^+(2286)$, and Ξ_{cc}, the first correction is that Ξ_{cc} is shifted down by the heavy-heavy interaction in the chromoelectric sector, see Eq. (26). However, both p and Λ_c are shifted down by the favorable chromomagnetic interaction among light quarks.

As the $(b\bar{c})$ meson has been observed, one should be able to detect (bcq) baryons with charm and beauty, with two $S=1/2$ states in the ground state, and one $S=3/2$ state. Next will come the double-beauty sector, and ultimately baryons with three heavy quarks.

2. Regularities

The masses exhibit a smooth behavior in flavor space, which is compatible with the expectation based on potential models incorporating flavor independence. Moreover, "heavy-quark symmetry implies that all of the mass splittings are independent of the heavy-quark flavor," to quote Isgur and Wise (1991). A comparison is shown in Fig. 36 of the known single-charm and single-beauty baryons. The comparison suffers from the small number of beauty baryons but it is clearly seen that the cost of single-strangeness excitation Ξ_Q-Λ_Q is similar for $Q=c$ and b.

For the double-strangeness excitations, the $\Omega_b(6165)^0$ of DØ is problematic. Most models predict Ω_b with mass of about 6050 MeV, which is 110–120 MeV lower than the observed mass. The measurement by CDF, 6054 MeV, is in better agreement with the expectations.

3. Hyperfine splittings

The hyperfine splitting also varies smoothly from one configuration to another. This is compatible with the mass dependence introduced in the chromomagnetic model: an explicit $m_i^{-1}m_j^{-1}$ in the operator, which is partially cancelled out by the reinforcement of the short-range correlations when the masses increase. However, a similar pattern could be reached in other approaches to hyperfine splitting. Figure 37 shows the regularities of the hyperfine effects in hyperons when the heavy quark is varied.

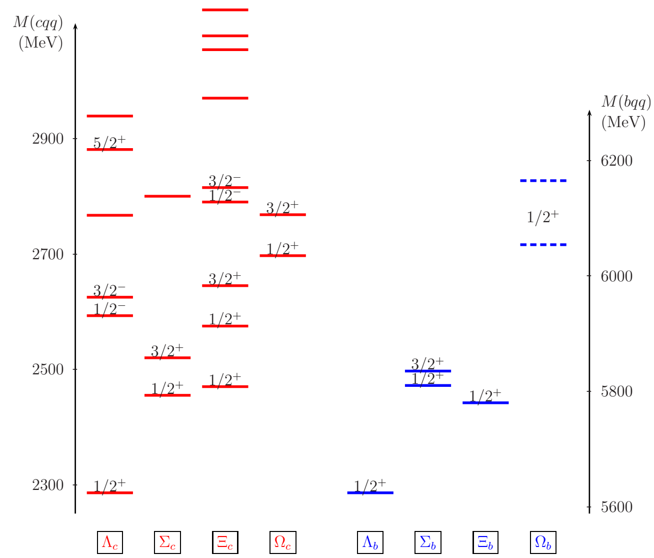

FIG. 36. (Color online) Comparison of the excitation energy single-charm and single-beauty baryons above the Λ_c (Λ_b mass). The quantum numbers are deduced from the quark model (Wohl, 2008a). For the Ω_b both DØ (top) and CDF (bottom) results are shown as dotted lines.

The Σ_Q^*-Σ_Q is expected to vanish as $M_Q \to \infty$, with a M_Q^{-1} in the limit where the change of the wave function is neglected. In this limit, the combination $2\Sigma_Q^* + \Sigma_Q - 3\Lambda_Q$ is expected to be constant, and this is rather well confirmed by the data, with about 613, 634, and 618 MeV for $Q=s$, c, and b, respectively.

To a good approximation, the hyperfine effect in the pair q_1q_2 is found independent of the third quark, this leading to a variety of sum rules if taken seriously; see, Lichtenberg *et al.* (1996) and Franklin (2008). Within the point of view of good diquarks, one can, indeed, measure the downward shift due to quark pairs in spin singlet, starting from the $S=3/2$ baryon where all pairs are in a spin triplet. As seen in Table XIV, one obtains $[ud] \approx 250$ MeV, for $[us] \approx 170$ MeV, $[uc] \approx 65$ MeV, and $[ub] \approx 20$ MeV.

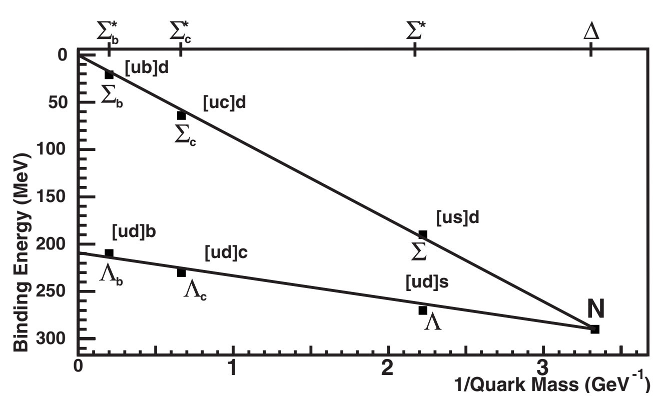

FIG. 37. Mass difference between spin-3/2 baryons (Δ, Σ^*, Σ_c^*, Σ_b^*) and spin-1/2 baryons. In spin-1/2 baryons, the light-light or a heavy-light-quark pair can have spin zero. The spin-0 diquark is indicated by $[q_1q_2]$. The masses are drawn as a function of the inverse (constituent) quark mass.

TABLE XIV. Masses (in MeV) of Λ and Σ and $\Sigma*$ baryons quoted from (Amsler *et al.*, 2008), and mass gaps δM between $J^P=1/2^+$ baryons containing "good" diquarks and $J^P=3/2^+$ baryons with all pairs in spin triplet. The quantum numbers of the heavy baryons are quark-model predictions.

1/2	Mass	1/2	Mass	3/2	Mass
Λ^0	1115.68 ± 0.01	Σ^0	1192.64 ± 0.04	$\Sigma*^0$	1383.7 ± 1.0
δM	$[ud]=-271$		$[us]=-191$		0 MeV
Λ_c^0	2286.46 ± 0.14	Σ_c^0	2457.76 ± 0.18	Σ_c^{*0}	2518.0 ± 0.5
δM	$[ud]=-231$		$[uc]=-60$		0 MeV
Λ_b^0	5619.7 ± 1.7	Σ_b^0	5811.5 ± 1.7	Σ_b^{*0}	5832.7 ± 1.9
δM	$[ud]=-213$		$[ub]=-21$		0 MeV
Ξ_c^0	2471.0 ± 0.4	$\Xi_c'^0$	2578.0 ± 2.9	Ξ_c^{*0}	2646.1 ± 1.2
δM	$[ds]=-174$		$[dc]=-70$		0 MeV

4. Isospin splittings

This was a subject of many investigations. Before the quark model, the neutron to proton mass difference has been given by Cottingham (1963) to electron-nucleon scattering. In the quark model, as discussed in Isgur (1980), there are many contributions to mass differences within an isospin multiplets, and the various terms often tend to cancel. There are the quark-mass difference $m_d - m_u$, the induced change of chromoelectric energy, the change in the strength of the chromomagnetic forces, the Coulomb repulsion, the magnetic interaction, etc. The effects have been estimated (Isgur, 1980; Varga *et al.*, 1999) and extended to heavy quarks (Lichtenberg, 1977; Franklin, 1999). There is also a contribution to isospin splittings from meson loops, with pions and baryons in the loops having different masses and couplings. This effect was emphasized recently for heavy baryons (Guo *et al.*, 2008).

D. Models of baryon excitations

While for the ground-state baryons there is a variety of pictures, some of them being directly guided by QCD, for the excitation spectrum, one should still rely on explicit constituent models, and among them the harmonic oscillator.

1. Harmonic oscillator

a. HO: equal masses

This is the simplest model, corresponding to Eq. (19) with all $m_i=m$ and Eq. (20). Then the relative motion is described by

$$\frac{\boldsymbol{p}_\rho^2}{m} + K\boldsymbol{\rho}^2 + \frac{\boldsymbol{p}_\lambda^2}{m} + K\boldsymbol{\lambda}^2, \tag{33}$$

leading the energy spectrum

$$\sqrt{\frac{K}{m}}(6 + 2l_\rho + 4\mathrm{n}_\rho + 2l_\lambda + 4\mathrm{n}_\lambda) = \sqrt{\frac{K}{m}}(6 + 2\mathsf{N}), \tag{34}$$

in an obvious notation for the orbital momenta $l_{\rho,\lambda} = 0,1,\ldots$ and radial numbers $\mathrm{n}_{\rho,\lambda}=0,1,\ldots$ attached to each degree of freedom. The wave functions are also explicitly known. For the ground state, it is the Gaussian (22). For excitations, it also contains a polynomial which reflects the rotation and permutation properties and ensures the orthogonality.

Note the first radial excitation of the nucleon and Δ, a symmetric combination of the states with $l_\rho=l_\lambda=0$ and either $\mathrm{n}_{\rho,\lambda}=(0,1)$ or (1, 0), which is *below* the first negative-parity excitation. This will be further discussed in connection with alternative models and with the data.

b. HO: unequal masses

For baryons with one heavy quark, (qqQ), the masses are (m,m,M). The case of double-charm baryons is deduced by $m \leftrightarrow M$. The second term in Eq. (33) has now a reduced mass μ with $\mu^{-1}=(2M^{-1}+m^{-1})/3$ replacing m. Then the energy levels are modified as

$$\sqrt{\frac{K}{m}}(3 + 2l_\rho + 4\mathrm{n}_\rho) + \sqrt{\frac{K}{\mu}}(3 + 2l_\lambda + 4\mathrm{n}_\lambda). \tag{35}$$

Hence the λ excitation are lower than their ρ analogs for single-flavor baryons. For baryons with double flavor, the first excitation are within the heavy-quark sector. The wave function is a slight generalization of Eq. (22), with $\sqrt{Km}\rho^2+\sqrt{K\mu}\lambda^2$ in the Gaussian and the corresponding changes in the normalization.

If the three constituents masses are different, then the Hamiltonian describing the relative motion is still of the type

$$\frac{\boldsymbol{p}_x^2}{m_x} + K\boldsymbol{x}^2 + \frac{\boldsymbol{p}_y^2}{m_y} + K\boldsymbol{y}^2, \tag{36}$$

with $\boldsymbol{x}$ and $\boldsymbol{y}$ combinations of the Jacobi variables ρ and λ which are obtained together with the reduced masses m_x and m_y by the diagonalization of a 2×2 matrix.

2. Potential models

If the potential V is not harmonic, the nonrelativistic Hamiltonian (19) can be solved numerically using powerful techniques developed in nuclear physics, such as Faddeev equations, hyperspherical expansion, or correlated Gaussians. While convergence is easily reached for the energy levels, some additional effort is usually required to measure the short-range correlations within the wave function.

Some approximations can be envisaged as an alternative to the full three-body calculation. Some of them are purely technical, for instance, truncating the hyperspherical expansion to the lowest partial wave. Others shed some light on the baryon structure. For instance, doubly-flavored baryons (QQq) have clear diquark-quark structure, but the internal diquark dynamics is influenced by the third quark, an effect which is unfortunately often forgotten.[2] (QQq) can also be treated H_2^+ in atomic physics, with QQ moving in a Born-Oppenheimer potential generated by the light degrees of freedom (Fleck and Richard, 1989).

It should be stressed that different models used for the interquark potential give similar ordering for the first levels. In the HO, the radial excitation energy is twice the orbital one. With a linear confinement, the ratio is smaller, but the radial excitation still remains above the orbital one, if the potential is local and flavor independent (Hogaasen and Richard, 1983). Pushing the radial excitation below the orbital one require drastic changes of the dynamics, like these of the OBE model.

3. Relativistic models

For relativistic models, the solution can be found by variational methods, i.e., by expanding the wave function on a basis, usually chosen as containing Gaussians of different range parameters. The level order of the first levels is similar to the pattern found in nonrelativistic models.

For high orbital excitations, an interesting result was obtained (Martin, 1986). The levels are well described in the semiclassical approximation. For low L, the lowest state is symmetric, all quarks sharing equally the orbital momentum. For higher L, there is a spontaneous breaking of symmetry, and in the ground state, two quarks have a relative $l_\rho=0$ while the third quark takes $l_\lambda=L$. Hence diquarks are generated *dynamically* at high L, even for a purely linear interaction. There is no need for short-range forces to form the diquark. With relativistic kinematics and linear confinement, both in the naive 1/2 rule version [Eq. (27)] or in the more elaborate Y-shape version [Eq. (29)] a linear Regge trajectory is obtained, with the same slope as for mesons.

4. Regge phenomenology

The Regge theory, first developed by Regge (1959, 1960), connects the high-energy behavior of the scattering amplitude with singularities in the complex angular momentum plane of the partial-wave amplitudes in the crossed (t) channel. It is based on rather general properties of the S matrix, on unitarity, analyticity, and crossing symmetry. The simplest singularities are poles (Regge poles). According to the Chew-Frautschi conjecture (Chew and Frautschi, 1961, 1962), the poles fall onto linear trajectories in M^2,J planes. In the Regge theory, the t-channel exchange of a particle with spin J is replaced by the exchange of a trajectory. Regge-trajectory exchange is thus a natural generalization of a usual exchange of a particle with spin J to complex values of J. The method established an important connection between high-energy scattering and the spectrum of hadrons. There is a discussion if Regge trajectories are linear, parallel, or not (Tang and Norbury, 2000; Inopin and Sharov, 2001). No systematic errors in the mass assignments were, however, included in these discussions. We assume linearity and do not see any significant deviation from linear trajectories.

[2] In the case of the harmonic oscillator, exactly 1/3 of the strength binding QQ is due to the third quark.

5. Solving QCD

a. QCD sum rules, lattice QCD

In QCD sum rules or in lattice QCD, one can reach the ground-state configuration of any given set of quantum numbers, in particular the leading Regge trajectory. The difficulty is only to build the corresponding operators.

The first excitations of the nucleons have received much attention (Melnitchouk *et al.*, 2003). With the large lattices available, one could presumably get access to the states on the leading Regge trajectory, each being the ground state in its J^P sector. This is probably delicate for the radial excitations, which are derived from the same operator as the lowest states and where one should first remove the leading contribution of the ground state. The theoretical uncertainty is thus larger. The question is whether, when the light-quark mass vanishes, one observes a change in the hierarchy of excitation, with the positive-parity excitation becoming lower than the negative-parity one. This is still controversial. The latest results are, however, encouraging: Mathur *et al.* (2005) compared the radial and orbital excitations of the nucleon as a function of the assumed light-quark mass m_n, and found that the former is usually above the latter except for very small m_n, where a crossing is observed, and thus the same ordering as the experimental one. This result indicates that the anomalous ordering is particular to the light-quark dynamics. It remains to be checked by others with attention in particular to finite size effects (Sasaki and Sasaki, 2005). Among the recent contributions, see Mathur *et al.* (2005), Sasaki *et al.* (2005), Basak *et al.* (2007), Drach *et al.* (2008), and Bulava *et al.* (2009). In this latter article, excitations up to $J=5/2$ have been studied.

b. AdS/QCD

A new approach to quantum field theory is presently pursued, the so-called AdS/CFT correspondence (anti de Sitter/conformal field theory), which establishes a duality between string theories defined on the five-dimensional AdS space-time and conformal field theo-

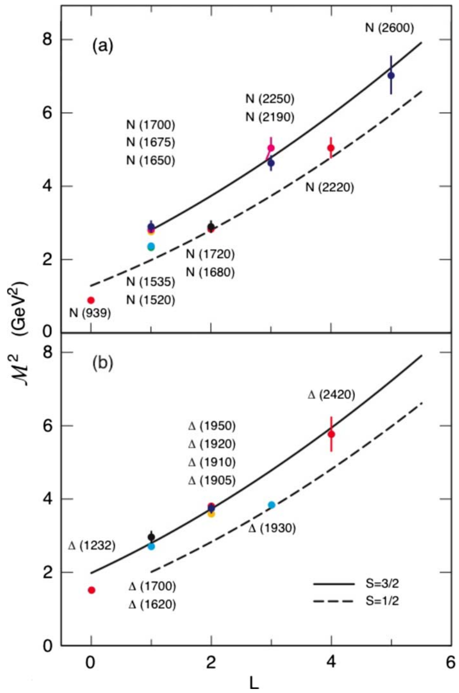

FIG. 38. (Color online) Light baryon orbital spectrum for (a) N^* and (b) Δ^*. The lower dashed curves correspond to baryon states dual to spin-1/2 modes in the bulk and the upper continuous curve to states dual to spin-3/2 modes. From de Teramond and Brodsky, 2005.

ries in physical space-time; see, Brodsky (2007). It is assumed that the effective strong coupling is approximately constant in an appropriate range of momentum transfer, and that the quark masses can be neglected. Then QCD becomes a nearly conformal field theory and the AdS/CFT correspondence can be applied to QCD. The hadron spectrum and strong interaction dynamics can then be calculated from a holographic dual string theory defined on five-dimensional AdS space. For an appropriate choice of the metrics, a semiclassical approximation to QCD follows which incorporates both color confinement and conformal short-distance behavior. Confinement is parametrized by a cutoff in AdS space in the infrared region ("hard wall") (Polchinski and Strassler, 2002). Applied to baryon spectroscopy, AdS/QCD yields a mass relation $M \propto L + \mathrm{N}$ (de Teramond and Brodsky, 2005; Brodsky and de Teramond, 2008), where L and N are orbital and radial excitation quantum numbers corresponding to $L = l_\rho + l_\lambda$ and $\mathrm{N} = \mathrm{n}_\rho + \mathrm{n}_\lambda$ in quark models. Spin 1/2 and 3/2 baryons require different AdS boundary conditions and lead to different offset masses. The predictions are shown in Fig. 38. The lower mass of nucleon resonances with $S = 1/2$ can be related to the effect of "good" diquarks (Jaffe and Wilczek, 2003; Wilczek, 2004): diquarks with vanishing spin and isospin are energetically favored compared to "bad" diquarks. Of course, Δ resonances have isospin 3/2 and contain no good diquarks. Problems occur for $\Delta(1232)$ which is too low in mass and for $\Delta_{1/2^-}(1620)$ and $\Delta_{3/2^-}(1700)$ which are on the "wrong" trajectory. $\Delta_{5/2^-}(1930)$ is treated as spin 1/2 state with $L = 3$; in Sec. IV.F, this state is combined with $\Delta_{1/2^-}(1900)$ and $\Delta_{3/2^-}(1940)$ to form a triplet with $L = 1$, $S = 3/2$, $N = 1$ quantum numbers in the third-excitation band. (de Teramond and Brodsky, 2005) require the existence of a further to-be-discovered Δ state with $J^P = 7/2^-$ at 1.9 to 2.0 GeV.

The use of orbital angular momentum L to classify baryon resonances has been often criticized, see Afonin (2009), de Teramond and Brodsky (2009), and Glozman (2009), for a refutation. In nonrelativistic models with anharmonic confinement and spin-dependent forces, and in relativistic models better suited for light quarks, each state contains a superposition of several angular momentum configurations. However, quark models with the same constituent quark rest mass for all excitations are probably not realistic. An alternative is the Nambu picture (Nambu and Jona-Lasinio, 1961) where the mass of a hadron is distributed along a string connecting nearly massless quarks. Perhaps the total angular momentum L occurring in recent mass formulas reflects the length of the inner flux tube linking the quarks.

Forkel *et al.* (2007a, 2007b) predicted the mass spectrum of light mesons and baryons using AdS/QCD in the soft-wall approximation. The approach relies on deformations of the AdS metric, governed by one free mass scale proportional to Λ_{QCD} and leads to the same boundary conditions for $S = 1/2$ and 3/2 baryons. Relations between ground-state masses and trajectory slopes

$$
\begin{aligned}
M^2 &= 4\lambda^2(\mathrm{L} + \mathrm{N} + 1/2), \quad \text{for mesons} \\
M^2 &= 4\lambda^2(\mathrm{L} + \mathrm{N} + 3/2), \quad \text{for baryons}
\end{aligned}
\tag{37}
$$

were derived. Using the slope of the Δ trajectory, baryon masses were calculated. However, it is argued (Forkel *et al.*, 2007b) that hyperfine interactions are not included in AdS/QCD and that the parameter λ in Eq. (37) should be re-tuned. This changes the offset (the predicted ground-state mass) and the Regge slope, and the result-

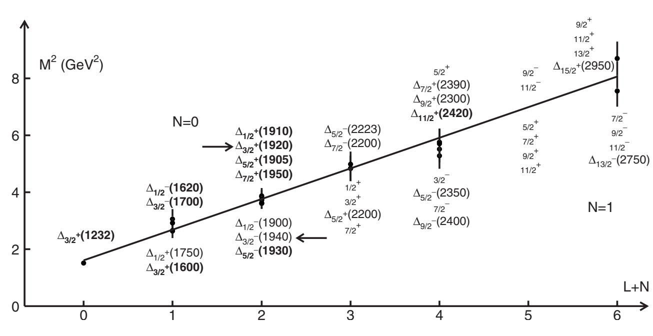

FIG. 39. Regge trajectory for Δ^* resonances as a function of the leading intrinsic orbital angular momentum L and the radial excitation quantum number N (corresponding to $n_1 + n_2$ in quark models) (Klempt, 2008). The line represents a prediction based on AdS/QCD correspondence (soft wall) (Forkel *et al.*, 2007a, 2007b). Resonances with N=0 and 1 are listed above or below the trajectory. The mass predictions are 1.27, 1.64, 1.92, 2.20, 2.43, 2.64, 2.84 GeV for $L + \mathrm{N} = 0, 1, \ldots, 6$, respectively.

TABLE XV. Nucleon and Δ resonances and suggested quantum numbers. The predicted masses are calculated using Eq. (38).

L	N	S	α_D	Resonance	Pred.
0	0	1/2	1/2	$N_{1/2^+}(940)$	943
0	1	1/2	1/2	$N_{1/2^+}(1440)$	1396
0	2	1/2	1/2	$N_{1/2^+}(1710)$	1735
0	3	1/2	1/2	$N_{1/2^+}(2100)$	2017
1	0	1/2	1/4	$N_{1/2^-}(1535)$, $N_{3/2^-}(1520)$	1516
1	1	1/2	1/4	$N_{1/2^-}(1905)$, $N_{3/2^-}(1860)$	1833
1	2	1/2	1/4	$N_{1/2^-}(2090)$, $N_{3/2^-}(2080)$	2102
1	0	3/2	0	$N_{1/2^-}(1650)$, $N_{3/2^-}(1700)$, $N_{5/2^-}(1675)$	1628
2	0	1/2	1/2	$N_{3/2^+}(1720)$, $N_{5/2^+}(1680)$	1735
2	0	3/2	0	$N_{1/2^+}(1880)$, $N_{3/2^+}(1900)$, $N_{5/2^+}(1870)$, $N_{7/2^+}(1990)$	1932
3	0	1/2	1/4	$N_{5/2^-}(2200)$, $N_{7/2^-}(2190)$	2102
3	0	3/2	0	$N_{9/2^-}(2250)$	2184
4	0	1/2	1/2	$N_{9/2^+}(2220)$	2265
5	0	1/2	1/4	$N_{11/2^-}(2600)$	2557
6	0	1/2	1/2	$N_{13/2^+}(2700)$	2693
0	0	3/2	0	$\Delta_{3/2^+}(1232)$	1261
0	1	3/2	0	$\Delta_{3/2^+}(1600)$	1628
1	0	1/2	0	$\Delta_{1/2^-}(1620)$,	1628
1	1	3/2	0	$\Delta_{1/2^-}(1900)$, $\Delta_{3/2^-}(1940)$, $\Delta_{5/2^-}(1930)$	1926
1	2	1/2	0	$\Delta_{1/2^-}(2150)$	2184
2	0	3/2	0	$\Delta_{1/2^+}(1910)$, $\Delta_{3/2^+}(1920)$, $\Delta_{5/2^+}(1905)$, $\Delta_{7/2^+}(1950)$	1926
3	0	1/2	0	$\Delta_{7/2^-}(2200)$	2184
3	1	3/2	0	$\Delta_{5/2^-}(2350)$, $\Delta_{9/2^-}(2400)$	2415
4	0	3/2	0	$\Delta_{7/2^+}(2390)$, $\Delta_{9/2^+}(2300)$, $\Delta_{11/2^+}(2420)$	2415
5	1	3/2	0	$\Delta_{13/2^-}(2750)$	2820
6	0	3/2	0	$\Delta_{15/2^+}(2950)$	2820

ing compromise might show problems for small and large angular momenta.

The predicted masses for Δ baryons are plotted as a function of L+N in Fig. 39, which includes all resonances [except the one-star $\Delta_{1/2^-}(2150)$ which would fit well with quantum numbers L=1, N=2 and 2.2 GeV predicted mass]. The agreement is excellent and the remaining problems seen in Fig. 38(b) disappear.

For nucleon resonances, we need to keep track that some diquarks have spin zero and are in S wave. Then Eq. (37) is rewritten as (Forkel and Klempt, 2009)

$$M^2 = a(L + N + 3/2) - b\alpha_D \ [\mathrm{GeV}^2] \tag{38}$$

with a=1.04 GeV^2 and b=1.46 GeV^2. For the lowest states, α_D can be interpreted as the fraction of good diquarks and calculated explicitly from standard quark-model wave functions. In Table XV, the same α_D is assumed along a trajectory, and its coefficient b is tuned to reproduce the Δ(1232)-N(940) splitting. Also shown are the quark spin, the orbital angular momentum, and the radial quantum number N. It is remarkable that the masses of all 48 N and Δ resonances are well reproduced using just two parameters. One parameter is related to confinement and was already used to describe the Δ mass spectrum and the second one accounts for hyperfine effects. It reduces the size of the nucleon by a fraction which depends on α_D.

The precision of the mass calculated by Eq. (38) is by far better than quark-model predictions even though the latter have a significantly larger number of parameters. The mean difference $\delta M/M$ is 2.5% for Eq. (38), 5.6% for the Capstick-Isgur model (with seven parameters) (Capstick and Isgur, 1986), and 5.1% (5.4%) for the two variants of the Bonn model (Löring *et al.*, 2001a) (five parameters). The Skyrme model (Karliner, 1986) with two parameters predicts only half of the observed states, with $\delta M/M$=9.1%. The masses of Table XIII were used for the comparison.

6. Hyperon resonances

Little experimental information is added since the review of Hey and Kelly (1983). We note that the mass spectrum of strange baryons is well reproduced by adding a term

$$M^2_{\Sigma*(1385)} - M^2_{\Delta(1232)} = 0.40 \ [\mathrm{GeV}^2] \tag{39}$$

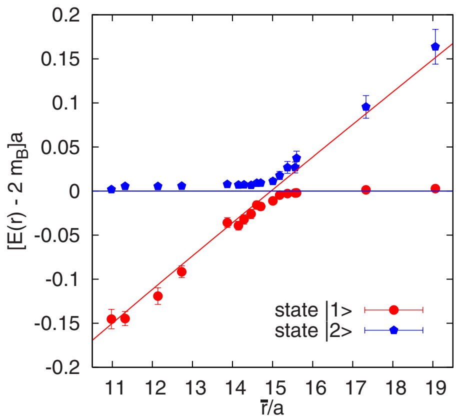

FIG. 40. (Color online) Pair creation on a lattice, calculated for mesons. A sea quark-antiquark pair is created in the vacuum. At large distances, two-meson states are energetically preferred. For static quarks, the levels cross at some distance R (with $a \approx 0.083$ fm), the string breaking introduces mixing of the energy levels defined by the potential $V(R)$ and the threshold $2m(B)$. From Michael, 2006.

to Eq. (38). The SU(3)$_f$ singlet states $\Lambda_{1/2^-}(1405)$, $\Lambda_{3/2^-}(1520)$, and probably $\Lambda_{7/2^-}(2100)$ have good-diquark fractions $\alpha_D = 3/2$.

E. Baryon decays

Hadron decays are a decisive element of any theory of strong interactions. The fact that so many resonances—expected in symmetric quark models—are missing in the data could find a natural explanation if the missing states have weak coupling only to $N\pi$. Indeed, this is what most models predict.

1. Hadron decays on the lattice

An intuitive understanding of hadron decays can be achieved by inspection of the potential energy between two static quarks. The energy can be described by the superposition of a Coulomb-like potential and a linearly rising (confinement) potential. At sufficiently large separations, for $R \approx 1.2$ fm, the total energy suffices to produce two (color-neutral) objects: string breaking occurs. String breaking in mesons can be simulated on a lattice (Michael, 2006). Figure 40 displays the energy levels due to a $q\bar{q}$ and a two-meson system in an adiabatic approximation. In a hadronic reaction, the sudden approximation—where the system follows the straight line—is more realistic, and mesons can be excited to large energies. Similar calculations for baryons have not yet been made but the physics picture should remain the same.

2. Models of hadron decays

The operators responsible for strong decays of baryon resonances are unknown. Models need to be constructed with some mechanism in mind; this can be either elementary meson emission from a baryon, quark pair creation, string breaking, or flux-tube breaking. In the latter three cases, a quark pair is created in a process which is often modeled by assuming $^3P_0$ quantum numbers for the quark pair. A survey of models, theoretical results, and a comparison with data is given by Capstick and Roberts (2000). They concluded that none of the models does "what can be termed an excellent job of describing what is known about baryon strong decays. The main features seem to be well described, but many of the details are simply incorrect." More recent widths calculations (Melde *et al.*, 2005; Sengl *et al.*, 2007) confirm this statement.

F. The band structure of baryon excitations

The harmonic oscillator provides a frame to classify baryons resonances. Nonharmonic corrections, relativistic effects, and in particular spin-dependent forces induce splitting of degenerate states and mixing of states with the same total spin and parity J^P but, of course, the number of expected states remains the same. In this section, the observed baryon resonances are mapped onto HO quark-model states, in an attempt to identify classes of resonances which are missing. The systematic of observed and missing resonances may provide hints at the dynamics, which lead to the observed spectrum of baryon resonances.

We focus the discussion on excited states of nucleon and Δ, and include low-mass Λ and Σ. There is not much known on the quantum numbers of Ξ and Ω baryons. An exception is the recent determination of the $\Xi_{1/2^+}(1690)$ quantum numbers from $\Lambda_c \to (\Lambda K_S^0)K^+$ decays (Petersen, 2006). A similar classification of baryon resonances was suggested by Melde *et al.* (2008). For low-lying states, most assignments agree; discrepancies show that the present data do not suffice to identify all states in a unique way.

1. First-excitation band

The first-excitation band $(D, L_N^P) = (70, 1_1^-)$ contains negative-parity resonances. With the SU(3)$_f$ decomposition

$$70 = {}^2 10 \oplus {}^4 8 \oplus {}^2 8 \oplus {}^2 1, \quad (40)$$

we expect as nonstrange baryons a SU(3)$_f$-octet spin doublet, a SU(3)$_f$-octet spin triplet (a degenerate quartet), and a SU(3)$_f$-decuplet spin doublet. In Table XVI, the low-mass negative-parity states are collected. The multiplet structure is easily recognized in the data. Configuration mixing is of course possible for states with the same J^P.

In the hyperon sector, a few expected states have not yet been observed. A missing state is indicated in Table XVI by an x. Based on Eqs. (37)–(39), we expect all missing Λ and Σ states to fall into the 1750–1850 MeV mass range. We have omitted the one-star $\Sigma_{3/2^-}(1580)$. The Crystal Ball Collaboration studied the reaction $K^- p \to \Lambda \pi^0$ in the c.m. energy range 1565–1600 MeV (Olmsted *et al.*, 2004). Their results disagreed with older

TABLE XVI. The negative-parity states of the first-excitation band $(D,L_{\mathrm{N}}^{P})=(70;1_1^-)$. An x stands for a missing state.

D; s	$J=1/2$	$J=3/2$	$J=5/2$
70, **8**; 1/2	$N_{1/2^-}(1535)$	$N_{3/2^-}(1520)$	
70, **8**; 3/2	$N_{1/2^-}(1650)$	$N_{3/2^-}(1700)$	$N_{5/2^-}(1675)$
70, **10**; 1/2	$\Delta_{1/2^-}(1620)$	$\Delta_{3/2^-}(1700)$	
1, **1**; 1/2	$\Lambda_{1/2^-}(1405)$	$\Lambda_{3/2^-}(1520)$	
70, **8**; 1/2	$\Lambda_{1/2^-}(1670)$	$\Lambda_{3/2^-}(1690)$	
70, **8**; 3/2	$\Lambda_{1/2^-}(1800)$	x	$\Lambda_{5/2^-}(1830)$
70, **8**; 1/2	$\Sigma_{1/2^-}(1620)$	$\Sigma_{3/2^-}(1670)$	
70, **8**; 3/2	$\Sigma_{1/2^-}(1750)$	x	$\Sigma_{5/2^-}(1775)$
70, **10**; 1/2	x	x	

fits which included the $\Sigma_{3/2^-}(1580)$ resonance. Instead, they proved the absence of any reasonably narrow resonance in this mass range.

In the Λ sector, the $\Lambda_{1/2^-}(1405)$ and $\Lambda_{3/2^-}(1520)$ are considerably lower in mass than $\Lambda_{1/2^-}(1670)$ and $\Lambda_{3/2^-}(1690)$. In quark models, this might be due to favorable hyperfine effects acting on a pair of light quarks with $l_\rho=0$ and spin 0. There is also a copious literature on the effect of coupling to decay channels, or multiquark components in these states (Choe, 1998; Oset and Ramos, 1998).

A similar effect can be observed in heavy-flavor baryons. The mass difference between the Λ_c^+ ground- state and the first-excited states (a doublet) is 325 MeV, rather low for an orbital excitation. Like the $\Lambda_{1/2^-}(1405)$, the two negative-parity states $\Lambda_c^+(2595)$ and $\Lambda_c^+(2625)$ benefit from the attractive spin-spin splitting for the light-quark pair.

The classification of low-mass negative-parity states in Table XVI is rather conventional. Nevertheless, we point out some trivialities. Pairs of states with $J^P=1/2^-$ or $3/2^-$ can mix [see Eq. (1) in Sec. I.C]. The mixing angle between the two $1/2^-$ states was calculated to be $-31.7°$ (Isgur and Karl, 1977); for the two $3/2^-$ states, it is 6°. The probability to find a $S=3/2$ in the $N_{1/2^-}(1535)$ is $\propto\sin^2\Theta_{1/2^-}=0.28$, and the mean mass separation between the triplet and the doublet is about 150 MeV. A mixing angle of 30° does not prevent identification of the leading component.

In this spirit, we try to also identify leading components for higher excitation bands. We are aware of the fact that with increasing mass the predicted complexity of the spectrum increases dramatically, and mixing of states is expected to become a severe problem. Hence the assignments will become more speculative. The reason why we include a discussion on higher excitation bands are threefold: First, there are unexpected clusters of resonances of different spin parities (but forming spin multiplets) spanning a narrow mass interval. Second, the observed multiplets can be arranged into a small number of (D,L_{N}^{P}) supermultiplets, which sometimes are completely filled while others remain empty. And third, the observed multiplets can be characterized by L and N, just those variables which result from AdS/QCD.

2. The second-excitation band

In the HO model, the second-excitation band contains states with either two units of angular momentum or one unit of radial excitation, with proper antisymmetrization in the case of identical quarks,

$$(D,L_{\mathrm{N}}^{P})=\underline{(56,2_2^+)},\underline{(70,2_2^+)}, \quad (41a)$$

$$(D,L_{\mathrm{N}}^{P})=(20,1_2^+), \quad (41b)$$

$$(D,L_{\mathrm{N}}^{P})=\underline{(56,0_2^+)},\underline{(70,0_2^+)}, \quad (41c)$$

either with $(l_\rho,l_\lambda)=(0,2)$ and $(2,0)$ yielding the $(56,2_2^+)$ multiplet or with $l_\rho,l_\lambda=1,1$ coupling to $L=0,1,2$ yielding $(70,2_2^+)$, $(20,1_2^+)$, and $(70,0_2^+)$. The $(56,0_2^+)$ supermultiplet comprises the first radial excitations with $(n_\rho,n_\lambda)=(0,1)$ or $(1,0)$. Both multiplets with $L^P=0$ contain nucleons with spin-parity $1/2^+$, while for decuplet states, $J^P=3/2^+$ for 56-plet members and $J^P=1/2^+$ for 70-plet members.

We begin with $(D,L_{\mathrm{N}}^{P})=(56,0_2^+)$. The most controversial state is the Roper resonance $N_{1/2^+}(1440)$. In the HO model, it is degenerate with other $N=2$ states, but in the experimental spectrum of the nucleon and Δ, it is almost degenerate, and even slightly below the $N=1$ states with negative parity. Anharmonic corrections push this state down, and this perturbative result is confirmed in the hypercentral approximation (Hogaasen and Richard, 1983), which is a better approximation to confinement that is not quadratic. Even in exact treatments of the three-body problem, but with local flavor-independent potentials of confining type, the Roper resonance comes always *above* the first negative-parity states.

The "wrong" mass of the Roper resonance has initiated a longstanding debate if it is dynamically generated or if it is the nucleon first radial excitation and a quark-model state. We think it is both. A discussion of the (im)possibility to distinguish meson-meson molecules from four-quark states can be found in Jaffe (2007). In Table XVII, the lowest-lying resonances having the same quantum numbers as their respective ground states and the mass square distance to them are listed. In colloquia, Nefkens calls them Roper, loper, soper, xoper, and doper (Nefkens, 2001), to underline that they play similar roles. If the Roper resonance should be generated by $\Delta\pi$ dynamics without any relation to the quark-model $(D,L_{\mathrm{N}}^{P})=(56,0_2^+)$ state, $\Sigma_{1/2^+}(1660)$ and $\Xi_{1/2^+}(1690)$ could be generated by the same mechanism [making use of $\Sigma_{3/2^+}(1385)\pi$ and $\Xi_{3/2^+}(1530)\pi$]. But there is no analogous mechanism which would lead to $\Lambda_{1/2^+}(1600)$ and $\Delta_{3/2^+}(1600)$. Understanding $N_{1/2^+}(1440)$ from the interaction of mesons and baryons is an important step in understanding baryons and their interactions; S-wave thresholds may have an important impact on the precise location of poles and on the observed

TABLE XVII. Members of the $(D,L_N^P)=(56,0_2^+)$ and $(D,L_N^P)=(70,0_2^+)$ multiplets in the second-excitation band and mass square difference (in GeV^2) to the respective ground state. The expected values for the mass square differences are 1.08 and 2.16 GeV^2, respectively [see Eq. (37) and Table XV]. An x stands for a missing state.

56, 8; 1/2	$N_{1/2^+}(1440)$	$\Lambda_{1/2^+}(1600)$	$\Sigma_{1/2^+}(1660)$	$\Xi_{1/2^+}(1690)$
δM^2	1.19 ± 0.11	1.31 ± 0.11	1.34 ± 0.11	1.13 ± 0.03
56, 10; 3/2	$\Delta_{3/2^+}(1600)$		x	x
δM^2	1.04 ± 0.15			
70, 8; 1/2	$N_{1/2^+}(1710)$	$\Lambda_{1/2^+}(1810)$	$\Sigma_{1/2^+}(1770)$	x
δM^2	2.04 ± 0.15	2.03 ± 0.15	1.72 ± 0.16	
70, 10; 1/2	$\Delta_{1/2^+}(1750)$		$\Sigma_{1/2^+}(1880)$	x
δM^2	1.54 ± 0.16		2.12 ± 0.11	

branching ratios. The pattern of states and their approximate mass values seem, however, not or hardly affected.

Commonly, $N_{1/2^+}(1710)$ and $\Delta_{1/2^+}(1750)$ are candidates assigned to $(D,L_N^P)=(70,0_2^+)$, and $\Sigma_{1/2^+}(1880)$ belongs to it as well. These baryons represent a new class: the two angular momenta l_ρ and l_λ are both one and couple to zero. $N_{1/2^+}(1710)$ could also be assigned to the fourth-excitation band, with two units of radial excitation, but this interpretation is forbidden for $\Delta_{1/2^+}(1750)$ and unlikely for $\Sigma_{1/2^+}(1880)$. The former is a one-star resonance, the latter one has two stars; the PDG entry $\Sigma_{1/2^+}(1880)$ represents all claims above $\Sigma_{1/2^+}(1770)$. Supposing their existence, we interpret the three states as members of the $(D,L^P)=(70,0^+)$ multiplet.

We now turn to $(D,L_N^P)=(56,2_2^+)$. In the nucleon spectrum, there should be (at 1.62 GeV) a spin doublet, in the Δ spectrum a spin quartet (at 1.92 GeV). These are all readily identified in the spectrum (see Table XVIII). For the Λ and Σ excitations, the corresponding states should be at 1.84 and 2.03 GeV. All but one state are observed.

TABLE XVIII. $(D,L_N^P)=(56,2_2^+)$, $(D,L_N^P)=(70,2_2^+)$, and $(D,L_N^P)=(20,1_2^+)$ resonances in the second-excitation band. An x stands for a missing state.

D; s	$J=1/2$	$J=3/2$	$J=5/2$	$J=7/2$
56, 8; 1/2		$N_{3/2^+}(1720)$	$N_{5/2^+}(1680)$	
56, 8; 1/2		$\Lambda_{3/2^+}(1890)$	$\Lambda_{5/2^+}(1820)$	
56, 8; 1/2		$\Sigma_{3/2^+}(1840)$	$\Sigma_{5/2^+}(1915)$	
56,10; 3/2	$\Delta_{1/2^+}(1910)$	$\Delta_{3/2^+}(1920)$	$\Delta_{5/2^+}(1905)$	$\Delta_{7/2^+}(1950)$
56,10; 3/2	x	$\Sigma_{3/2^+}(2080)$	$\Sigma_{5/2^+}(2070)$	$\Sigma_{7/2^+}(2030)$
70, 8; 3/2	$N_{1/2^+}(1880)$	$N_{3/2^+}(1900)$	$N_{5/2^+}(1870)$	$N_{7/2^+}(1990)$
70, 8; 3/2	x	x	$\Lambda_{5/2^+}(2110)$	$\Lambda_{7/2^+}(2020)$
70, 8; 3/2	x	x	x	(Σ)
70, 8; 1/2		x	x	(N,Λ,Σ)
70,10; 1/2		x	x	(Δ,Σ)
20, 8; 1/2	x	x		(N,Λ,Σ)

The situation is more difficult for $(D,L_N^P)=(70,2_2^+)$. We expect a spin doublet (1.78 GeV; 1.90 GeV) and a spin quartet (1.92 GeV; 2.03 GeV) of octet states (mass estimates are for nonstrange and strange baryons). The anchor for $L=2$, $S=3/2$ states are those having $J^P=7/2^+$. These are the two-star $N_{7/2^+}(1990)$ and the one-star $\Lambda_{7/2^+}(2020)$. The nucleon quartet can be completed, the Λ quartet misses two states, and there is no evidence for a second Σ quartet. Most of the states have one or two stars, except the three-star $\Lambda_{5/2^+}(2110)$.

The interpretation of $\Sigma_{3/2^+}(2080)$, $\Sigma_{5/2^+}(2070)$, and $\Sigma_{7/2^+}(2030)$ is ambiguous; in Table XVIII these states are assigned to the decuplet but they may as well be octet states. As 56-plet, they are strange partners of the quartet of Δ resonances mentioned above which are observed clearly in πN scattering. As 70-plet, they would be partners of the more elusive $N_{1/2^+}(1880)$, $N_{3/2^+}(1900)$, $N_{5/2^+}(1870)$, and $N_{7/2^+}(1990)$.

In the second-excitation band, the 56-plet is nearly complete and most states are well established. Spatial wave functions can be constructed which require excitation of one oscillator only. The 70-plet spatial wave functions have components in which a single oscillator is excited and components with both oscillators being excited. Several candidates exist, mostly however with one- or two-star status.

In the nonstrange sector, four supermultiplets, underlined in Eq. (41), are nearly full while the $(D,L_N^P)=(20,1_2^+)$ multiplet is empty. It has an antisymmetric spatial wave function which is $\rho\times\lambda\psi_0$ in the HO model. Clearly, the wave function has no component with only one oscillator excited. Assuming that in πN scattering and in production experiments, only one of the oscillators is excited, we can "understand" the absence of this state in the observed spectrum, provided mixing with nearby states having identical quantum numbers is small.

3. The third-excitation band

In the third band, the number of expected states increases significantly. In the harmonic-oscillator basis, the following multiplets are predicted:

$$(D,L_N^P)=\underline{(56,1_3^-)},2\times(70,1_3^-),(20,1_3^-), \tag{42a}$$

$$(D,L_N^P)=(70,2_3^-), \tag{42b}$$

$$(D,L_N^P)=(56,3_3^-),\underline{(70,3_3^-)},(20,3_3^-), \tag{42c}$$

Thus, 45 N^* and Δ^* resonances are expected while only 12 resonances are found in the 1800–2300 MeV mass range. Most of them are decorated with 1 or 2 stars, and some of them will be assigned to the fifth band. All candidates belong just to the two underlined multiplets. The breakdown into states of defined spin and parity is given in Table XIX.

We first look for nucleon resonances with mass below 2.3 GeV and large angular momenta. These are $N_{7/2^-}(2190)$ and $N_{9/2^-}(2250)$. Based on the Regge trajec-

TABLE XIX. Number of expected states in the third-excitation band and observed states in the 1.8 to 2.4 GeV mass range (N and Δ).

	$N_{1/2^-}$	$N_{3/2^-}$	$N_{5/2^-}$	$N_{7/2^-}$	$N_{9/2^-}$
Exptd	7	9	8	5	1
Obsvd	2	2	1	1	1
	$\Delta_{1/2^-}$	$\Delta_{3/2^-}$	$\Delta_{5/2^-}$	$\Delta_{7/2^-}$	$\Delta_{9/2^-}$
Exptd	3	5	4	2	1
Obsvd	2	1	2	1	1

tory of Fig. 39, we assign $L=3$ to both of them. We propose the assignments of Table XX as $(D,L_N^P)=(70,3_3^-)$ states: $N_{9/2^-}(2250)$ is a four-star "stretched" state with $L=3$, $S=3/2$; these often leave a more significant trace in the data then states which would fall onto a daughter Regge trajectory. Likewise, we propose $N_{7/2^-}(2190)$ to have $L=3$, $S=1/2$ with spin and orbital angular momenta aligned. The two states $N_{5/2^-}(2200)$ and $N_{7/2^-}(2190)$ could also be members of the spin quartet. The $N_{5/2^-}(2070)$ is observed, jointly with $N_{1/2^-}(1535)$ and $N_{3/2^+}(1720)$, to have strong coupling to $N\eta$. The pattern is used in Bartholomy *et al.* (2007) to argue that the state has $S=1/2$. The two resonances $N_{1/2^-}(2090)$ and $N_{3/2^-}(2080)$ are tentatively interpreted as second radial excitations and are assigned to $(D,L_N^P)=(70,1_5^-)$.

There is a striking sequence of negative-parity Δ states in the 1900–2000 MeV region, the $\Delta_{1/2^-}(1900)$, $\Delta_{3/2^-}(1940)$, and $\Delta_{5/2^-}(1930)$ resonances. They could belong to two different doublets with $L=1$ and 3; the partner of $\Delta_{5/2^-}(1930)$ would then be $\Delta_{7/2^-}(2200)$. In view of the absence of a large $\boldsymbol{L}\cdot\boldsymbol{S}$ splitting in other cases, the mass separation seems rather large, and we do not follow this path. A future discovery of a $7/2^-$ state below 2 GeV—as predicted by Cohen and Glozman (2002b)—would lead to a different interpretation.

We assign the three states to a triplet in the $(D,L_N^P)=(56,1_3^-)$ multiplet. The triplet is separated in mass square from the doublet $\Delta_{1/2^-}(1620)$, $\Delta_{3/2^-}(1700)$ by 0.94 GeV^2 [which is similar to the $N(1440)$-$N(940)$ mass square difference]. If this is true, there must be a spin-doublet nucleon pair of resonances with $J=1/2^-$ and $3/2^-$ below 1.9 GeV (to allow for a mass shift by a finite good-diquark fraction). This pair indeed exists, even though with debatable confidence. The states are listed in Table XX. The 56-multiplet is full.

TABLE XX. The negative-parity states of the third-excitation band $(D,L_N^P)=(56,1_3^-)$ and $(D,L_N^P)=(70,3_3^-)$. An x stands for a missing state.

D; s		$J=1/2$	$J=3/2$	$J=5/2$
56, **8**; 1/2		$N_{1/2^-}(1905)$	$N_{3/2^-}(1860)$	
56, **10**; 3/2		$\Delta_{1/2^-}(1900)$	$\Delta_{3/2^-}(1940)$	$\Delta_{5/2^-}(1930)$
D; s	$J=3/2$	$J=5/2$	$J=7/2$	$J=9/2$
70, **8**; 1/2		$N_{5/2^-}(2070)$	$N_{7/2^-}(2190)$	
70, **8**; 3/2	x	$N_{5/2^-}(2200)$	x	$N_{9/2^-}(2250)$
70, **10**; 1/2		x	$\Delta_{7/2^-}(2200)$	

The assignment of the three states $\Delta_{1/2^-}(1900)$, $\Delta_{3/2^-}(1940)$, and $\Delta_{5/2^-}(1930)$ assumes that they are of the same kind. For quark models, they are found at a rather low mass, $M\approx 2200$ MeV is expected. Gonzalez *et al.* (2009) suggested to explain at least $\Delta_{5/2^-}(1930)$ as $\rho\Delta$ bound state while the other two are predicted to have a large $\rho\Delta$ component.

Does this finding imply that we can neglect $\Delta_{5/2^-}(1930)$ for our discussion of quark-model states? We do not believe so. Chiral dynamics is an important tool to understand properties of baryon (and meson) resonances. But it addresses the same objects. The famous $N_{1/2^-}(1535)$ can be understood as dynamically generated resonance. But it is a quark-model state as well. Resonances are not independent of their decays; they can often be constructed from their decays, but this does not imply that they are supernumerous from the quark-model point of view.

$\Delta_{9/2^-}(2400)$ has a mass which makes it unlikely to have (dominantly) $L=5$ intrinsic orbital angular momentum. With $L=3$, it needs a quark spin $S=3/2$. Using quark-model arguments only, $\Delta_{7/2^-}(2200)$ and $\Delta_{9/2^-}(2400)$ could both be $(D,L_N^P)=(56,3_3^-)$ multiplet members. However, there is a 200 MeV mass difference between the two states and, in view of Fig. 39, we assign $\Delta_{7/2^-}(2200)$ to the $(D,L_N^P)=(70,3_3^-)$ and $\Delta_{9/2^-}(2400)$ to $(D,L_N^P)=(56,3_5^-)$. We thus propose that odd-angular-momentum Δ states are in a 56-plet if and only if there is a simultaneous excitation of the radial quantum number. The $\Delta_{5/2^-}(2350)$ resonance could be a spin partner of either $\Delta_{7/2^-}(2200)$ or $\Delta_{9/2^-}(2400)$, or the entry may comprise two resonances. The $\Delta_{1/2^-}(2150)$ is the third state with these quantum numbers. It might be a second radial excitation and belong to $(D,L_N^P)=(70,1_5^-)$.

4. Further-excitation bands

In the fourth band, the number of states is exploding while data are scarce. Expected is a large number of multiplets (43),

$$(D,L_N^P) = 2\times(56,0_4^+),2\times(70,0_4^+), \tag{43a}$$

$$(D,L_N^P) = (20,1_4^+),(70,1_4^+), \tag{43b}$$

$$(D,L_N^P) = 2\times(56,2_4^+),3\times(70,2_4^+),(20,2_4^+), \tag{43c}$$

$$(D,L_N^P) = (70,3_4^+),(20,3_4^+), \tag{43d}$$

$$(D,L_N^P) = \underline{(56,4_4^+)},2\times(70,4_4^+), \tag{43e}$$

while only few of them are found (Table XXI). The large number of expected states is one of the unsolved issues in baryon spectroscopy. It is known as the problem of the *missing resonances*. Equation (43) gives the decom-

TABLE XXI. Number of expected states in the fourth-excitation band and observed states in the 2.1–2.5 GeV mass range (N and Δ).

	$N_{1/2^+}$	$N_{3/2^+}$	$N_{5/2^+}$	$N_{7/2^+}$	$N_{9/2^+}$	$N_{11/2^+}$
Exptd	10	14	16	12	7	2
Obsvd	0	0	0	0	1	0
	$\Delta_{1/2^+}$	$\Delta_{3/2^+}$	$\Delta_{5/2^+}$	$\Delta_{7/2^+}$	$\Delta_{9/2^+}$	$\Delta_{11/2^+}$
Exptd	5	8	8	7	3	1
Obsvd	0	0	1	1	1	

position of expected states into multiplets. While 93 N and Δ resonances are expected, four are found. All four observed states, $N_{9/2^+}(2220)$, $\Delta_{7/2^+}(2390)$, $\Delta_{9/2^+}(2300)$, and $\Delta_{11/2^+}(2420)$, when interpreted as $L=4$ $S=1/2$ nucleon and $S=3/2$ Δ resonances, belong to the $(D,L_{\mathrm{N}}^{P})=(56,4_4^+)$ supermultiplet, in which only two states, a $N_{7/2^+}$ and a $\Delta_{5/2^+}$, are missing.

The spectrum continues with $\Delta_{5/2^-}(2350)$ and $\Delta_{9/2^-}(2400)$ ($L=3$, $N=1$), $N_{11/2^-}(2600)$ ($L=5$, $N=0$) in the 5th, with $N_{13/2^+}(2700)$ and $\Delta_{15/2^+}(2950)$ ($L=6$, $N=0$) in the 6th, and $\Delta_{13/2^-}(2750)$ ($L=5$, $N=1$) in the 7th band. The number of expected states increases dramatically. We conjecture that at high masses, beyond 2.3 GeV, all observed nucleons have $\boldsymbol{J}=\boldsymbol{L}+\boldsymbol{S}$ have spin 1/2 and all Δ resonances, spin 3/2.

5. Dynamical conclusions

In the low-mass region, in the first-excitation shell, the quark model gives a perfect match of the number of expected and observed states. Starting from N=2, only states are realized in which the ρ and the λ oscillator are excited coherently (e.g., with a wave function $\propto\rho^2+\lambda^2$), while states with both oscillators excited simultaneously (e.g., with a wave function $\propto\rho\times\lambda$) have not been observed. If mixing were important, their absence in the spectrum would pose a severe problem for any quark model.

Positive-parity nucleon resonances with $L=2$, $S=3/2$ will have $J^P=7/2^+$; indeed, a two-star $N_{7/2^+}(1990)$ exists. Above there is a $N_{9/2^+}(2220)$ but no $11/2^+$ partner which should exist if $N_{9/2^+}(2220)$ had $L=4$, $S=3/2$. Instead it likely has $L=4$, $S=1/2$. Likewise, $N_{13/2^+}(2700)$ exists but no $15/2^+$ nucleon, and we assign $L=6$, $S=1/2$. The four states $N(940)$, $N_{5/2^+}(1680)$, $N_{9/2^+}(2220)$, and $N_{13/2^+}(2700)$ belong to the leading nucleon Regge trajectory.

Negative-parity nucleon resonances with the largest total angular momenta (in a given mass interval) are $N_{5/2^-}(1675)$, $N_{9/2^-}(2250)$, and $N_{11/2^-}(2600)$, where the former two resonances have $L=1$ and 3 and $S=3/2$, and the latter one $L=5$, $S=1/2$. We conclude that for up to $L=3$ nucleon resonances can have spin $S=1/2$ or have spin $S=3/2$ while for high masses, the observed nucleon resonances have spin $S=1/2$.

High-spin positive-parity Δ resonances are readily identified as $\Delta_{3/2^+}(1232)$, $\Delta_{7/2^+}(1950)$, $\Delta_{11/2^+}(2420)$, and $\Delta_{15/2^+}(2950)$ with $L=0$, 2, 4, and 6 and $S=3/2$ as leading contributions (and possibly some small higher-L components). The observed positive-parity Δ resonances can all be assigned to spin $S=3/2$ multiplets. The $\Delta_{1/2^+}(1750)$ resonance is the only positive-parity $I=3/2$ resonances which belongs to a 70-plet.

The negative-parity sector is a bit more complicated. Δ resonances with $L=1$, $S=3/2$ are forbidden for $n_\lambda=0$, and resonances have either $S=1/2$, $n_\lambda=0$ (and belong to a 70-plet) or $S=3/2$, $n_\lambda=1$ (and belong to a 56-plet). For $L=3$, Δ resonances still have either $S=1/2$, $n_\lambda=0$ and belong to $70,3_3^-$, or they have $S=3/2$, $n_\lambda=1$ $(56,1_3^-)$ even though HO wave functions do not forbid either $S=3/2$, $n_\lambda=0$ $(56,3_3^-)$ or $S=1/2$, $n_\lambda=1$ $(70,1_3^-)$. For $L=5$, only $S=3/2$ and $n_\lambda=1$ is observed.

In summary, most observed Δ resonances fall into 56-plets, in 70-plets Δ resonances are seen only up to the third shell. Nucleon resonances above the third shell are in a 56-plet when they have positive, in a 70-plet for negative parity. There are no states which would need to be assigned to a 20-plet. In other words, the experimentally known resonances above the third shell can be described by a diquark in S wave (with the ρ oscillator in the ground state) and the λ oscillator carrying the full excitation.

This rule leads to a selection of allowed multiplets which are summarized in Table XXII.

G. Exotic baryons

The search for exotic mesons, spin-parity exotics, and crypto-exotic states has been a continuous stimulation of the field. Examples are the $\pi_1(1400)$ and $\pi_1(1600)$ mesons with $J^{PC}=1^{-+}$ (quantum numbers which cannot come from $q\bar{q}$), the flavor exotic states $Z^{\pm}(4050)$, $Z^{\pm}(4248)$, and $Z^{\pm}(4430)$ (Abe *et al.*, 2008; Mizuk *et al.*, 2008) (decaying into a pion and a $c\bar{c}$ resonance), or me-

TABLE XXII. Observed multiplets at large angular momenta

N^* with $P=+$: N^* with $P=-$:	spin $S=1/2$	$l_\lambda=L$; $n_\rho=0$
Δ^* with $P=+$: Δ^* with $P=-$:	spin $S=3/2$	$l_\lambda=L$; $n_\rho=0$ $l_\lambda=L$; $n_\rho=1$

sons like $f_0(980)$, $a_0(980)$, $f_0(1500)$, and $X(3872)$ (Abe *et al.*, 2008) which have attracted many theoretical papers trying to understand their nature either as quarkonium states or as crypto-exotic states, as glueballs, as weakly or tightly bound tetraquarks or as molecular states (among other more exotic interpretations). The existence of exotic mesons as additional states in meson spectroscopy is not beyond doubt; see Klempt and Zaitsev (2007) for a critical review and Crede and Meyer (2009) for a more optimistic view.

Intruders into the world of baryons would be identified unambiguously when they have quantum numbers which differ from those of qqq baryons. There are no spin-parity exotic quantum numbers in baryon spectroscopy, but flavor exotic states (containing an antiquark in the flavor wave function) might exist. Most discussion is directed to the question if crypto-exotic baryons exist.

Examples of baryons which may deserve an interpretation beyond the quark model are $N_{1/2^+}(1440)$, which is found at an unexpectedly low mass, $N_{1/2^-}(1535)$, a resonance which is observed at the expected mass but with an unusual large decay branching ratio to $N\eta$, and the $\Lambda_{1/2^-}(1405)$ and $\Lambda_{3/2^-}(1520)$ resonances with their low mass and unusual splitting. A consistent (Liu and Zou, 2006; Zou, 2008)—even though controversial (Liu and Zou, 2007; Sibirtsev, Haidenbauer, and Meißner, 2007)—picture for these possibly crypto-exotic baryons ascribes the mass pattern to a large $qqqq\bar{q}$ fraction in the baryonic wave functions.

1. Pentaquarks

The question of the existence of multiquark hadrons has been raised at the beginning of the quark model, and is regularly revisited, due either to fleeting experimental evidence or to theoretical speculations. In the late 1960s some analyses suggested a possible resonance with baryon number $B=1$ and strangeness $S=-1$, opposite to that of the Λ or Σ hyperons.

In 1976, a stable dihyperon H was proposed (Jaffe, 1977), whose tentative binding was due to coherence in the chromomagnetic interaction. In 1987, Gignoux *et al.* and independently Lipkin (Gignoux *et al.*, 1987; Lipkin, 1987) showed that the same mechanism leads to a stable $(Q\bar{q}^4)$ below the threshold for spontaneous dissociation into $(Q\bar{q})+(\bar{q}^3)$. This calculation, and Jaffe's for his $H=(u^2d^2s^2)$, gave 150 MeV of binding if the light quark are treated in the $\mathrm{SU}(3)_f$ limit (and Q infinitely heavy for the pentaquark) and if the short-range correlation $\langle\delta^{(3)}(r_{ij})\rangle$ is borrowed from ordinary baryons. However, relaxing these strong assumptions always goes in the direction of less and less binding, and even instability. The H was searched for in dozens of experiments (Ashery, 1996). The 1987-vintage pentaquark was searched for by the experiment E791 at Fermilab (Aitala *et al.*, 1998), but the results are not conclusive.

Some years ago, a lighter pentaquark was found in photoproduction, called $\Theta^+(1540)$ (Nakano *et al.*, 2003), inspired by the theoretical speculation in a chiral soliton model predicting a (anti)decuplet of narrow baryons (Diakonov *et al.*, 1997), following in turn a number of earlier papers. [For the width, see also Jaffee (2004) and Wiegel (2007)]. The $\Theta^+(1540)$ was confirmed in a series of low-statistics experiments. The decuplet was enriched by the doubly-charged $\Phi(1860)$ (Alt *et al.*, 2004); the missing members were identified with $N_{1/2^+}(1710)$ and $\Sigma_{1/2^+}(1890)$. A narrow peak in the pD^{*-} and $\bar{p}D^{*+}$ distributions signaled a baryon with an intrinsic $\bar{c}$ quark, $\Theta_c^0(3100)$ (Aktas *et al.*, 2004).

These observations initiated a large number of further experimental and theoretical studies which were reviewed by Dzierba *et al.* (2005) and Hicks (2005). Recent experiments had partly a significant increase in statistics but no narrow pentaquark state was confirmed. If it exists, the $\Theta^+(1540)$ must be very narrow: from the absence of a signal in the reaction $K^+d\to K^0pp$, an upper limit of about 1 MeV can be derived (Arndt *et al.*, 2003b; Cahn, 2004; Sibirtsev *et al.*, 2004; Workman *et al.*, 2006). The list of experiments and upper limits for pentaquark production can be found in PDG (Wohl, 2008b) from where we quote the final conclusion: *The whole story—the discoveries themselves, the tidal wave of papers by theorists and phenomenologists that followed, and the eventual "undiscovery"—is a curious episode in the history of science.* The evidence for a pentaquark interpretation (Kuznetsov, 2008) of a narrow peak in the $n\eta$ invariant mass spectrum at 1680 MeV is weak; the peak is observed in photoproduction of η mesons off neutrons in a deuteron (Kuznetsov, 2007; Fantini *et al.*, 2008; Jaegle *et al.*, 2008) but the data are not really in conflict with standard properties of $N_{1/2^-}(1535)$ and $N_{1/2^-}(1650)$ and interference between them (Döring *et al.*, 2008; Anisovich *et al.*, 2009).

2. Dynamically generated resonances

A number of baryon resonances has been suggested to be due to the dynamics of the meson-baryon interaction. Before entering a discussion of individual cases, we specify different views of the meaning of "dynamically generated resonances." The $\Delta(1232)$ resonance can be considered as πN resonance (Chew and Low, 1956), and this remains the most efficient tool to describe π-nucleus scattering, as a propagation of Δ-hole excitations. Alternatively, the $\Delta(1232)$ is easily described in the quark model, mainly as a state of three light quarks, (qqq), with spins aligned, but its higher Fock states certainly accounts for an overlap with πN. Some quark models are supplemented by explicit accounts for hadron-hadron components; see, Vijande *et al.* (2009) for mesons with charm and strangeness. Years ago, a model-independent analyses of the effect of hadronic loops was proposed by Törnqvist and Zenczykowski (1984, 1986).

When a resonance is close to the threshold for an important decay mode, in particular for decays into two hadrons in S wave, the molecular component can become large. For the $\Delta(1232)$, this is mostly a matter of taste whether it is first described as a quark state acquiring hadron-hadron components, or built first from the interaction of its decay products, i.e., generated dynamically.

The problem becomes of course much more delicate when dynamical resonances are predicted atop the quark-model states, or when the light-quark baryons are disregarded altogether and replaced by a systematics of meson-baryon excitations. A convincing formalism is available: an effective field theory in terms of hadrons, with the symmetries of QCD, and coupling adjusted by fitting the low-energy strong-interaction data (Gasser and Leutwyler, 1984, 1985). However, it is not obvious which spectrum would emerge.

Dynamically generated states can possibly be identified by a study of their behavior as a function of the number of colors (Lutz and Kolomeitsev, 2002). Hanhart (2008) pointed out that the analytical structure of the meson-baryon scattering matrix at important thresholds is different for (tightly-bound) qqq states and (weakly bound) molecular states, and this provides a means to identify the nature of a resonance. Chiral dynamics with unitarity constraints and explicit resonance fields have provided a good picture of meson-nucleon scattering. When such a formalism is implemented, additional resonances (genuine quark-model states) are sometimes no longer required to fit the data; see Meißner (2000) and Döring *et al.* (2004).

We now turn to a discussion of some specific cases.

a. The Roper resonance

The Roper resonance $N_{1/2^+}(1440)$ is the lowest-mass nucleon resonance and has the quantum numbers of the nucleon. Its most natural explanation as first radial excitation is incompatible with quark models in which the radial excitation requires two harmonic-oscillator quanta while the negative-parity states like $N_{1/2^-}(1535)$ require one quantum only. Even including anharmonicity, the mass of the first radial excitation should always be above the first orbital-angular-momentum excitation. Within the constituent quark model with one-gluon-exchange (Capstick and Isgur, 1986) or instanton-induced forces (Löring *et al.*, 2001a), the Roper resonance $N_{1/2^+}(1440)$ should have a mass 80 MeV above the $N_{1/2^-}(1535)$ mass, and not $\approx$100 MeV below it.

Models using Goldstone-boson exchange interactions (Glozman and Riska, 1996) improve on the Roper mass but this success is counterbalanced by two shortcomings: the interaction is (1) inappropriate to calculate the full hadronic spectrum, and (2) restricted to light baryons. Only the lowest-mass excitations were calculated with a comparatively large number of adjustable parameters.

The Roper resonance has a surprisingly large width, and the transition photocoupling amplitude has even the wrong sign (Capstick and Keister, 1995). Some calculations on a lattice support the idea that the Roper resonance is not the radial excitation of the nucleon (Borasoy, Bruns, Meißner, and Lewis, 2006; Burch *et al.*, 2006) [but others come to the contrary conclusion (Mathur *et al.*, 2005; Mahbub *et al.*, 2009)]. These difficulties, to explain the properties of the Roper resonance, encouraged attempts to interpret the data dynamically, without introducing a resonance. In a coupled-channel meson exchange model based on an effective chiral-symmetric Lagrangian by Krehl *et al.* (2000), no genuine qqq resonance was needed to fit πN phase shifts and inelasticity, in agreement with Schneider *et al.* (2006). Thus, $N_{1/2^+}(1440)$ is often interpreted as an intruder into the world of qqq baryons. Yet, the sign change in the helicity amplitude (Fig. 41) as a function of Q^2 (Aznauryan *et al.*, 2008; Aznauryan, 2009) does not support this interpretation; it rather suggest a node in the wave function and thus a radially excited state. The result does of course not rule out a $qqqq\bar{q}$ $(N\pi)$ component in the wave function as suggested by Julia-Diaz and Riska (2006) and Li and Riska (2006).

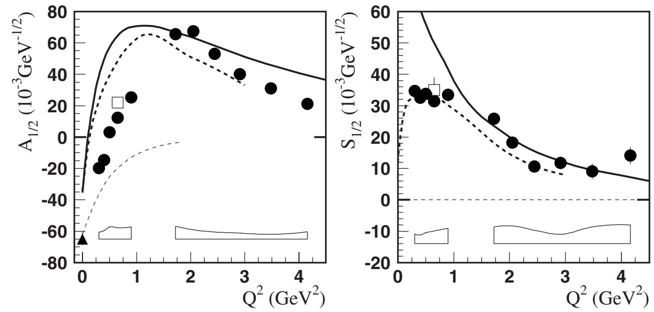

FIG. 41. Helicity amplitudes for the $\gamma^* p \to N(1440)P_{11}$ transition. The full circles are recent results from CLAS (Aznauryan, 2009) and open boxes are results of an earlier analysis which included 2π electroproduction data (Aznauryan *et al.*, 2005). The bands show the model uncertainties. The full triangle at $Q^2=0$ is the PDG estimate (Amsler *et al.*, 2008). The thick curves correspond to quark models assuming that $N(1440)P_{11}$ is a first radial excitation of the $3q$ ground state: (Capstick and Keister, 1995) dashed and (Aznauryan, 2007) solid. The thin dashed curves are obtained assuming that $N(1440)P_{11}$ is a gluonic baryon excitation (q^3G hybrid state) (Li *et al.*, 1992).

There has been the claim that the Roper resonance region might house two resonances (Morsch and Zupranski, 2000), one at 1390 MeV with a small elastic width and large coupling to $N\pi\pi$, and a second one at higher mass—around 1460 MeV—with a large elastic width and small $N\pi\pi$ coupling. This idea was tested by Sarantsev *et al.* (2008) analyzing the overconstrained set of reactions $\pi^- p \to N\pi$, $\pi^- p \to n\pi^0\pi^0$, $\gamma p \to N\pi$, and $\gamma p \to p\pi^0\pi^0$ (see Fig. 42). A second pole was rejected unless its width was sufficiently narrow to allow the resonance to have its full phase motion in between the masses at which data are available. We note that in EBAC no photoproduced Roper resonance was found in fits to the total cross section (Kamano *et al.*, 2009a, 2009b). But, of course, such fits are much less sensitive to the underlying dynamics than event-based likelihood fits performed by Sarantsev *et al.* (2008).

We mention here a few further $N_{1/2^+}$ states: a narrow $N(1680)$ which might have been observed in $n\eta$ photoproduction was already discussed as $N_{1/2^+}(1680)$ in the section on pentaquarks. A $N_{1/2^+}(1880)$ was recently re-

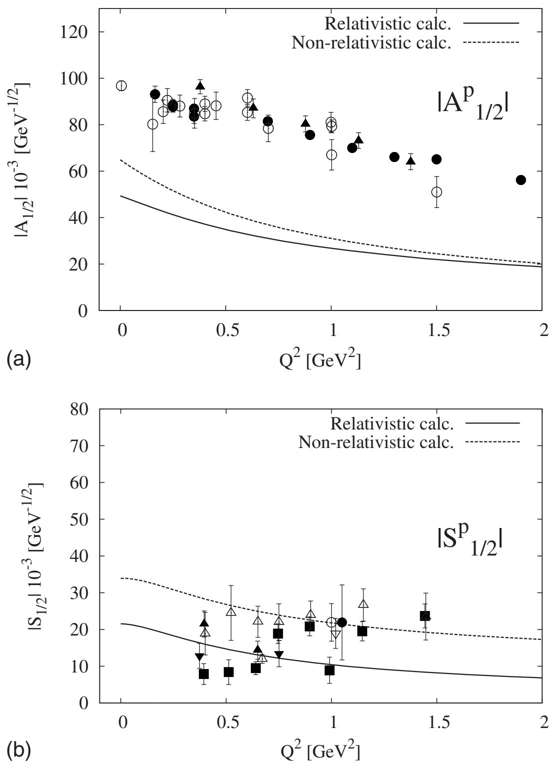

FIG. 42. Transverse (top) and longitudinal (bottom) helicity amplitudes for the $\gamma^* p \to N_{1/2^-}(1535)$ transition. The data points are from CLAS (Denizli *et al.*, 2007). The value at the photon point is from Amsler *et al.* (2008). The lines represent calculations by Jido *et al.* (2008).

ported by Castelijns *et al.* (2008) from photoproduction and has been observed by Manley *et al.* (1984) in the reaction $\pi^- p \to p\pi^+\pi^-$. The latter observation is listed in the PDG under $N_{1/2^+}(2100)$. The $N_{1/2^+}(1710)$ resonance, questioned in the most recent analysis of πN elastic scattering (Arndt *et al.* (2006)), was required in fits to $\pi N \to N\eta$ and $\pi N \to \Lambda K$ (Ceci *et al.*, 2006a, 2006b).

b. $N_{1/2^-}(1535)$ three-quark resonance or $N\eta$-ΣK coupled-channel effect?

This resonance is observed at a mass expected in quark models but its large decay branching ratio to $N\eta$ invited speculations that it might be created dynamically. An effective chiral Lagrangian, relying on an expansion in increasing powers of derivatives of the meson fields and quark masses, has been successful in understanding many $N_{1/2^-}(1535)$ properties (and of the meson-baryon system at low energies) (Kaiser *et al.*, 1995). More recent studies—with more data but similar conclusions—are presented in Döring *et al.* (2008), Hyodo *et al.* (2008), and Geng *et al.* (2009). Döring and Nakayama (2010a, 2010b) studied the pole structure of $N_{1/2^-}(1535)$ and $N_{1/2^-}(1650)$. If a dynamically generated $N_{1/2^-}(1535)$ is introduced and an additional pole (as quark-model state), the latter pole moves far into the complex plane and provides an almost energy-independent background while the dynamically generated $N_{1/2^-}(1535)$ pole appears as a stable object. However, the dynamical generation of $N_{1/2^-}(1535)$ is tied to its strong couplings to $K\Lambda$ and $K\Sigma$. If theses couplings are reduced by about 40% or 50%, the dynamically generated resonance disappears.

Experimentally, response functions, photocouplings, and ηN coupling strengths as functions of the invariant squared momentum transfer (measured for $Q^2 = 0.13$–$3.3\ \mathrm{GeV}^2$) were deduced from a measurement of cross sections for the reaction $ep \to e'\eta p$ for total center-of-mass energies $W = 1.5$–2.3 GeV (Denizli *et al.*, 2007). The helicity amplitudes were calculated within a coupled-channel chiral unitary approach assuming that $N_{1/2^-}(1535)$ is dynamically generated from the strong interaction of mesons and baryons (Jido *et al.*, 2008). The Q^2 dependence is reproduced, the absolute height not (a quantity which is difficult to determine reliably from the data). The ratios obtained between the $S_{1/2}$ and $A_{1/2}$ for the two charge states of the $N_{1/2^-}(1535)$ agree qualitatively with experiment. They are not inconsistent with this resonance being dynamically generated. However, there are indications—e.g., the harder Q^2 dependence in the data compared to the prediction—that a genuine quark-state component could improve the agreement between experiment and the model.

c. $\Lambda_{1/2^-}(1405)$

One of the first historical examples is $\Lambda_{1/2^-}(1405)$, which was suggested to be a $\bar{K}N$ quasibound state (Dalitz and Tuan, 1959, 1960). This approach has been often revisited, since the $\Lambda_{1/2^-}(1405)$ is one of the resonances having a mass which is difficult to reproduce in quark models. It falls just below the $N\bar{K}$ threshold; hence the attractive interaction between N and $\bar{K}$ and the coupling to the $\Sigma\pi$ channel could lead to a threshold enhancement or attract the pole of a not-too-far qqq resonance (Dalitz *et al.*, 1967). In models exploiting chiral symmetry and imposing unitarity, $\Lambda_{1/2^-}(1405)$ can be generated dynamically from the interaction of mesons and baryons in coupled channels.

This is a unique or rare example where the predictions of chiral dynamics and the quark model are at variance. Quark models predict one $1/2^-$ resonance at 1400 MeV, $\Lambda_{1/2^-}(1405)$. A detailed study within a chiral unitary model revealed that the $N\bar{K}-\Sigma\pi$ coupled-channel effects is considerably more complex. Jido *et al.* (2003) suggested that $\Lambda_{1/2^-}(1405)$ may contain two resonances; one—mainly $SU(3)_f$ singlet—at 1360 MeV with a larger width and a stronger coupling to $\pi\Sigma$ and the other one at 1426 MeV, which is mostly $SU(3)_f$ octet and couples more strongly to the $N\bar{K}$. The lower mass state is mostly observed in the $\pi^- p \to K^0\pi\Sigma$ reaction while the reaction $K^- p \to \pi^0\pi^0\Sigma^0$ produces a relatively narrow ($\Gamma = 38$ MeV) peak at 1420 MeV (Magas *et al.*, 2005; Oller, 2006). However, it is not yet clear how much SU(3) breaking invalidates these conclusions; possibly, the second pole could even dissolve in the background (Borasoy, Meißner, and Nissler, 2006).

We propose to test these ideas by a measurement of $J/\psi \to \Lambda_{1/2^-}\text{-}\bar{\Lambda}_{1/2^-}$, where $\Lambda_{1/2^-}$ stands for the conventional $\Lambda_{1/2^-}(1405)$ resonance or the two-resonance structure of Jido *et al.* (2003) and to measure the frequency with which the following decay sequences occur:

$$J/\psi \to (\Lambda_{1/2^-} \to \pi\Sigma)(\bar{\Lambda}_{1/2^-} \to \pi\bar{\Sigma}), \tag{44a}$$

$$J/\psi \to (\Lambda_{1/2^-} \to \bar{K}N)(\bar{\Lambda}_{1/2^-} \to \pi\bar{\Sigma}), \tag{44b}$$

$$J/\psi \to (\Lambda_{1/2^-} \to \bar{K}N)(\bar{\Lambda}_{1/2^-} \to K\bar{N}). \tag{44c}$$

In J/ψ decays $SU(3)_f$ singlet and octet states can be produced pairwise, but simultaneous production of one octet and one singlet state is suppressed. If there were two states, there should be correlations between $\Lambda_{1/2^-}(1405)$ and $\bar{\Lambda}_{1/2^-}$ decays; for a single-state resonances, the decays are uncorrelated. We anticipate that the latter prediction is correct. Assuming a two-pole structure of $\Lambda_{1/2^-}(1405)$, the correlation in the $\Lambda_{1/2^-}(1405) \to \Sigma\pi(+\text{c.c.})$ decay modes is calculated by Li and Oset (2004). We note in passing that Wohl (2008a) compared light and heavy baryons and concludes that $\Lambda_{1/2^-}(1405)$ is a three-quark resonance.

3. Baryonic hybrids

Baryons with properties incompatible with quark-model predictions can be suspected to be baryonic hybrids. This fate is shared by a number of states, the Roper resonance $N_{1/2^+}(1440)$ being one example. Likewise, $\Lambda_{1/2^+}(1600)$ (Kisslinger, 2004), $\Sigma_{1/2^+}(1600)$, and $\Xi_{1/2^+}(1660)$ have low masses and could be hybrids as well. The mass gap between $\Lambda_{1/2^-}(1405)$ and $\Lambda_{3/2^-}(1520)$ is larger than expected in quark models but can be reproduced assuming them to be of hybrid nature (Kittel and Farrar, 2005), where a possible hybrid nature is also suggested for $\Lambda_c(2593)$ and $\Lambda_c(2676)$.

First bag-model predictions suggested that some hybrids could have masses just below 2 GeV (Barnes and Close, 1983; Golowich *et al.*, 1983), making a hybrid interpretation of $N_{1/2^+}(1440)$ unlikely. Also in a nonrelativistic flux-tube model, the lowest hybrid-baryon mass was estimated to be 1870 ± 100 MeV (Barnes *et al.*, 1995; Capstick and Page, 2002). Within a relativistic quark model, Gerasyuta and Kochkin (2002) arrived at hybrid masses suggesting that $N_{1/2^+}(1710)$ and $\Delta_{3/2^+}(1600)$ could be hybrid baryons. QCD sum rules predict, however, a hybrid mass of 1500 MeV and $N_{1/2^+}(1440)$ remains a hybrid candidate (Kisslinger and Li, 1995).

The most convincing experimental evidence providing an interpretation of the Roper resonance is derived from recent measurements of nucleon resonance transition form factors. Figure 41 shows the transverse and longitudinal electrocoupling amplitudes $A_{1/2}$ and $S_{1/2}$ of the transition to the $N_{1/2^+}(1440)$ resonance. At the photon point $A_{1/2}$ is negative. The amplitude rises steeply with Q^2 and a sign change occurs near $Q^2=0.5$ GeV^2. At $Q^2=2$ GeV^2 the amplitude has about the same magnitude but opposite sign as at $Q^2=0$. Then it falls off slowly. The longitudinal amplitude $S_{1/2}$ is large at low Q^2 and drops off smoothly with increasing Q^2. The bold curves represent various quark-model calculations and the thin dashed line is for a gluonic excitation (Li *et al.*, 1992). The hybrid hypothesis misses the sign change in $A_{1/2}$; $S_{1/2}$ is predicted to vanish identically. In contrast, most quark models qualitatively reproduce the experimental findings: the Roper $N_{1/2^+}(1440)$ resonance is the first radial excitation of the nucleon.

4. Parity doublets, chiral multiplets

The existence of parity doublets in the baryon spectrum has been noticed as early as 1968 by Minami (1968), and arguments in favor of their existence were given even before [see Afonin (2007) for a review]. Parity doublets are expected in a world of chiral symmetry. The large mass difference between the nucleon and its chiral partner with $J=1/2$ but negative parity, $N_{1/2^-}(1535)$, provides evidence that chiral symmetry is broken spontaneously. Glozman deserves the credit to have consistently pointed out—in at least 20 papers on arXiv, we quote here (Glozman, 2000; Cohen and Glozman, 2002a, 2002b)—that at high masses mesons and baryons often occur in nearly mass-degenerate pairs of states with given spin but opposite parity: parity doublets are observed and possibly even parity quartets in which all (four) nucleon and Δ states with identical J^P are degenerate in mass. Bicudo *et al.* (2009) argued that the mass splittings between these parity partners decrease with increasing baryon mass, and that the decreasing mass difference can be used to probe the running quark mass in the midinfrared power-law regime.

Table XXIII summarizes the experimental status of multiplets for $J^P=1/2^\pm,\dots,9/2^\pm$. In spite of an intense discussion in the literature, reviewed by Jaffe *et al.* (2006) and Glozman (2007), there is no consensus whether parity doubling emerges from the spin-orbital dynamics of the three-quark system, if it reflects a deep symmetry in QCD, or if they do not exist at all in nature. With the present status of the data, this question will likely remain unsettled. New data and new analyses are needed.

In the harmonic oscillator approximation, a three-quark system is characterized by successive shells of positive and negative parity. Formally, this corresponds to masses being proportional to $L+2\text{N}$. Parity doubling is not expected. In AdS/QCD parity doubling arises naturally due to the $L+\text{N}$ dependence of the nucleonic mass levels. Within their collective model of baryons by Bijker *et al.* (1994, 1997), parity doubling is explained by the "geometric structure" of excitations (Iachello, 1989). In Regge phenomenology, the separation of states scales with $\delta M^2=\text{const}$, or $M_1-M_2=\text{const}/(M_1+M_2)$. Experimentally, the masses of states with positive and negative parity often show mass degeneracy, but not in all cases. Clearly, a definition is needed when two masses are called mass degenerate (within experimental errors) or not. In Table XXIII, we have not accepted as parity

TABLE XXIII. Parity doublets and chiral multiplets of N^* and Δ^* resonances of high mass. List and star rating are from Table XIII.

$J=\frac{1}{2}$	$\mathrm{N}_{1/2^+_{***}}(1710)$	$\mathrm{N}_{1/2^-_{****}}(1650)$	$\Delta_{1/2^+}(1750)$	$\Delta_{1/2^-_{****}}(1620)$
$J=\frac{3}{2}$	$\mathrm{N}_{3/2^+_{****}}(1720)$	$\mathrm{N}_{3/2^-_{***}}(1700)$	$\Delta_{3/2^+_{***}}(1600)$	$\Delta_{3/2^-_{****}}(1700)$
$J=\frac{5}{2}$	$\mathrm{N}_{5/2^+_{****}}(1680)$	$\mathrm{N}_{5/2^-_{****}}(1675)$	no chiral partners	
$J=\frac{1}{2}$	$\mathrm{N}_{1/2^+_{**}}(1880)$	$\mathrm{N}_{1/2^-_{*}}(1905)$	$\Delta_{1/2^+_{****}}(1910)$	$\Delta_{1/2^-_{**}}(1900)$
$J=\frac{3}{2}$	$\mathrm{N}_{3/2^+_{*}}(1900)$	$\mathrm{N}_{3/2^-_{**}}(1860)$	$\Delta_{3/2^+_{***}}(1920)$	$\Delta_{3/2^-_{**}}(1940)$
$J=\frac{5}{2}$	$\mathrm{N}_{5/2^+_{**}}(1870)$	no chiral partner	$\Delta_{5/2^+_{****}}(1905)$	$\Delta_{5/2^-_{**}}(1930)$
$J=\frac{7}{2}$	$\mathrm{N}_{7/2^+_{**}}(1990)$	no chiral partner	$\Delta_{7/2^+_{****}}(1950)$	no chiral partner
$J=\frac{7}{2}$	no chiral partner	$\mathrm{N}_{7/2^-_{****}}(2190)$	no chiral partner	$\Delta_{7/2^-_{*}}(2200)$
$J=\frac{9}{2}$	$\mathrm{N}_{9/2^+_{****}}(2220)$	$\mathrm{N}_{9/2^-_{****}}(2250)$	$\Delta_{9/2^+_{**}}(2300)$	$\Delta_{9/2^-_{**}}(2400)$

partners having a mass spacing in the order of the normal shell separation. Based on quantitative tests, Klempt (2003) and Shifman and Vainshtein (2008) remained skeptical if the observed mass pattern are related to a fundamental symmetry of QCD; it could as well be due a dynamical symmetry such as the absence of spin-orbit forces.

V. SUMMARY AND PROSPECTS

The recent years have seen a remarkable boost in our knowledge of baryons with heavy flavors, with the number of known baryons with b quarks increasing from 1 to 7 in the last four years, and that of charmed states from 16 to 34. However, many points remain to be clarified: in most cases, the quantum numbers of heavy-flavor baryons are deduced from quark-model expectation, and a direct measurement would be desirable. One exception is the $\Lambda_c(2880)$, determined experimentally to be $J^P=5/2^+$ exploiting the decay angular distribution in the sequential $\Lambda_c(2880)^+\to(\Sigma_c(2455)\pi)^+$ decay (Fig. 5), but the mass spectrum suggests rather spin 1/2 or 3/2 and negative parity. The heaviest baryon known so far, Ω_b, may have a mass of 6.165 GeV, which seems almost 100 MeV too high by comparison with the strangeness-excitation energy in the sector of charmed baryons, but this result has been challenged recently.

The double-charmed baryon Ξ_{cc}^+ has been seen in only one experiment, and the measured mass seems too low as compared to model prediction. It is surprising that the mechanism of double $c\bar{c}$ production which is responsible for the observation of $J/\psi+\eta_c$ in e^+e^- collisions does not produce more often $cc+\overline{cc}$, whose hadronization would lead to double-charm baryons. Triple-charm [or (ccb), (cbb), or (bbb)] spectroscopy will be to baryons what heavy quarkonium is for mesons: a laboratory for high-precision QCD studies. It is expected, for instance, that the analog of the Roper resonance for these baryons would be stable, and lie below the negative-parity excitations.

The experimental prospects for heavy baryon spectroscopy are bright provided the chances are used. Remember that discussions and even workshops are regularly held to use the production potential of heavy-ion collisions for the spectroscopy of exotic and heavy-flavored hadrons, but the corresponding upgrade of detectors, triggers, and analysis programs has not yet started.

Doubled-charmed baryons will probably be produced abundantly at LHC and even (ccc) states are not beyond the possibility. See Berezhnoi *et al.* (1998) and Gomshi Nobary and Sepahvand (2007) for estimates of the production rates. The upgrade of BELLE will improve the statistics in B decays and background e^+e^- annihilation events very substantially; most information we have at present stems from the predecessors BABAR, the present BELLE and from CLEO. PANDA offers a further unique possibility to study the physics of heavy flavors.

Light baryon spectroscopy has come again into the focus of a large community. The quark model still provides the most convincing picture. Even its simplest version, the harmonic oscillator, accounts for the number of expected states at low masses, and the description is improved using a better central potential and spin-dependent forces. In its relativistic variants, electromagnetic properties such helicity amplitudes of photoproduction, magnetic moments, and form factors can be calculated as well. However, at higher excitations, the quark model leads to the problem of "missing resonances." Here we recall that the masses of ground-state baryons do not arise from the motion of relativistic quarks but rather from chiral symmetry breaking. Possibly, chiral symmetry breaking is also the primary source for the masses of excited baryons, where chiral symmetry could be broken in an extended volume.

The question of dynamically generated resonances will require further clarification. The states predicted by quark-gluon dynamics need long-range corrections with higher Fock configurations, which are dominated by the meson-baryon interaction. On the other hand, resonances can be described starting from a purely hadronic picture, with the recent improvements provided by effective theories and chiral dynamics, but in this approach, short-range corrections lead back to interacting quarks. The situation is perhaps similar to that of atoms in a magnetic field, for which both the weak- and strong-field limits are relatively simple. For intermediate fields, the truncated weak- and strong-field expansions give different predictions that a superficial observer could misinterpret as a doubling of the atomic levels. For baryon resonances, quark-model wave functions and meson-baryon states have clearly a sizable overlap, hence their superposition should be handled with care.

Experimentally, intense efforts are undertaken to carry out photoproduction experiments with linearly and circularly polarized photons and protons polarized along the direction of the incoming photon beam, or transversely. The reaction $\gamma p \to \Lambda K^+$ offers the best chance to perform a complete experiment, in which the full photoproduction amplitude can be reconstructed in an energy-independent partial-wave analysis. Important steps have been marked by experiments like CBELSA, CLAS, GRAAL, LEPS, and different experiments at MAMI; several groups are attacking the difficult task of extracting from the data resonant and nonresonant contributions in energy-dependent partial-wave analyses. The confirmation of a few states [$N_{3/2^+}(1900)$, $\Delta_{3/2^+}(1920)$, and $\Delta_{3/2^-}(1940)$], which had been observed in the old analyses of Höhler and of Cutkosky and which were missing in the recent analysis of the GWU group substantiates the hope that photoproduction of multiparticle final states is a well-suited method for uncovering new baryon resonances.

The known baryon resonances show few surprising results. First, the apparent absence (or smallness) of forces beyond confinement and hyperfine interactions leads to clear spin multiplets and thus allows one to assign intrinsic orbital and spin angular momenta to a given baryon resonance. The four nearly mass-degenerate states $\Delta_{1/2^+}(1910)$, $\Delta_{3/2^+}(1920)$, $\Delta_{5/2^+}(1905)$, and $\Delta_{7/2^+}(1950)$ form a quartet of resonances. It is counting the number of states and not relying on a model which determines the total quark spin to $S=3/2$ and the orbital angular momentum to $L=2$. Mixing with other states is not excluded, but giving mixing angles is (so far) a model-dependent statement. On this basis, all nucleon and Δ resonances can be assigned to a few SU(6) multiplets while other multiplets remain completely empty. At large masses, all known resonances are compatible with nucleon excitations having a total quark spin $S=1/2$ and Δ excitations having $S=3/2$. At low energies, including the second-excitation shell, the full richness offered by the three-particle problem seems to be realized, except for one multiplet with an antisymmetric orbital wave function in which the angular momenta of the two oscillators with $l_\rho=1$ and $l_\lambda=1$ couple to a total angular momentum $L=1$. Based on the systematics of baryon masses, we expect a spin doublet $N_{1/2^+}$ and $N_{3/2^+}$ at a mass of about 1.75–1.85 GeV. Since both oscillators are excited, direct production of these states may be suppressed. But the two states could mix with the two known states $N_{1/2^+}(1710)$ and $N_{3/2^+}(1720)$, and we expect a pattern which is difficult to resolve. Indeed, inconsistencies in the properties of the two resonances as produced in photoproduction and in πN elastic scattering may be a first hint for these elusive resonances. In the intermediate region, in the third shell, some multiplets are completely filled while others remain empty. There is no obvious systematic behavior which states are observed and which ones are not. It is an open question if these states are not realized because of an unknown dynamical selection rule or if they just have escaped experimental verification. We note that in most cases there is, for isospin I and strangeness S, only one resonance is found experimentally with a set of quantum numbers L, N, S, and J, while the quark model predicts an increasing (with mass) number of states all having the same quantum numbers.

The masses of nucleon and Δ resonances exhibit intriguing spin-parity doublets, pairs of states with $J^P=J^\pm$, and even evidence for four mass-degenerate nucleon and two Δ resonances, all having the same J. The absence of strong spin-orbit forces leads to a degeneracy of states with given L and S but coupling to different J. Thus, the spectrum reveals a high level of symmetries. Different interpretations have been offered to explain the symmetries, restoration of chiral symmetry in the high-mass region (Table XXIII), and AdS/QCD (Table XV). The two interpretations predict different mass values for the lowest-mass $\Delta_{7/2^-}$ state. In AdS/QCD this state should have intrinsic $L=3$, $S=1/2$, and 2.12 GeV mass. When chiral symmetry is restored, it should be found at 1.95 GeV. A search for the lowest-mass $\Delta_{7/2^-}$ resonance is thus urgently needed.

Photoinduced reactions seems to favor production of low-angular-momentum states while pion-induced reactions (at least πN elastic scattering) is rich in high-angular-momentum states. To get a complete picture, hadron-induced reactions will be needed for a full understanding of the baryon resonance spectrum. Bugg (2009) mentioned that relatively simple experiments with no charged-particle tracking and with no magnetic field but a good electromagnetic calorimeter and a polarized target would give decisive new information on the hadronic mass spectrum, for both mesons and baryons, provided a good pion beam—which in the 1960s used to be the most natural thing in the world—would be available. A perfect laboratory for such experiments would be JPARC at KEK.

The chances for breakthroughs in the spectroscopy of light and heavy baryons are there and need to be pursued. The additional degrees of freedom in baryons—compared to the much simpler mesons—offer the possibility to test how strong QCD responds in such a complex environment: which of the multitude of configurations are realized and what are the effective agents and forces leading to the highly degenerate pattern of energy levels. A related question is whether iterating the binding mechanisms seen at work for baryons lead to exotic hadrons, in particular multiquark states.

ACKNOWLEDGMENTS

This review was initiated by the stimulating environment of the Sonderforschungsbereich SFB/TR16. E.K. is indebted to all his colleagues in SFB/TR16. Special thanks go to Ulrike Thoma and to her contributions in an early stage of this review. Illuminating discussions with Bernard Metsch and Herbert Petry are gratefully acknowledged as well as the cooperation with Alexey Anisovich, Victor Nikonov, and Andrey Sarantsev within the Bonn-Gatchina Partial Wave Analysis Group. We also benefited from comments on an early version of this review, in particular by Eulogio Oset and Ulf Meißner.

LIST OF ABBREVIATIONS

$\boldsymbol{I}$	isospin having components I_k,
I	isospin quantum number
$\boldsymbol{J}=\boldsymbol{L}+\boldsymbol{S}$	total angular momentum
J,L,S,l_ρ,l_λ	corresponding quantum numbers,
$\boldsymbol{L}$	$\boldsymbol{L}=\boldsymbol{l}_\rho+\boldsymbol{l}_\lambda$
L	sum $L=l_\rho+l_\lambda$
$M_{p,n}$	proton and neutron mass
N	band number
$N(xxx)$	nucleon N with mass xxx
$\mathrm{N}=\mathrm{n}_\rho+\mathrm{n}_\lambda$	radial number
P	parity
Q	charge
$Q=c,b$	heavy quarks
S	strangeness
$\boldsymbol{S}=s_1+s_2+s_3$	total quark spin
Y	hypercharge
$\Upsilon=(b\bar{b})$	bottomonium family
p,n	proton and neutron
$q=u,d,s$	include strangeness
u,d	light quarks
α,α_s	electromagnetic and strong couplings
$\kappa_{p,n}$	anomalous magnetic moments
ρ,λ	Jacobi variables for the three-body problem
$+e$	unit charge

REFERENCES

Aaltonen, T., *et al.*, 2007a, Phys. Rev. Lett. **99**, 202001.
Aaltonen, T., *et al.*, 2007b, Phys. Rev. Lett. **99**, 052002.
Aaltonen, T., *et al.*, 2009, Phys. Rev. D **80**, 072003.
Abazov, V. M., *et al.*, 2006, Nucl. Instrum. Methods Phys. Res. A **565**, 463.
Abazov, V. M., *et al.*, 2007, Phys. Rev. Lett. **99**, 052001.
Abazov, V. M., *et al.*, 2008, Phys. Rev. Lett. **101**, 232002.
Abe, K., *et al.*, 2007, Phys. Rev. Lett. **98**, 262001.
Abe, K., *et al.*, 2008, Phys. Rev. Lett. **100**, 142001.
Ablikim, M., *et al.*, 2006, Phys. Rev. Lett. **97**, 062001.
Abrams, G. S., *et al.*, 1974, Phys. Rev. Lett. **33**, 1453.
Acosta, D. E., *et al.*, 2005, Phys. Rev. D **71**, 032001.
Afonin, S. S., 2007, Int. J. Mod. Phys. A **22**, 4537.
Afonin, S. S., 2009, e-print arXiv:0904.0737.
Ahrens, J., *et al.*, 2000, Phys. Rev. Lett. **84**, 5950.
Ahrens, J., *et al.*, 2001, Phys. Rev. Lett. **87**, 022003.
Ahrens, J., *et al.*, 2005, Phys. Lett. B **624**, 173.
Ahrens, J., *et al.*, 2006a, Phys. Rev. Lett. **97** 202303.
Ahrens, J., *et al.*, 2006b, Phys. Rev. C **74**, 045204.
Ahrens, J., *et al.*, 2007, Eur. Phys. J. A **34**, 11.
Aitala, E. M., *et al.*, 1998, Phys. Rev. Lett. **81**, 44.
Ajaka, J., *et al.*, 2006, Phys. Rev. Lett. **96**, 132003.
Ajaka, J., *et al.*, 2008, Phys. Rev. Lett. **100**, 052003.
Aker, E., *et al.*, 1992, Nucl. Instrum. Methods Phys. Res. A **321**, 69.
Aktas, A., *et al.*, 2004, Phys. Lett. B **588**, 17.
Albrecht, H., *et al.*, 1989, Nucl. Instrum. Methods Phys. Res. A **275**, 1.
Albrecht, H., *et al.*, 1993, Phys. Lett. B **317**, 227.
Albrecht, H., *et al.*, 1997, Phys. Lett. B **402**, 207.
Albrow, M. G., *et al.*, 1970, Nucl. Phys. B **25**, 9.
Albrow, M. G., *et al.*, 1972, Nucl. Phys. B **37**, 594.
Albuquerque, R. A., S. Narison, and M. Nielsen, 2009, Phys. Lett. B **684**, 236.
Alekseev, I. G., *et al.*, 1991, Nucl. Phys. B **348**, 257.
Alekseev, I. G., *et al.*, 1995, Phys. Lett. B **351**, 585.
Alekseev, I. G., *et al.*, 1997, Phys. Rev. C **55**, 2049.
Alekseev, I. G., *et al.*, 2000, Phys. Lett. B **485**, 32.
Alekseev, I. G., *et al.*, 2006, Eur. Phys. J. C **45**, 383.
Alexander, J. P., *et al.*, 1999, Phys. Rev. Lett. **83**, 3390.
Alt, C., *et al.*, 2004, Phys. Rev. Lett. **92**, 042003.
Ambrozewicz, P., *et al.*, 2007, Phys. Rev. C **75**, 045203.
Ammar, R., *et al.*, 2001, Phys. Rev. Lett. **86**, 1167.
Amsler, C., *et al.*, 2008, Phys. Lett. B **667**, 1.
Anciant, E., *et al.*, 2000, Phys. Rev. Lett. **85**, 4682.
Anderson, R. L., *et al.*, 1969, Phys. Rev. Lett. **23**, 721.
Anderson, R. L., *et al.*, 1976, Phys. Rev. D **14**, 679.
Anisovich, A., 2009, e-print arXiv:0911.5277, Eur. Phys. J. (to be published).
Anisovich, A., V. Anisovich, M. Matveev, V. Nikonov, J. Nyiri, and A. Sarantsev, 2008, *Mesons and Baryons* (World Scientific, Singapore), p. 580.
Anisovich, A., E. Klempt, A. Sarantsev, and U. Thoma, 2005, Eur. Phys. J. A **24**, 111.
Anisovich, A. V., *et al.*, 2005, Eur. Phys. J. A **25**, 427.
Anisovich, A. V., *et al.*, 2007a, Eur. Phys. J. A **34**, 129.
Anisovich, A. V., *et al.*, 2007b, Eur. Phys. J. A **34**, 243.
Anisovich, A. V., *et al.*, 2009, Eur. Phys. J. A **41**, 13.
Arndt, R. A., W. J. Briscoe, T. W. Morrison, I.-I. Strakovsky,

R. L. Workman, and A. B. Gridnev, 2005, Phys. Rev. C **72**, 045202.
Arndt, R. A., W. J. Briscoe, I.-I. Strakovsky, and R. L. Workman, 2002, Phys. Rev. C **66**, 055213.
Arndt, R. A., W. J. Briscoe, I.-I. Strakovsky, and R. L. Workman, 2005, Phys. Rev. C **72**, 058203.
Arndt, R. A., W. J. Briscoe, I.-I. Strakovsky, and R. L. Workman, 2006, Phys. Rev. C **74**, 045205.
Arndt, R. A., W. J. Briscoe, I.-I. Strakovsky, and R. L. Workman, 2008, Eur. Phys. J. A **35**, 311
Arndt, R. A., W. J. Briscoe, I.-I. Strakovsky, R. L. Workman, and M. M. Pavan, 2004, Phys. Rev. C **69**, 035213.
Arndt, R. A., I.-I. Strakovsky, and R. L. Workman, 2003a, Int. J. Mod. Phys. A **18**, 449.
Arndt, R. A., I. I. Strakovsky, and R. L. Workman, 2003b, Phys. Rev. C **67**, 048201; **69**, 019901(E) (2004).
Artru, X., M. Elchikh, J.-M. Richard, J. Soffer, and O. V. Teryaev, 2009, Phys. Rep. **470**, 1.
Artuso, M., *et al.*, 2001, Phys. Rev. Lett. **86**, 4479.
Ashery, D., 1996, Hyperfine Interact. **103**, 253.
Assafiri, Y., *et al.*, 2003, Phys. Rev. Lett. **90**, 222001.
Aston, D., *et al.*, 1988, Phys. Lett. B **215**, 799.
Aston, D., *et al.*, 1990, Invited talk given at the 15th APS Division of Particles and Fields General Meeting, Houston, TX, 1990, SLAC Report No. SLAC-PUB-5236.
Athar, S. B., *et al.*, 2005, Phys. Rev. D **71**, 051101.
Aubert, B., *et al.*, 2002, Nucl. Instrum. Methods Phys. Res. A **479**, 1.
Aubert, B., *et al.*, 2005, Phys. Rev. D **72**, 052006.
Aubert, B., *et al.*, 2006a, in *A study of* $\Xi_c(2980)^+$ *and* $\Xi_c(3077)^+$*, 33rd International Conference on High Energy Physics (ICHEP 06)*, Moscow, Russia, 2006, edited by A. Sissakian and G. Kozlov (World Scientific, Singapore).
Aubert, B., *et al.*, 2006b, in Ξ_c' *production at BABAR, 33rd International Conference on High Energy Physics (ICHEP 06)*, Moscow, Russia, 2006, edited by A. Sissakian and G. Kozlov (World Scientific, Singapore).
Aubert, B., *et al.*, 2006c, Phys. Rev. Lett. **97**, 232001.
Aubert, B., *et al.*, 2006d, Phys. Rev. D **74**, 011103.
Aubert, B., *et al.*, 2007, Phys. Rev. Lett. **98**, 012001.
Aubert, B., *et al.*, 2008a, Phys. Rev. D **77**, 012002.
Aubert, B., *et al.*, 2008b, Phys. Rev. D **78**, 112003.
Aubert, J. J., *et al.*, 1974, Phys. Rev. Lett. **33**, 1404.
Augustin, J. E., *et al.*, 1974, Phys. Rev. Lett. **33**, 1406.
Avakian, H., *et al.*, 2004, Phys. Rev. D **69**, 112004.
Avery, P., *et al.*, 1989, Phys. Rev. Lett. **62**, 863.
Aznauryan, I. G., 2007, Phys. Rev. C **76**, 025212.
Aznauryan, I. G., 2009, Phys. Rev. C **80**, 055203.
Aznauryan, I. G., V. D. Burkert, G. V. Fedotov, B. S. Ishkhanov, and V. I. Mokeev, 2005, Phys. Rev. C **72**, 045201.
Aznauryan, I. G., V. D. Burkert, and T. S. H. Lee, 2008, e-print arXiv:0810.0997.
Aznauryan, I. G., *et al.*, 2008, Phys. Rev. C **78**, 045209.
Bagan, E., M. Chabab, H. G. Dosch, and S. Narison, 1993, Phys. Lett. B **301**, 243.
Bagan, E., H. G. Dosch, P. Gosdzinsky, S. Narison, and J. M. Richard, 1994, Z. Phys. C **64**, 57.
Ballam, J., *et al.*, 1972, Phys. Rev. D **5**, 545.
Ballam, J., *et al.*, 1973, Phys. Rev. D **7**, 3150.
Barber, D. P., *et al.*, 1982, Z. Phys. C **12**, 1.
Barber, D. P., *et al.*, 1984, Z. Phys. C **26**, 343.
Bari, G., *et al.*, 1991a, Nuovo Cimento Soc. Ital. Fis., A **104**, 1787.
Bari, G., *et al.*, 1991b, Nuovo Cimento Soc. Ital. Fis., A **104**, 571.
Barker, I. S., A. Donnachie, and J. K. Storrow, 1975, Nucl. Phys. B **95**, 347.
Barmin, V. V., *et al.*, 2003, Phys. At. Nucl. **66**, 1715.
Barnes, T., and F. E. Close, 1983, Phys. Lett. B **123**, 89.
Barnes, T., F. E. Close, and E. S. Swanson, 1995, Phys. Rev. D **52**, 5242.
Barnes, V. E., *et al.*, 1964, Phys. Rev. Lett. **12**, 204.
Barrow, S. P., *et al.*, 2001, Phys. Rev. C **64**, 044601.
Bartalini, O., *et al.*, 2002, Phys. Lett. B **544**, 113.
Bartalini, O., *et al.*, 2005, Eur. Phys. J. A **26**, 399.
Bartalini, O., *et al.*, 2007, Eur. Phys. J. A **33**, 169.
Barth, J., *et al.*, 2003a, Eur. Phys. J. A **18**, 117.
Barth, J., *et al.*, 2003b, Eur. Phys. J. A **17**, 269.
Barth, J., *et al.*, 2003c, Phys. Lett. B **572**, 127.
Bartholomy, O., *et al.*, 2005, Phys. Rev. Lett. **94**, 012003.
Bartholomy, O., *et al.*, 2007, Eur. Phys. J. A **33**, 133.
Basak, S., *et al.*, 2007, Phys. Rev. D **76**, 074504.
Basdevant, J. L., and S. Boukraa, 1986, Z. Phys. C **30**, 103.
Battaglieri, M., *et al.*, 2001, Phys. Rev. Lett. **87**, 172002.
Battaglieri, M., *et al.*, 2003, Phys. Rev. Lett. **90**, 022002.
Battaglieri, M., *et al.*, 2008, Phys. Rev. Lett. **102**, 102001.
Battaglieri, M., *et al.*, 2009, Phys. Rev. D **80**, 072005.
Beck, R., 2006, Eur. Phys. J. A **28**(s01), 173.
Berezhnoi, A. V., V. V. Kiselev, A. K. Likhoded, and A. I. Onishchenko, 1998, Phys. Rev. D **57**, 4385.
Bernard, V., 2008, Prog. Part. Nucl. Phys. **60**, 82.
Bernard, V., N. Kaiser, and U.-G. Meißner, 1995, Int. J. Mod. Phys. E **4**, 193.
Bernotas, A., and V. Simonis, 2008, e-print arXiv:0808.1220.
Biagi, S. F., *et al.*, 1983, Phys. Lett. B **122**, 455.
Biagi, S. F., *et al.*, 1985, Z. Phys. C **28**, 175.
Bicudo, P., M. Cardoso, T. Van Cauteren, and F. J. Llanes-Estrada, 2009, Phys. Rev. Lett. **103**, 092003.
Bienlein, J. K., and E. D. Bloom, 1981, *Proposal for investigating b and* $\bar{b}$ *spectroscopy at DORIS using the Crystal Ball*, Program Research Committee 81/09 (unpublished).
Bijker, R., F. Iachello, and A. Leviatan, 1994, Ann. Phys. **236**, 69.
Bijker, R., F. Iachello, and A. Leviatan, 1997, Phys. Rev. D **55**, 2862.
Bijker, R., F. Iachello, and A. Leviatan, 2000, Ann. Phys. (N.Y.) **284**, 89.
Biselli, A. S., *et al.*, 2008, Phys. Rev. C **78**, 045204.
Blomqvist, K. I., *et al.*, 1998, Nucl. Instrum. Methods Phys. Res. A **403**, 263.
Bock, A., *et al.*, 1998, Phys. Rev. Lett. **81**, 534.
Borasoy, B., P. C. Bruns, U. G. Meißner, and R. Lewis, 2006, Phys. Lett. B **641**, 294.
Borasoy, B., U. G. Meißner, and R. Nissler, 2006, Phys. Rev. C **74**, 055201.
Borasoy, B., U. G. Meißner, and R. Nissler, 2007, Eur. Phys. J. A **34**, 161.
Bradford, R., *et al.*, 2006, Phys. Rev. C **73**, 035202.
Bradford, R., *et al.*, 2007, Phys. Rev. C **75**, 035205.
Brambilla, N., *et al.*, 2004, CERN Yellow Report No. CERN-2005-005 (unpublished), p. 487.
Briscoe, W., R. Arndt, I. Strakovsky, and R. Workman, 2005, *International Workshop on the Physics of Excited Baryons (NSTAR 05)*, Tallahassee, Florida, edited by S. Capstick, V. Crede, and P. Eugenio (World Scientific, Singapore).
Brodsky, S. J., 2007, Eur. Phys. J. A **31**, 638.

Brodsky, S. J., and G. F. de Teramond, 2008, in *International School of Subnuclear Physics: 45th Course: Searching for the "Totally Unexpected"*, in the LHC Era, Erice, Italy, edited by A. Zichichi, e-print arXiv:0802.0514.
Brown, G. E., and M. Rho, 1979, Phys. Lett. B **82**, 177.
Brown, R. M., *et al.*, 1978, Nucl. Phys. B **144**, 287.
Bugg, D. V., 2009, Adv. High Energy Phys. **2009**, 52750.
Bulava, J. M., *et al.*, 2009, Phys. Rev. D **79**, 034505.
Burch, T., *et al.*, 2006, Phys. Rev. D **74**, 014504.
Butterworth, J. M., and M. Wing, 2005, Rep. Prog. Phys. **68**, 2773.
Cahn, R. N., and G. H. Trilling, 2004, Phys. Rev. D **69**, 011501.
Capstick, S., and N. Isgur, 1986, Phys. Rev. D **34**, 2809.
Capstick, S., and B. D. Keister, 1995, Phys. Rev. D **51**, 3598.
Capstick, S., and P. R. Page, 2002, Phys. Rev. C **66**, 065204.
Capstick, S., and W. Roberts, 2000, Prog. Part. Nucl. Phys. **45**, S241.
Carman, D. S., *et al.*, 2003, Phys. Rev. Lett. **90**, 131804.
Carman, D. S., *et al.*, 2009, Phys. Rev. C **79**, 065205.
Castelijns, R., *et al.*, 2008, Eur. Phys. J. A **35**, 39.
Cazzoli, E. G., *et al.*, 1975, Phys. Rev. Lett. **34**, 1125.
Ceci, S., A. Svarc, and B. Zauner, 2006a, Phys. Rev. Lett. **97**, 062002.
Ceci, S., A. Svarc, and B. Zauner, 2006b, Few-Body Syst. **39**, 27.
Ceci, S., A. Svarc, B. Zauner, M. Manley, and S. Capstick, 2008, Phys. Lett. B **659**, 228.
Chan, H.-M., *et al.*, 1978, Phys. Lett. B **76**, 634.
Chekanov, S., *et al.*, 2004, Phys. Lett. B **591**, 7.
Cheng, B., D.-X. Wang, and A. Zhang, 2009, e-print arXiv:0906.3934.
Cheng, H.-Y., and C.-K. Chua, 2007, Phys. Rev. D **75**, 014006.
Chew, G. F., and S. C. Frautschi, 1961, Phys. Rev. Lett. **7**, 394.
Chew, G. F., and S. C. Frautschi, 1962, Phys. Rev. Lett. **8**, 41.
Chew, G. F., M. L. Goldhaber, F. E. Low, and S. C. Frautschi, 1956, Phys. Rev. **101**, 1570.
Chew G. F., M. L. Goldberger, F. E. Low, and Y. Nambu, 1957, Phys. Rev. **106**, 1345.
Chiang, W.-T., and F. Tabakin, 1997, Phys. Rev. C **55**, 2054.
Chiang, W.-T., S. N. Yang, L. Tiator, M. Vanderhaeghen, and D. Drechsel, 2003, Phys. Rev. C **68**, 045202.
Chistov, R., *et al.*, 2006, Phys. Rev. Lett. **97**, 162001.
Choe, S., 1998, Eur. Phys. J. A **3**, 65.
Chung, Y., H. G. Dosch, M. Kremer, and D. Schall, 1982, Nucl. Phys. B **197**, 55.
Cohen, T. D., and L. Y. Glozman, 2002a, Phys. Rev. D **65**, 016006.
Cohen, T. D., and L. Y. Glozman, 2002b, Int. J. Mod. Phys. A **17**, 1327.
Copley, L. A., N. Isgur, and G. Karl, 1979, Phys. Rev. D **20**, 768; **23**, 817(E) (1981).
Corthals, T., D. G. Ireland, T. Van Cauteren, and J. Ryckebusch, 2007, Phys. Rev. C **75**, 045204.
Corthals, T., J. Ryckebusch, and T. Van Cauteren, 2006, Phys. Rev. C **73**, 045207.
Corthals, T., T. Van Cauteren, P. Van Craeyveld, J. Ryckebusch, and D. G. Ireland, 2007, Phys. Lett. B **656**, 186.
Cottingham, W. N., 1963, Ann. Phys. (N.Y.) **25**, 424.
Cox, C. R., *et al.*, 1969, Phys. Rev. **184**, 1453.
Craig, K., *et al.*, 2003, Phys. Rev. Lett. **91**, 102301.
Crede, V., and C. A. Meyer, 2009, Prog. Part. Nucl. Phys. **63**, 74.
Crede, V., *et al.*, 2005, Phys. Rev. Lett. **94**, 012004.
Crede, V., *et al.*, 2009, Phys. Rev. C **80**, 055202.
Csorna, S. E., *et al.*, 2001, Phys. Rev. Lett. **86**, 4243.
Cutkosky, R. E., C. P. Forsyth, J. B. Babcock, R. L. Kelly, and R. E. Hendrick, 1980, *4th International Conference on Baryon Resonances*, Toronto, Canada, 1980 (University of Toronto, Toronto).
Cutkosky, R. E., C. P. Forsyth, R. E. Hendrick, and R. L. Kelly, 1979, Phys. Rev. D **20**, 2839.
Dalitz, R. H., and S. F. Tuan, 1959, Phys. Rev. Lett. **2**, 425.
Dalitz, R. H., and S. F. Tuan, 1960, Ann. Phys. (N.Y.) **10**, 307.
Dalitz, R. H., T. C. Wong, and G. Rajasekaran, 1967, Phys. Rev. **153**, 1617.
Dalton, M., *et al.*, 2009, Phys. Rev. C **80**, 015205.
Danilov, M. V., and R. V. Mizuk, 2008, Phys. At. Nucl. **71**, 605.
Dannhausen, H. W., *et al.*, 2001, Eur. Phys. J. A **11**, 441.
De Grand, T. A., R. L. Jaffe, K. Johnson, and J. E. Kiskis, 1975, Phys. Rev. D **12**, 2060.
De Masi, R., *et al.*, 2008, Phys. Rev. C **77**, 042201.
Denizli, H., *et al.*, 2007, Phys. Rev. C **76**, 015204.
De Rújula, A., H. Georgi, and S. L. Glashow, 1975, Phys. Rev. D **12**, 147.
de Teramond, G. F., and S. J. Brodsky, 2005, Phys. Rev. Lett. **94**, 201601.
de Teramond, G. F., and S. J. Brodsky, 2009, e-print arXiv:0903.4922.
Diakonov, D., V. Petrov, and M. V. Polyakov, 1997, Z. Phys. A **359**, 305.
Di Salvo, R., *et al.*, 2009, Eur. Phys. J. A **42**, 151.
Donoghue, J. F., C. Ramirez, and G. Valencia, 1989, Phys. Rev. D **39**, 1947.
Döring, M., E. Oset, and M. J. Vicente Vacas, 2004, Phys. Rev. C **70**, 045203.
Döring, M., and K. Nakayama, 2010a, Phys. Lett. B **683**, 145.
Döring, M., and K. Nakayama, 2010b, Eur. Phys. J. A **43**, 83.
Döring, M., E. Oset, and B. S. Zou, 2008, Phys. Rev. C **78**, 025207.
Dosch, H. G., M. Jamin, and S. Narison, 1989, Phys. Lett. B **220**, 251.
Drach, V., *et al.*, 2008, PoS **LAT2008**, 123.
Drechsel, D., S. S. Kamalov, and L. Tiator, 2007, Eur. Phys. J. A **34**, 69.
Drechsel, D., and T. Walcher, 2008, Rev. Mod. Phys. **80**, 731.
Drell, S. D., and A. C. Hearn, 1966, Phys. Rev. Lett. **16**, 908.
Dugger, M., *et al.*, 2002, Phys. Rev. Lett. **89**, 222002.
Dugger, M., *et al.*, 2006, Phys. Rev. Lett. **96**, 062001.
Dugger, M., *et al.*, 2007, Phys. Rev. C **76**, 025211.
Dugger, M., *et al.*, 2009, Phys. Rev. C **79**, 065206.
Durand, J., B. Julia-Diaz, T. S. H. Lee, B. Saghai, and T. Sato, 2008, Phys. Rev. C **78**, 025204.
Dürr, S., *et al.*, 2008, Science **322**, 1224.
Dutz, H., *et al.*, 2003, Phys. Rev. Lett. **91**, 192001.
Dziembowski, Z., M. Fabre de la Ripelle, and G. A. Miller, 1996, Phys. Rev. C **53**, R2038.
Dzierba, A. R., C. A. Meyer, and A. P. Szczepaniak, 2005, J. Phys.: Conf. Ser. **9**, 192.
Ebert, D., R. N. Faustov, and V. O. Galkin, 2008, Phys. Lett. B **659**, 612.
Ecker, G., J. Gasser, A. Pich, and E. de Rafael, 1989, Nucl. Phys. B **321**, 311.
Edwards, K. W., *et al.*, 1995, Phys. Rev. Lett. **74**, 3331.
Egiyan, H., *et al.*, 2006, Phys. Rev. C **73**, 025204.
Elsner, D., *et al.*, 2006, Eur. Phys. J. A **27**, 91.
Elsner, D., *et al.*, 2007, Eur. Phys. J. A **33**, 147.

Elsner, D., *et al.*, 2009, Eur. Phys. J. A **39**, 373.

Engelfried, J., *et al.*, 1998, Nucl. Instrum. Methods Phys. Res. A **409**, 439.

Erbe, R., *et al.*, 1968, Phys. Rev. **175**, 1669.

Fantini, A., *et al.*, 2008, Phys. Rev. C **78**, 015203.

Fedotov, G., *et al.*, 2009, Phys. Rev. C **79**, 015204.

Feuster, T., and U. Mosel, 1998a, Phys. Rev. C **58**, 457.

Feuster, T., and U. Mosel, 1998b, Phys. Rev. C **59**, 460.

Fleck, S., and J. M. Richard, 1989, Prog. Theor. Phys. **82**, 760.

Fleck, S., and J. M. Richard, 1990, Part. World **1**, 67.

Flynn, J. M., F. Mescia, and A. S. B. Tariq, 2003, J. High Energy Phys. **07**, 066.

Forkel, H., M. Beyer, and T. Frederico, 2007a, Int. J. Mod. Phys. E **16**, 2794.

Forkel, H., M. Beyer, and T. Frederico, 2007b, J. High Energy Phys. **07**, 077.

Forkel, H., and E. Klempt, 2009, Phys. Lett. B **679**, 77.

Frabetti, P. L., *et al.*, 1994, Phys. Rev. Lett. **72**, 961.

Frabetti, P. L., *et al.*, 1996, Phys. Lett. B **365**, 461.

Franklin, J., 1999, Phys. Rev. D **59**, 117502.

Franklin, J., 2008, e-print arXiv:0811.2143.

Frolov, V. V., *et al.*, 1999, Phys. Rev. Lett. **82**, 45.

Gabler, A. R., *et al.*, 1994, Nucl. Instrum. Methods Phys. Res. A **346**, 168.

Gaillard, M. K., B. W. Lee, and J. L. Rosner, 1975, Rev. Mod. Phys. **47**, 277.

Gaiser, J., *et al.*, 1986, Phys. Rev. D **34**, 711.

García-Recio, C., J. Nieves, E. Ruiz Arriola, and M. J. Vicente Vacas, 2003, Phys. Rev. D **67**, 076009.

Garcilazo, H., J. Vijande, and A. Valcarce, 2007, J. Phys. G **34**, 961.

Gasser, J., and H. Leutwyler, 1984, Ann. Phys. (N.Y.) **158**, 142.

Gasser, J., and H. Leutwyler, 1985, Nucl. Phys. B **250**, 465.

Gell-Mann, M., 1962, Phys. Rev. **125**, 1067.

Gell-Mann, M., and Y. Ne'eman, 1964, *The Eightfold Way*, Frontiers in Physics (Benjamin, New York).

Geng, L. S., E. Oset, B. S. Zou, and M. Doring, 2009, Phys. Rev. C **79**, 025203.

Gerasimov, S. B., 1966, Sov. J. Nucl. Phys. **2**, 430 [Yad. Fiz. **2**, 598 (1966)].

Gerasyuta, S. M., and V. I. Kochkin, 2002, Phys. Rev. D **66**, 116001.

Gignoux, C., B. Silvestre-Brac, and J. M. Richard, 1987, Phys. Lett. B **193**, 323.

Glander, K. H., *et al.*, 2004, Eur. Phys. J. A **19**, 251.

Glozman, L. Y., 2000, Phys. Lett. B **475**, 329.

Glozman, L. Y., 2007, Phys. Rep. **444**, 1.

Glozman, L. Y., 2009, e-print arXiv:0903.3923.

Glozman, L. Y., and D. O. Riska, 1996, Phys. Rep. **268**, 263.

Godfrey, S., and N. Isgur, 1985, Phys. Rev. D **32**, 189.

Goldhaber, G., *et al.*, 1976, Phys. Rev. Lett. **37**, 255.

Goloskokov, S. V., 2008, Microtecnic **162**, 25.

Golowich, E., E. Haqq, and G. Karl, 1983, Phys. Rev. D **28**, 160.

Gomez Tejedor, J. A., and E. Oset, 1996, Nucl. Phys. A **600**, 413.

Gomshi Nobary, M. A., and R. Sepahvand, 2007, Phys. Rev. D **76**, 114006.

Gonzalez, P., E. Oset, and J. Vijande, 2009, Phys. Rev. C **79**, 025209.

Gopal, G. P., 1980, *4th International Conference on Baryon Resonances*, Toronto, Canada, 1980 (University of Toronto, Toronto).

Greenberg, O. W., 1964, Phys. Rev. Lett. **13**, 598.

Greenberg, O. W., and H. J. Lipkin, 1981, Nucl. Phys. A **370**, 349.

Guberina, B., B. Melic, and H. Stefancic, 2000, Phys. Lett. B **484**, 43.

Guberina, B., R. Ruckl, and J. Trampetic, 1986, Z. Phys. C **33**, 297.

Guo, F.-K., C. Hanhart, and U.-G. Meißner, 2008, J. High Energy Phys. **09**, 136.

Guo, L., *et al.*, 2007, Phys. Rev. C **76**, 025208.

Gutz, E., *et al.*, 2008, Eur. Phys. J. A **35**, 291.

Hadjidakis, C., *et al.*, 2005, Phys. Lett. B **605**, 256.

Han, M. Y., and Y. Nambu, 1965, Phys. Rev. **139**, B1006.

Hanhart, C., 2008, Eur. Phys. J. A **35**, 271.

Hasenfratz, P., R. R. Horgan, J. Kuti, and J. M. Richard, 1980, Phys. Lett. B **94**, 401.

Hasenfratz, P., and J. Kuti, 1978, Phys. Rep. **40**, 75.

Haupt, C., B. Metsch, and H.-R. Petry, 2006, Eur. Phys. J. A **28**, 213.

He, X.-G., X.-Q. Li, X. Liu, and X.-Q. Zeng, 2007, Eur. Phys. J. C **51**, 883.

Helbing, K., 2006, Prog. Part. Nucl. Phys. **57**, 405.

Hey, A. J. G., and R. L. Kelly, 1983, Phys. Rep. **96**, 71.

Hicks, K., *et al.*, 2007, Phys. Rev. C **76**, 042201.

Hicks, K., *et al.*, 2009, Phys. Rev. Lett. **102**, 012501.

Hicks, K. H., 2005, Prog. Part. Nucl. Phys. **55**, 647.

Hleiqawi, I., *et al.*, 2007, Phys. Rev. C **75**, 042201.

Hogaasen, H., and J. M. Richard, 1983, Phys. Lett. B **124**, 520.

Höhler, G., 2004, private communication.

Höhler, G., F. Kaiser, R. Koch, and E. Pietarinen, 1979, Physics Data **12-1**, 1.

Höhler, G., and R. L. Workman, 2008, see Amsler *et al.*, 2008.

Horn, I., *et al.*, 2008a, Phys. Rev. Lett. **101**, 202002.

Horn, I., *et al.*, 2008b, Eur. Phys. J. A **38**, 173.

Hyodo, T., D. Jido, and A. Hosaka, 2008, Phys. Rev. C **78**, 025203.

Hyslop, J. S., R. A. Arndt, L. D. Roper, and R. L. Workman, 1992, Phys. Rev. D **46**, 961.

Iachello, F., 1989, Phys. Rev. Lett. **62**, 2440.

Iijima, T., and E. Prebys, 2000, Nucl. Instrum. Methods Phys. Res. A **446**, 75.

Inopin, A., and G. S. Sharov, 2001, Phys. Rev. D **63**, 054023.

Ioffe, B. L., 1981, Nucl. Phys. B **188**, 317; **191**, 591(E) (1981).

Iori, M., *et al.*, 2007, e-print arXiv:hep-ex/0701021.

Isgur, N., 1980, Phys. Rev. D **21**, 779; **23**, 817(E) (1981).

Isgur, N., 2001, in *Excited Nucleons and Hadronic Structure, N^**2000, Newport News, 2000, edited by V. D. Burkert, L. Elonadrihiri, J. J. Kelly (World Scientific, Singapore), p. 403.

Isgur, N., and G. Karl, 1977, Phys. Lett. B **72**, 109.

Isgur, N., and M. B. Wise, 1991, Phys. Rev. Lett. **66**, 1130.

Jaegle, I., *et al.*, 2008, Phys. Rev. Lett. **100**, 252002.

Jaffe, R. L., 1977, Phys. Rev. Lett. **38**, 195; **38**, 617(E) (1977).

Jaffe, R. L., 2004, Eur. Phys. J. C **35**, 221.

Jaffe, R. L., 2005, Phys. Rep. **409**, 1.

Jaffe, R. L., 2007, AIP Conf. Proc. **964**, 1.

Jaffe, R. L., D. Pirjol, and A. Scardicchio, 2006, Phys. Rep. **435**, 157.

Jaffe, R. L., and F. Wilczek, 2003, Phys. Rev. Lett. **91**, 232003.

Jessop, C. P., *et al.*, 1999, Phys. Rev. Lett. **82**, 492.

Jido, D., M. Doering, and E. Oset, 2008, Phys. Rev. C **77**, 065207.

Jido, D., J. A. Oller, E. Oset, A. Ramos, and U. G. Meißner, 2003, Nucl. Phys. A **725**, 181.

Joo, K., *et al.*, 2002, Phys. Rev. Lett. **88**, 122001.
Joo, K., *et al.*, 2003, Phys. Rev. C **68**, 032201.
Joo, K., *et al.*, 2005, Phys. Rev. C **72**, 058202.
Julia-Diaz, B., T. S. H. Lee, A. Matsuyama, and T. Sato, 2007, Phys. Rev. C **76**, 065201.
Julia-Diaz, B., T. S. H. Lee, A. Matsuyama, T. Sato, and L. C. Smith, 2008, Phys. Rev. C **77**, 045205.
Julia-Diaz, B., and D. O. Riska, 2006, Nucl. Phys. A **780**, 175.
Julia-Diaz, B. and D. O. Riska, 2009, Phys. Rev. C **80**, 025207.
Junkersfeld, J., *et al.*, 2007, Eur. Phys. J. A **31**, 365.
Kaiser, N., P. B. Siegel, and W. Weise, 1995, Nucl. Phys. A **594**, 325.
Kalleicher, F., *et al.*, 1997, Z. Phys. A **359**, 201.
Kamano, H., B. Julia-Diaz, T. S. H. Lee, A. Matsuyama, and T. Sato, 2009a, Phys. Rev. C **79**, 025206.
Kamano, H., B. Julia-Diaz, T. S. H. Lee, A. Matsuyama, and T. Sato, 2009b, Phys. Rev. C **80**, 065203.
Karliner, M., B. Keren-Zur, H. J. Lipkin, and J. L. Rosner, 2009, Ann. Phys. **324**, 2.
Karliner, M., and M. P. Mattis, 1986, Phys. Rev. D **34**, 1991.
Kashevarov, V. L., 2009, Eur. Phys. J. A **42**, 141.
Kernel, G., *et al.*, 1989a, Phys. Lett. B **216**, 244.
Kernel, G., *et al.*, 1989b, Phys. Lett. B **225**, 198.
Kernel, G., *et al.*, 1990, Z. Phys. C **48**, 201.
Kirchbach, M., M. Moshinsky, and Y. F. Smirnov, 2001, Phys. Rev. D **64**, 114005.
Kisslinger, L. S., 2004, Phys. Rev. D **69**, 054015.
Kisslinger, L. S., and Z. P. Li, 1995, Phys. Rev. D **51**, R5986.
Kittel, O., and G. R. Farrar, 2005, e-print arXiv:hep-ph/0508150.
Klein, F., *et al.*, 2008, Phys. Rev. D **78**, 117101.
Klempt, E., 2003, Phys. Lett. B **559**, 144.
Klempt, E., 2008, Eur. Phys. J. A **38**, 187.
Klempt, E., A. V. Anisovich, V. A. Nikonov, A. V. Sarantsev, and U. Thoma, 2006, Eur. Phys. J. A **29**, 307.
Klempt, E., B. C. Metsch, C. R. Munz, and H. R. Petry, 1995, Phys. Lett. B **361**, 160.
Klempt, E., and A. Zaitsev, 2007, Phys. Rep. **454**, 1.
Knapp, B., *et al.*, 1976, Phys. Rev. Lett. **37**, 882.
Knöchlein, G., D. Drechsel, and L. Tiator, 1995, Z. Phys. A **352**, 327.
Kohri, H., *et al.*, 2009, e-print arXiv:0906.0197.
Kokkedee, J. J. J., 1969, *The Quark Model*, Frontiers in Physics (Benjamin, New York), based on a series of lectures given at CERN in Autumn 1967.
Koniuk, R., and N. Isgur, 1980a, Phys. Rev. D **21**, 1868.
Koniuk, R., and N. Isgur, 1980b, Phys. Rev. Lett. **44**, 845.
Kopp, S. E., 1996, Nucl. Instrum. Methods Phys. Res. A **384**, 61.
Körner, J. G., M. Kramer, and D. Pirjol, 1994, Prog. Part. Nucl. Phys. **33**, 787.
Kozlenko, N. G., *et al.*, 2003, Phys. At. Nucl. **66**, 110.
Krambrich, D., *et al.*, 2009, Phys. Rev. Lett. **103**, 052002.
Krehl, O., C. Hanhart, S. Krewald, and J. Speth, 2000, Phys. Rev. C **62**, 025207.
Krusche, B., and S. Schadmand, 2003, Prog. Part. Nucl. Phys. **51**, 399.
Kuznetsov, A., *et al.*, 2008, Acta Phys. Pol. B **39**, 1949.
Kuznetsov, V., *et al.*, 2007, Phys. Lett. B **647**, 23.
LaCourse, D., and M. G. Olsson, 2008, Phys. Rev. D **39**, 2751.
Langgärtner, W., *et al.*, 2001, Phys. Rev. Lett. **87**, 052001.
Lawall, R., *et al.*, 2005, Eur. Phys. J. A **24**, 275.
Lee, T. S. H., 2007, Int. J. Mod. Phys. E **18**, 1215.
Lesiak, T., 2008, Phys. Lett. B **665**, 9.
Lewis, R., N. Mathur, and R. M. Woloshyn, 2001, Phys. Rev. D **64**, 094509.
Li, C., and E. Oset, 2004, Phys. Rev. C **70**, 065202.
Li, Q. B., and D. O. Riska, 2006, Phys. Rev. C **74**, 015202.
Li, S., X. Shen, and F. T. B. Collaboration, 2009, e-print arXiv:0905.1562.
Li, Z.-P., V. Burkert, and Z.-J. Li, 1992, Phys. Rev. D **46**, 70.
Lichtenberg, D., 1996, *Third International Workshop on Diquarks and other Models of Compositeness (DIQUARKS III)*, Turin, Italy (World Scientific, Singapore).
Lichtenberg, D. B., 1977, Phys. Rev. D **16**, 231.
Lichtenberg, D. B., R. Roncaglia, and E. Predazzi, 1996, Phys. Rev. D **53**, 6678.
Lipkin, H. J., 1987, Phys. Lett. B **195**, 484.
Liu, B. C., and B. S. Zou, 2006, Phys. Rev. Lett. **96**, 042002.
Liu, B. C., and B. S. Zou, 2007, Phys. Rev. Lett. **98**, 039102.
Liu, X., H.-W. Ke, Q.-P. Qiao, Z.-T. Wei, and X.-Q. Li, 2008, Phys. Rev. D **77**, 035014.
Lleres, A., *et al.*, 2007, Eur. Phys. J. A **31**, 79.
Lleres, A., *et al.*, 2009, Eur. Phys. J. A **39**, 149.
Löring, U., K. Kretzschmar, B. C. Metsch, and H. R. Petry, 2001, Eur. Phys. J. A **10**, 309.
Löring, U., B. C. Metsch, and H. R. Petry, 2001a, Eur. Phys. J. A **10**, 395.
Löring, U., B. C. Metsch, and H. R. Petry, 2001b, Eur. Phys. J. A **10**, 447.
Lowe, J., *et al.*, 1991, Phys. Rev. C **44**, 956.
Lutz, M. F. M., and E. E. Kolomeitsev, 2002, Nucl. Phys. A **700**, 193.
MacCormick, M., *et al.*, 1996, Phys. Rev. C **53**, 41.
Magas, V. K., E. Oset, and A. Ramos, 2005, Phys. Rev. Lett. **95**, 052301.
Mahbub, M. S., *et al.*, 2009, Phys. Lett. **679**, 418.
Manley, D. M., R. A. Arndt, Y. Goradia, and V. L. Teplitz, 1984, Phys. Rev. D **30**, 904.
Manley, D. M., and E. M. Saleski, 1992, Phys. Rev. D **45**, 4002.
Manley, D. M., *et al.*, 2002, Phys. Rev. Lett. **88**, 012002.
Manweiler, R., *et al.*, 2008, Phys. Rev. C **77**, 015205.
Mart, T., and A. Sulaksono, 2006, Phys. Rev. C **74**, 055203.
Martin, A., 1986, Z. Phys. C **32**, 359.
Martin, J. F., *et al.*, 1975, Nucl. Phys. B **89**, 253.
Mathur, N., *et al.*, 2005, Phys. Lett. B **605**, 137.
Matsuyama, A., T. Sato, and T. S. H. Lee, 2007, Phys. Rep. **439**, 193.
Mattson, M., *et al.*, 2002, Phys. Rev. Lett. **89**, 112001.
Meadows, B. T., 1980, *Proceedings Baryon 1980*, Toronto (University of Toronto, Toronto), pp. 283–300.
Mecking, B. A., *et al.*, 2003, Nucl. Instrum. Methods Phys. Res. A **503**, 513.
Meißner, Ulf-G., and J. A. Oller, 2000, Nucl. Phys. A **673**, 311.
Melde, T., W. Plessas, and B. Sengl, 2008, Phys. Rev. D **77**, 114002.
Melde, T., W. Plessas, and R. F. Wagenbrunn, 2005, Phys. Rev. C **72**, 015207.
Melnitchouk, W., *et al.*, 2003, Phys. Rev. D **67**, 114506.
Merkel, H., *et al.*, 2007, Phys. Rev. Lett. **99**, 132301.
Metsch, B., U. Loring, D. Merten, and H. Petry, 2003, Eur. Phys. J. A **18**, 189.
Mibe, T., *et al.*, 2005, Phys. Rev. Lett. **95**, 182001.
Michael, C., 2006, PoS **LAT2005**, 008.
Migura, S., D. Merten, B. Metsch, and H.-R. Petry, 2006a, Eur. Phys. J. A **28**, 41.

Migura, S., D. Merten, B. Metsch, and H.-R. Petry, 2006b, Eur. Phys. J. A **28**, 55.
Minami, S., 1968, Prog. Theor. Phys. **40**, 1068.
Mizuk, R., *et al.*, 2005, Phys. Rev. Lett. **94**, 122002.
Mizuk, R., *et al.*, 2008, Phys. Rev. D **78**, 072004.
Mokeev, V. I., *et al.*, 2009, Phys. Rev. C **80**, 045212.
Mokhtari, A., *et al.*, 1985, Phys. Rev. Lett. **55**, 359.
Mokhtari, A., *et al.*, 1987, Phys. Rev. D **35**, 810.
Morand, L., *et al.*, 2005, Eur. Phys. J. A **24**, 445.
Morrow, S. A., *et al.*, 2009, Eur. Phys. J. A **39**, 5.
Morsch, H. P., and P. Zupranski, 2000, Phys. Rev. C **61**, 024002.
Nacher, J. C., E. Oset, M. J. Vicente, and L. Roca, 2001, Nucl. Phys. A **695**, 295.
Nadkarni, S., and H. B. Nielsen, 1986, Nucl. Phys. B **263**, 1.
Nakabayashi, T., *et al.*, 2006, Phys. Rev. C **74**, 035202.
Nakano, T., *et al.*, 2003, Phys. Rev. Lett. **91**, 012002.
Nakano, T., *et al.*, 2009, Phys. Rev. C **79**, 025210.
Nakayama, K., Y. Oh, and H. Haberzettl, 2008, e-print arXiv:0803.3169.
Nambu, Y., and G. Jona-Lasinio, 1961, Phys. Rev. **122**, 345.
Nanova, M., *et al.*, 2008, Eur. Phys. J. A **35**, 333.
Narison, S., 2004, *QCD as a Theory of Hadrons: From Partons to Confinement* (Cambridge University Press, Cambridge).
Nasseripour, R., *et al.*, 2008, Phys. Rev. C **77**, 065208.
Naumann, J., *et al.*, 2003, Nucl. Instrum. Methods Phys. Res. A **498**, 211.
Nefkens, B., 2001, 18th Students Workshop on Electromagnetic Interactions in Bosen/Saar (unpublished).
Nefkens, B. M. K., S. Prakhov, and A. Starostin, 2002, International Workshop on Chiral Fluctuations in Hadronic Matter, Orsay, France, edited by Z. Aouissat, C. Isselhorst, P. Schuck, and J. Wambach (unpublished).
Niiyama, M., *et al.*, 2008, Phys. Rev. C **78**, 035202.
Nikonov, V. A., A. V. Anisovich, E. Klempt, A. V. Sarantsev, and U. Thoma, 2008, Phys. Lett. B **662**, 245.
Nussinov, S., and M. A. Lampert, 2002, Phys. Rep. **362**, 193.
Ocherashvili, A., *et al.*, 2005, Phys. Lett. B **628**, 18.
Oller, J. A., 2006, Eur. Phys. J. A **28**, 63.
Oller, J. A., E. Oset, and A. Ramos, 2000, Prog. Part. Nucl. Phys. **45**, 157.
Olmsted, J., *et al.*, 2004, Phys. Lett. B **588**, 29.
Oset, E., and A. Ramos, 1998, Nucl. Phys. A **635**, 99.
Osipenko, M., *et al.*, 2009, Phys. Rev. D **80**, 032004.
Pasquini, B., D. Drechsel, and L. Tiator, 2006, Int. J. Mod. Phys. A **27**, 231.
Penner, G., and U. Mosel, 2002a, Phys. Rev. C **66**, 055211.
Penner, G., and U. Mosel, 2002b, Phys. Rev. C **66**, 055212.
Petersen, B. A., 2006, *33rd International Conference on High Energy Physics (ICHEP 06)*, Moscow, 2006, edited by A. Sissakian and G. Kozlov (World Scientific, Singapore).
Pocanic, D., *et al.*, 1994, Phys. Rev. Lett. **72**, 1156.
Polchinski, J., and M. J. Strassler, 2002, Phys. Rev. Lett. **88**, 031601.
Prakhov, S., *et al.*, 2004a, Phys. Rev. C **70**, 034605.
Prakhov, S., *et al.*, 2004b, Phys. Rev. C **69**, 045202.
Prakhov, S., *et al.*, 2004c, Phys. Rev. C **69**, 042202.
Prakhov, S., *et al.*, 2005, Phys. Rev. C **72**, 015203.
Ratti, S. P., 2003, Nucl. Phys. B, Proc. Suppl. **115**, 33.
Regge, T., 1959, Nuovo Cimento **14**, 951.
Regge, T., 1960, Nuovo Cimento **18**, 947.
Reinders, L. J., H. Rubinstein, and S. Yazaki, 1985, Phys. Rep. **127**, 1.
Rho, M., D. O. Riska, and N. N. Scoccola, 1992, Z. Phys. A **341**, 343.
Richard, J. M., 1981, Phys. Lett. B **100**, 515.
Richard, J. M., 1992, Phys. Rep. **212**, 1.
Richard, J. M., and P. Taxil, 1983, Ann. Phys. **150**, 267.
Ripani, M., *et al.*, 2003, Phys. Rev. Lett. **91**, 022002.
Rosner, J. L., 2007, J. Phys. G **34**, S127.
Sadler, M. E., *et al.*, 2004, Phys. Rev. C **69**, 055206.
Santoro, J. P., *et al.*, 2008, Phys. Rev. C **78**, 025210.
Sarantsev, A. V., V. A. Nikonov, A. V. Anisovich, E. Klempt, and U. Thoma, 2005, Eur. Phys. J. A **25**, 441.
Sarantsev, A. V., *et al.*, 2008, Phys. Lett. B **659**, 94.
Sasaki, K., and S. Sasaki, 2005, Phys. Rev. D **72**, 034502.
Sasaki, K., S. Sasaki, and T. Hatsuda, 2005, Phys. Lett. B **623**, 208.
Schneider, S., S. Krewald, and U.-G. Meißner, 2006, Eur. Phys. J. A **28**, 107.
Schumacher, R., 2008, Eur. Phys. J. A **35**, 299.
Schwille, W. J., *et al.*, 1994, Nucl. Instrum. Methods Phys. Res. A **344**, 470.
Seftor, C. J., *et al.*, 1989, Phys. Rev. D **39**, 2457.
Semay, C., F. Brau, and B. Silvestre-Brac, 2001, Phys. Rev. C **64**, 055202.
Sengl, B., T. Melde, and W. Plessas, 2007, Phys. Rev. D **76**, 054008.
Sevior, M. E., *et al.*, 1991, Phys. Rev. Lett. **66**, 2569.
Shifman, M., and A. Vainshtein, 2008, Phys. Rev. D **77**, 034002.
Shifman, M. A., A. I. Vainshtein, and V. I. Zakharov, 1979, Nucl. Phys. B **147**, 385.
Shklyar, V., H. Lenske, and U. Mosel, 2005, Phys. Rev. C **72**, 015210.
Shklyar, V., H. Lenske, and U. Mosel, 2007, Phys. Lett. B **650**, 172.
Shklyar, V., H. Lenske, U. Mosel, and G. Penner, 2005, Phys. Rev. C **71**, 055206.
Shuryak, E. V., and J. L. Rosner, 1989, Phys. Lett. B **218**, 72.
Shyam, R., O. Scholten, and H. Lenske, 2010, Phys. Rev. C **81**, 015204.
Sibirtsev, A., J. Haidenbauer, and U. G. Meißner, 2007, Phys. Rev. Lett. **98**, 039101.
Sibirtsev, A., *et al.*, 2004, Phys. Lett. B **599**, 230.
Sibirtsev, A., *et al.*, 2007, Eur. Phys. J. A **34**, 49.
Sibirtsev, A., *et al.*, 2009a, Eur. Phys. J. A **40**, 65.
Sibirtsev, A., *et al.*, 2009b, Eur. Phys. J. A **41**, 71.
Solovieva, E., *et al.*, 2005, Phys. Lett. B **672**, 1.
Stanley, D. P., and D. Robson, 1980, Phys. Rev. Lett. **45**, 235.
Starostin, A., *et al.*, 2005, Phys. Rev. C **72**, 015205.
Stepanyan, S., *et al.*, 2003, Phys. Rev. Lett. **91**, 252001.
Strauch, S., *et al.*, 2005, Phys. Rev. Lett. **95**, 162003.
Sumihama, M., *et al.*, 2006, Phys. Rev. C **73**, 035214.
Suzuki, N., T. Sato, and T. S. H. Lee, 2009, Phys. Rev. C **79**, 025205.
Tang, A., and J. W. Norbury, 2000, Phys. Rev. D **62**, 016006.
Tariq, A. S. B., 2007, PoS **LAT2007**, 136.
Thoma, U., *et al.*, 2008, Phys. Lett. B **659**, 87.
Thomas, A. W., S. Theberge, and G. A. Miller, 1981, Phys. Rev. D **24**, 216.
't Hooft, G., 1976, Phys. Rev. D **14**, 3432.
Törnqvist, N. A., and P. Zenczykowski, 1984, Phys. Rev. D **29**, 2139.
Törnqvist, N. A., and P. Zenczykowski, 1986, Z. Phys. C **30**, 83.
Trilling, G., 2008, see Yao *et al.*, 2006.
Ungaro, M., *et al.*, 2006, Phys. Rev. Lett. **97**, 112003.
Valcarce, A., F. Fernandez, P. Gonzalez, and V. Vento, 1996,

Phys. Lett. B **367**, 35.
Van Dyck, A., T. Van Cauteren, J. Ryckebusch, B. C. Metsch, and H. R. Petry, 2008, Prog. Part. Nucl. Phys. **61**, 175.
van Pee, H., *et al.*, 2007, Eur. Phys. J. A **31**, 61.
Varga, K., M. Genovese, J.-M. Richard, and B. Silvestre-Brac, 1999, Phys. Rev. D **59**, 014012.
Viehhauser, G., 2000, Nucl. Instrum. Methods Phys. Res. A **446**, 97.
Vijande, J., A. Valcarce, and F. Fernandez, 2009, Phys. Rev. D **79**, 037501.
Vijande, J., A. Valcarce, and J. M. Richard, 2007, Phys. Rev. D **76**, 114013.
Vrana, T. P., S. A. Dytman, and T. S. H. Lee, 2000, Phys. Rep. **328**, 181.
Walcher, T., 1988, Annu. Rev. Nucl. Part. Sci. **38**, 67.
Weigel, H., 2008, Lect. Notes Phys. **743**, 1.
Weigel, R. L., 2007, Phys. Rev. D **75**, 114018.
Weis, M., *et al.*, 2008, Eur. Phys. J. A **38**, 27.
Wieland, F. W., *et al.*, 2010, unpublished.
Wilczek, F., 2004, in *Solicited Contribution to the Ian Kogan Memorial Volume*, edited by M. Shifman, A. Vainshtein, and J. Wheater (World Scientific, Singapore), pp. 322–338.
Williams, M., *et al.*, 2009a, Phys. Rev. C **80**, 045213.
Williams, M., *et al.*, 2009b, Phys. Rev. C **80**, 065208.
Williams, M., *et al.*, 2009c, Phys. Rev. C **80**, 065209.
Wohl, C. G., 2008a, see Amsler *et al.*, 2008.
Wohl, C. G., 2008b, see Amsler *et al.*, 2008
Workman, R., 1999, Few-Body Syst., Suppl. **11**, 94.
Workman, R. L., and R. A. Arndt, 2009, Phys. Rev. C **79**, 038201.
Workman, R. L., *et al.*, 2006, Phys. At. Nucl. **69**, 90.
Wright, A. M., *et al.*, 1995, in *7th International Conference on the Structure of Baryons*, Santa Fe, New Mexico, edited by B. F. Gibson (World Scientific, Singapore).
Wu, C., *et al.*, 2005, Eur. Phys. J. A **23**, 317.
Yao, W. M., *et al.*, 2006, J. Phys. G **33**, 1.
Ynduráin, F. J., 1999, *The Theory of Quark and Gluon Interactions*, 3rd ed., Texts and Monographs in Physics (Springer, Berlin).
Zabrodin, A., *et al.*, 1999, Phys. Rev. C **60**, 055201.
Zegers, R. G. T., *et al.*, 2003, Phys. Rev. Lett. **91**, 092001.
Zhu, L. Y. *et al.*, 2003, Phys. Rev. Lett. **91**, 022003.
Zhu, L. Y. *et al.*, 2005, Phys. Rev. C **71**, 044603.
Zou, B. S., 2008, Eur. Phys. J. A **35**, 325.